WILEY-VCH

DOI: 10.1002/ ((please add manuscript number))
Article type: Full Paper

PEPDROID: Development of a Generic DREIDING-based Force Field for the Assessment of Peptoid Secondary Structures

*Sébastien Hoyas, Vincent Lemaur, Quentin Duez, Fabrice Saintmont, Emilie Halin, Julien De Winter, Pascal Gerbaux, Jérôme Cornil**

((Optional Dedication))

S. Hoyas, Dr. V. Lemaur, Prof. J. Cornil
Laboratory for Chemistry of Novel Materials
University of Mons
Mons 7000, Belgium
E-mail: Jerome.Cornil@umons.ac.be
Q. Duez, F. Saintmont, E. Halin, Dr. J. De Winter, Prof. P. Gerbaux
Synthesis and Mass Spectrometry Laboratory
University of Mons
Mons 7000, Belgium

Keywords: peptoid, foldamer, force field, Dreiding, molecular dynamics

α-peptoids are peptido-mimetic foldamers based on poly-N-substituted glycines that currently receive a growing interest in view of their larger structural diversity, easier synthetic pathways and larger thermal stability compared to peptides. The selection of the side chains appended to the nitrogen atoms is often crucial to constrain the peptoids into well-defined and active rigid structures for applications. To shed light on the secondary structure of peptoids, accurate methods for structural characterization are mandatory and typically involve the association of CD and NMR spectroscopies. Molecular simulations can also prove highly complementary to rationalize the relationship between their primary and secondary structures although much less studies have been reported to date compared to the body of knowledge accumulated on peptides. To this end, we have developed the PEPDROID force field by evaluating a new set of parameters to be incorporated in the original DREIDING force field and applied to (α or β) peptoids bearing different type of side chains. We demonstrate the ability of PEPDROID to assess the secondary structure of peptoids by generating Ramachandran-like plots matching those previously obtained at a quantum-chemical level for model systems. For further sake of

validation, we demonstrate that PEPDROID can reproduce the well-known "threaded loop" structure of a peptoid nonamer bearing (*S*)-1-phenylethyl side chains, as well as the crystalline structure of a β-peptoid hexamer forming helical structures.

1. Introduction

Peptoids, or poly-N-substituted glycines, are peptide regioisomers representing a class of peptido-mimetic polymers. The characteristic chemical feature of these molecules lies in the fact that the side chains (R) are appended to the amide nitrogen atoms instead of the α-carbon atoms like in peptides (**Scheme 1 A**).[1] Peptoid synthesis is performed using a stepwise solid-phase synthesis and involves the use of primary amines (R-NH_2) carrying the side chain R.[1,2] The key advantage of the peptoid synthesis lies in the absence of protection/deprotection steps between the coupling steps, except when the side chain bears reactive moieties.[2] Thus, peptoids exhibit a large diversity in terms of primary structure due to the large array of commercially available primary amines (over 300) in comparison to the 20 amino acids available for peptides. In contrast to peptides, the substitution of the amide nitrogen atoms prevents the creation of intramolecular hydrogen bonds, thus dramatically improving their thermal resistance as well as the resistance to proteolysis.[3,4] Nevertheless, peptoids can form stable secondary structures in solution through the selection of an appropriate side chain group (homopeptoids) or an appropriate set of side chains (heteropeptoids).[3,5,6] For example, a (*S*)-1-phenylethyl (*Nspe*) side chain gives rise to the formation of a *cis*-amide helical secondary structure driven by steric hindrance effects and stereoelectronic interactions, as attested by circular dichroism (CD) and nuclear magnetic resonance (NMR) data.[7] In contrast, aryl side chains fully induce the *trans*-amide bond conformation due to the steric hindrance and electronic repulsion between the carbonyl and aryl moieties.[8] Due to their highly modular and tunable structures, peptoids are increasingly used in biomedical applications,[4] as antifouling agents,[9] or even more importantly as biomaterials, for instance as chiral chromatography

supports for the resolution of racemic mixtures to cope with the growing demand in pharmaceutical industries to develop chiral selectors.[10] However, establishing the relationship between the structure (primary or secondary) and the function of peptoids is not straightforward and is still in its infancy. The enantioselective properties of peptoids is assumed to be linked to the formation of a helical structure within the chromatography column, although no clear evidences have been reported to date.[10] In view of the large diversity of available side chains and their possible combinations, exploring this relationship is a gigantic task. On the other hand, another class of peptoids referred to as "β-peptoids", in relation to β-peptides, has been introduced.[11,12] These molecules bear a second methylene unit in the repeat unit, giving more flexibility to the backbone (**Scheme 1 A**). In this case, the choice of an appropriate side chain R also enables the backbone to adopt well-defined secondary structures.[12–14] In this challenging context of identifying the α- or β-peptoid sequences that drive the formation of a targeted specific secondary structure with specific properties, molecular modelling can prove very helpful. Indeed, this approach can be used to decipher the conformational preferences of oligo-peptoids bearing a particular side chain at the atomistic level, as exemplified in recent theoretical studies.[15–18] Moreover, due to the large structural diversity, theoretical methods can be used to design, prior to synthesis, peptoid sequences that exhibit specific properties[19], in particular in the context of chiral resolution.[10,17]

Over the past 20 years, a large variety of modeling techniques has been used to investigate the secondary structures of peptoids.[5,15,16,18,20,21] Quantum-mechanical (QM) modeling is the most powerful tool to obtain high-resolution structures but is only applicable to small model molecules (i.e., hundreds of atoms), such as small peptoid fragments, in view of the large computational costs for larger molecules; the time scale of such simulations is also extremely limited when turning to dynamical aspects.[15,16] In contrast, molecular mechanics and dynamics (MM/MD) are particularly adapted methods to investigate large systems over a long time scale and hence to explore a large conformational space.[18,21–23] These methods rely on the use of a

force field whose empirical expression represents the potential energy of the system. The quality of these simulations is strongly dependent on the quality of the force field which must be accurately developed to compete with the quality of QM results at a reduced computational cost. So far, only a few studies have reported the use of force fields to describe peptoids. Most of them rely on peptide force fields when dealing with α-peptoids (CHARMM, AMBER) or more generic force fields such as GAFF or OPLS for β-peptoids.[13,15,18,24–26] However, since these force fields have been primarily optimized for peptides and not for peptoids, the quality of the results can be lowered for peptoids, as shown by Weiser *et al*. in a recent review.[27] In this context, Mirijanian et *al.* have recently developed the MF-TOID force field, based on the CHARMM22 peptide force field.[18] Their parametrization for peptoids is mainly done by the transfer of atom parameters from the peptide backbone and the alanine side chain to similar atoms present in the peptoid backbone.[18,23] Moreover, only methyl side chains have been taken into account in the parametrization, thus leading to potential transferability issues.[18] In order to validate their force field, they generated Ramachandran-like plots, which represent the potential energy surface (PES) resulting from the variation of two dihedral angles along the backbone, and compared them to those generated at a quantum-mechanical level.[16] While they obtained a qualitative agreement, their partial parameterization reveals some limitations since the force field over-stabilizes by around 5 kcal/mol the α-helical conformation compared to the real global minimum (*cis*-α_D conformation).[15,18,27] This directly impacts the PES since the global minimum, called $C_{7\beta}$ conformation (**Figure 3**),[15] is not recovered. Since the mere consideration of methyl side chains already produces artefacts, we can speculate that the description of more complex side chains, such as (*S*)-1-phenylethyl, would also be affected.

This has motivated the development of PEPDROID as a generic force field built from the original DREIDING force field in which a new set of parameters have been specifically determined for peptoids.[28] A key feature of the modified force field is to incorporate torsional

profiles obtained by fitting high-level quantum-mechanical calculations obtained on α- and β-peptoids. Another very attractive feature is that its transferability to any desired side chain is facilitated by the fact that the backbone torsional energy profiles are defined independently from those of the side chains. The validation of the new set of parameters in PEPDROID is achieved via the generation of Ramachandran-like plots for model systems and their comparison to those previously obtained by Butterfoss *et al.* or Renfrew *et al.* at the QM level.[16,20] A second validation check successfully passed has been to reproduce experimental structures reported for α and β-peptoids, in particular the well-known "threaded loop" formed by the (*S*)-1-phenylethyl nonamer (α-*Nspe*$_9$), as demonstrated by CD and NMR,[29] and the β-peptoid helix formed by the (*S*)-1-naphtylethyl hexamer (β-*N1snpe*$_6$), as revealed by CD and XRD.[13]

2. Methods

Developing a force field is a challenging task since many parameters must be properly defined. Hence, we decided to partly modify the DREIDING force field originally parameterized for generic organic, biological, and main-group inorganic molecules.[28] The functional form of the potential energy implemented in DREIDING in the Materials Studio 6.0 package is presented in **Equation (1)**. It contains four terms describing bonded interactions and three terms for the non-bonded interactions. A key characteristic of this force field is the explicit contribution of hydrogen bonds, allowing for a complete analysis of each energy contribution.

$$E_{pot}(R)= \sum_{bonds} {}^1\!/_2\, K_0(R-R_0)^2 + \sum_{angles} {}^1\!/_2\, K_0[\theta-\theta_0]^2 + \sum_{dihedrals,\ n=1}^{6} {}^1\!/_2\, B_n(1- d_n \cos(n\varphi)) + \sum_{improper} K_0(1-\omega) + \sum_{electrostatic} 322.0637 \frac{q_i q_j}{\varepsilon R} + \sum_{van\ der\ Waals} D_0 \left[\left(\frac{R_0}{R}\right)^{12} - \left(\frac{R_0}{R}\right)^{6}\right] + \sum_{hydrogen\ bonds} D_0 \left[5\left(\frac{R_0}{R}\right)^{12} - 6\left(\frac{R_0}{R}\right)^{10}\right] \cos^4\phi \qquad (1)$$

DREIDING is a robust force field already used in many different areas, such as in the modeling of small biomolecules,[30] polymers,[31–33] and peptides.[34,35] An adjustment of a few parameters,

mostly those related to the torsional terms, based on quantum-mechanical calculations is most often necessary to describe more accurately the systems.[31,33] As a matter of fact, dihedrals are considered as 'soft' bonded terms since changes in the energy associated to the whole range of torsion angles rarely exceed a few kcal/mol so that a non-accurate description of these terms can promote totally different molecular shapes. However, these interactions do not govern alone the 3D structure (conformation) of a system because non-bonded interactions (vdW, electrostatic and H-bonds) also play a significant role. We therefore paid a special attention to these terms by confronting DREIDING against high-level QM calculations for different peptoidic systems. Apart from dihedrals and non-bonded interactions, we also checked the reliability of the default parameters used for the equilibrium bond lengths, bond angles, and angles in the improper terms.

All molecular mechanics calculations have been carried out in the Materials Studio 6.0 package. For the reparameterization part and the generation of Ramachandran-like plots, we kept all default settings except that we selected the Conjugate Gradient as the minimization algorithm. We set to 200 Å the cutoff value to ensure accounting for all non-bonded interactions in these non-periodic systems. Partial charges on atoms were set by the Gasteiger method and the electrostatic term follows Coulomb's law (r^{-1}) instead of the dressed potential in r^{-2} defined by default; the dielectric constant is set to 1 (vacuum).[36] Quantum-mechanical calculations were performed at the Hartree-Fock/Möller-Plesset 2 level with a cc-pVDZ basis set (MP2/cc-pVDZ) using the Gaussian09 package revision A02. We discuss below the tests and changes made for the different terms of the force field.

2.1. Stretching term

In order to validate bond length parameters, we optimized at both the QM and MM levels an isolated α-peptoid monomer bearing (*S*)-1-phenylethyl side chains *Nspe* (**Scheme 2 A**). When comparing the bond lengths calculated with both methods, we found a good quantitative agreement between the MP2 and original DREIDING parameters, leading to a RMSD lower

than 3% (see Supporting Information, **Table S1**). We also performed the same procedure for a β-peptoid bearing methyl side chains (**Scheme 2 B**) and found again a comparable agreement between QM and MM data (Supporting Information, **Table S2**). Since bond lengths are not expected to govern predominantly the 3D structure of peptoids, such small deviations compared to the benchmark calculations fully validate the DREIDING default parameters for the stretching term.

2.2. Bending term

We adopt here the same methodology as previously described for bond lengths by comparing data generated at the QM and MM level for bond angles. For the same α- and β-peptoids (**Scheme 2 A, B**), we found a RMSD lower than 3% (see SI, **Table S1** & **S2**), validating again the use of the DREIDING default parameters.

2.3. Torsional term

As described earlier, the torsional profile is a very critical energy term in the description of 3D structures. The functional form of the dihedral potential energy is displayed in **Equation 2**, where B_n is the barrier height, d_n the phase factor and n the periodicity.

$$E_{dihedrals} = \sum_{\text{dihedrals, n=1}}^{6} {}^{1}/_{2}\, B_n(1\text{-}d_n \cos(n\varphi)) \qquad (2)$$

Since we intend to come up with a generic force field, we decomposed the peptoid structure into two components: the backbone versus the side chains. The backbone is characterized by three distinct torsion angles (ω,φ,ψ) for α-peptoids (**Scheme 1 C**) and two for the side chains (χ_1, χ_2) (see **Scheme 1 E** for *Nspe*). Note that the β-peptoid backbone presents an additional dihedral angle (θ) compared to the α-peptoid backbone, while the amide bond dihedral (ω) is the same as for the α-peptoid backbone (**Scheme 1 D**). Since similar dihedrals are found in both α and β-peptoids, we kept the same labelling and added a prime on the angles of β-peptoids for sake of distinction (**Scheme 1 D**). In order to validate whether DREIDING is adapted to accurately describe the dihedral angles of α-peptoids, we generated each torsion energy profile

for peptoid fragments containing a dihedral of interest (**Figure 1 A**) at the MP2 and DREIDING levels. From a technical point of view, whatever the level of the calculations (MP2 or Molecular Mechanics), for a given set of dihedrals (ω,φ,ψ), we optimize all geometrical parameters except the three angles when building torsional profiles associated to one of these dihedrals. For example, to build the ω angle torsion profile, ω is scanned by step of 10° while the two other angles are constrained to their MP2 equilibrium values and all other parameters are free to relax. These energy profiles were then converted into population profiles by using the Boltzmann equation at 298 K (**Equation (3)**). We also generated such profiles following the same procedure for the dihedrals of different side chains (χ_1, χ_2), namely (*S*)-1-phenylethyl (*Nspe*), n-propyl (*Nnpr*) and benzyl (*Npm*), **Scheme 1 B**.

$$\text{Normalized Population Fraction} = \frac{e^{\frac{-E_i}{kT}}}{\sum_i e^{\frac{-E_i}{kT}}} \qquad (3)$$

When we compare the shape of the energetic profiles, we notice large deviations between QM and the DREIDING default values (see SI**, Figure S1**), thus preventing the use of DREIDING to accurately describe peptoid 3D structures. As a result, we fitted the dihedral parameters, namely the barrier height B_n, the phase factor d_n and the periodicity n **(Equation (2))** to reproduce the MP2 population profiles. These parameters were systematically adjusted to yield a low RMSD between the QM and MM population profiles (see Supporting Information, **Table S4)**. The results of this fitting procedure are presented in **Figure 1** and is validated by examining the normalized population counts obtained with the new profiles (**Figure 1 A,** 3rd panel). The same methodology has been applied to the dihedral angles of the different side chains (χ_1, χ_2) (**Scheme 1 B**) since the DREIDING default parameters also led to a poor agreement with the MP2 calculations (see SI **Figures S2, S3 a, S6 a,c**)**.** For example, the profiles for the (*S*)-1-phenylethyl (*Nspe*) are displayed in **Figure 1 B**, while the energy and population profiles obtained for the other side chains can be found in the Supporting Information (**Figure S6 b, d**).

The same procedure has also been applied to the β-peptoid backbone dihedrals (**Figures S3 a, b**).

It is worth stressing that the key advantage of decoupling the backbone versus side-chain components is that we can easily incorporate any new side chain in PEPDROID after a proper fitting procedure of the set of parameters of the new side chains.

2.4. Inversion term

For peptoids, only nitrogen atoms are concerned by the inversion energy term. The default value in DREIDING for the equilibrium angle is set to 0°, implying that the nitrogen atoms and the three connected atoms are in the same molecular plane. The equilibrium inversion angle obtained at the QM level and with the DREIDING force field for the peptoid monomer (**Scheme 2 A**) is estimated to be 4.3° and 0.6°, respectively, thus giving confidence on the default parameter of DREIDING.

2.5. van der Waals interactions

The original DREIDING force field describes van der Waals (vdW) interactions by a 12-6 Lennard-Jones potential (**Equation (1)**). Each atom type is characterized by specific vdW parameters corresponding to the equilibrium distance and the well depth (R_0 and D_0 respectively) derived from *ab initio* calculations on homonuclear bonds to reproduce a large data set of crystal structures and sublimation energies [28]; heteronuclear interactions are then defined as the arithmetic and geometric mean for the equilibrium distance and well depth, respectively (**Equation (3)**).

$$R_{0ij} = 1/2\left(R_{0ii}+R_{0jj}\right) \;\&\; D_{0ij} = \left[D_{0ii}D_{0jj}\right]^{1/2} \qquad (3)$$

Recently, it has been shown that the vdW parameters used for the hydrogen atom in DREIDING are too large,[37,38] leading for example to an underestimation of computed gas densities. Reparametrizing the vdW parameters (R_0 and D_0) for hydrogen is therefore essential. To do so, a new value of R_0 has been recently estimated in our group via an independent study aiming at the comparison of experimental cross-section values of polymer chains by ion mobility mass

spectrometry and corresponding theoretical estimates, see more details in the SI. The RMSD is minimized for a distance R_0 of 2.83 Å (to be compared to the default value of 3.195 Å); note that a distance of 2.85 Å was adopted in DREIDING calculations reported by Kulkarni *et al.*[39] To optimize the well depth D_0, we have compared experimental vaporization enthalpies of different solvents to our force field calculations while varying the well-depth value D_0 and keeping the equilibrium distance constant, see Supporting Information for details on the complete procedure. We obtained the lowest average RMSD for the default well depth value (0.0152 kcal/mol). These values of R_0 and D_0 have been adopted in PEPDROID.

3. Results and Discussion

3.1. Ramachandran-like plots

In order to validate the new set of parameters implemented in PEPDROID, we generated Ramachandran-like plots of model peptoid structures. These 2D diagrams are often used with proteins to rationalize their secondary structures.[40] These plots span the full range of two dihedral angles and provide a landscape of the potential energy surface; they have been marginally applied so far to peptoids.[16,18,20] Since the amide bond can adopt two conformations, namely *cis* and *trans*, both need to be considered to effectively get an insight into the total PES of peptoids. We thus generated Ramachandran-like plots for the backbone dihedrals (φ, ψ) of the smallest model peptoid containing each different backbone dihedral, either in *cis* or *trans* conformation ($\omega = 0°$ or 180° respectively) (**Figure 2**). For each data point of the 2D plot, we optimized all geometrical parameters of the molecules except for the two scanned angles and the ω angle constrained to 0° or 180° for the *cis* and *trans* conformations, respectively. These plots were compared to those generated at the B3LYP/6-311+G(2d,p)//HF/6-31G* level by Butterfoss *et al.* for a model peptoid containing an additional amide unit (**Figure 2 c**).[16] The PES generated with our PEPDROID force field for the *cis*-model is in good quantitative agreement with that generated at the QM level (**Figure 2 A** & **C**). Two global minima, corresponding to the so-called *cis*-α_D conformations, are found at dihedral angles around ± 90°

and 180° for φ and ψ, respectively (**Figure 3**), in agreement with previous QM results.[15] Moreover, the *cis*-α conformation is round 1.5 kcal/mol higher in energy than the *cis*-α_D. Therefore, PEPDROID overcomes the limitation encountered by the previously reparameterized MF-TOID force field, which points to the *cis*-α conformation (φ = ±60°, ψ = ±60°) as the global minimum (see **Figure S4** for comparison).[14] The Ramachandran-plot of the *trans* peptoid model displays a very similar landscape when compared to that obtained by Butterfoss et al,[16] although some minor discrepancies are found owing to the fact that their peptoid contains an additional backbone unit which makes the analysis more complex. In particular, the global minimum for our model peptoid in the *trans* conformation corresponds to the *trans*-$C_{7\beta}$ conformation, as already identified by high-level QM calculations by Moelhe *et al.* for the same model peptoid.[15] We have calculated at the MP2/cc-pVDZ level the relative energies of the *trans*-α_D and $C_{7\beta}$ structures for our model peptoid and found that the fully optimized $C_{7\beta}$ structure is slightly more stable by 0.78 kcal/mol compared to *trans*-α_D; in agreement with the 0.97 kcal/mol energy difference obtained with PEPDROID) (**Figure 3**); Although such subtle effects are not expected to be always fully reproduced with PEPDROID, the key aspect here is that PEPDROID can locate the most stable structures in the peptoid conformational space.

We investigated next the influence of the *Nspe* side chain on the PES of the backbone dihedrals (φ, ψ) and hence on the secondary structure of the peptoids. We used here the same approach as previously described for the backbone, namely we generated Ramachandran-like plots for the *cis* and *trans* amide conformations for a model peptoid bearing a *Nspe* side chain (**Scheme 2 D**). In contrast to methyl side chains, we observe now an asymmetric PES, in both the *cis* or *trans* conformation, indicating that a chiral sterically hindered side chain restrains the available conformational space (**Figure 4**). For the *cis* conformers, we get once again a good quantitative agreement with the quantum-chemical data reported by Butterfoss *et al.*,[16] with the global

minimum corresponding to the α_D conformation ($\varphi \sim -80°$, $\psi \sim 180°$). For the *trans* form, our Ramachandran-like plot points to the $C_{7\beta}$ conformation as the global minimum. Our calculations scanning the full range of each dihedral angle are not readily comparable to the QM results reported by Butterfoss *et al.* since they restricted their analysis to two specific values of χ_1 and were led to the conclusion that the *trans*-α_D conformation is the global minimum.[16] When performing MP2 geometry optimizations on the global minimum extracted from PEPDROID and from Ref. 16 by Butterfoss *et al.*,[16] we find the *trans*-$C_{7\beta}$ conformation to be slightly more stable than the *trans*-α_D structure by 0.41 kcal/mol (0.51 kcal/mol with PEPDROID, see SI **Table S3**), thus confirming the robustness of the description of stable secondary structures of peptoids provided by PEPDROID. Moreover, it also validates our reparameterization method since we accurately describe the PES either in *cis* or *trans* although the side chains dihedrals were initially reparametrized only in the *cis* conformation ($\omega = 0°$). Recently, Renfrew *et al.* also investigated the PES of peptoids at the QM level with a special emphasis on the influence of the side chain dihedrals (see *Nnpr*, *Npm*, *Nspe*, *N1snpe* **Scheme 1 B**).[20] We thus generated Ramachandran-like plots (χ_1, χ_2) for the same model peptoid as they considered by scanning the dihedrals χ_1 and χ_2 of the *Nspe* side chain with the amide bond in *cis* or *trans* conformation (SI, **Figure S5**). Our results match very well the data of Renfrew *et al.*,[20] thus giving us a supplementary evidence that the new set of parameters of PEPDROID is reliable. We carried out the same methodology as explained above for two other side chains, *Nnpr* and *Npm* (**Scheme 1 B**). Ramachandran-like plots were generated for the combination of the side chain dihedrals χ_1 and χ_2 and are again in good agreement with the results of Renfrew *et al.* (SI, **Figures S6 a-d, S7, S8**).[20] Importantly, we still accurately describe the PES of the system (SI, **Figure S9**) when we apply the dihedral parameters developed for one side chain to another one displaying the same saturated spacer (*Nspe* versus *N1snpe* where the phenyl unit is

replaced by a naphthyl unit – **Scheme 1 B**), thus ensuring the good transferability of our force field.[20]

In order to assess the quality of PEPDROID to describe the conformational dynamics of peptoids, we selected the global minimum of the model peptoid bearing methyl side chains in the *cis* and *trans* conformation from the Ramachandran-like plots (*cis*-α_D and *trans*-$C_{7\beta}$, **Figure 2**) and submitted them to molecular dynamics simulations. We first performed an equilibration MD run for 10 ns (NVT, Nosé-Hoover thermostat, 298 K, 1 fs timestep) followed by an analysis MD run for 10 ns using the same parameters. We have then extracted 1000 structures from the second MD and computed several structural parameters, such as the evolution of dihedral angles, bond angles, and bond lengths along the MD trajectory to evaluate the fluctuations around the optimized structure at the QM level (MP2/cc-pVDZ).

cis-α_D conformation

The structural analysis of the model peptoid in the *cis* conformation is illustrated in **Figure 5**where we also display the deviations around the QM optimized parameters. The distributions obtained for two representative bonds along the MD trajectory are well-centered around the QM values. The same conclusion can be drawn for the bond angle values, with small deviations around the reference value. In the case of the dihedral angles, we observe two distributions for the φ angle (around 90° and 270°) resulting from the fact that these two conformations are isoenergetic (at both the QM and MM levels, **Table S5**) and that frequent switchings between the two forms occur during the dynamics. (**Figure 5 E**). In contrast, the ψ angle slightly fluctuates around the equilibrium value (around 180°) even though some higher-lying energy minima (around 60° and 300°) are weakly populated.

trans-$C_{7\beta}$ conformation

The same conclusions can be drawn for this conformation for which the deviations from the QM reference value for bond lengths and angles are also quite small during the MD run (**Figure 6 A, B, C**). We observe multiple distributions for the dihedral angles linked to switching

processes between multiple local minima spotted in the Ramachandran plot (see Supporting Information, **Table S5**). Indeed, the φ angle has two distributions around 100° and 250°, which correspond to the *trans*-$C_{7\beta}$ or the *trans*-α_D conformations, depending on the ψ value. In the early stage of the analysis MD **Figure 6 E** (0 – 2000 fs), the φ angle fluctuates around 100° while the ψ angle switches back and forth between 180° and 300°; note that the starting geometry for the equilibration MD has a φ value of 230° which evolves rapidly to ~ 100° during the MD. The combination (φ = 100°, ψ = 180°) is associated to the *trans*-α_D conformation while the combination (φ = 100°, ψ = 300°) is associated to the *trans*-$C_{7\beta}$ conformation. In a later stage (2000 – 9000 fs), the φ angle switches to values around 250° and the ψ angle around 70° or 180°. We can thus conclude that the MD simulations allow for an exploration of the conformational space in full consistency with the energy landscape provided in the Ramachandran plots, without divergence along the runs.

3.2. Simulation of known experimental structures

Ramachandran-like plots are very useful to validate force fields through the exploration of the conformational space of small peptoid fragments. Another way to test our force field is to demonstrate its ability to reproduce available high-resolution experimental structures.

3.2.1. α -Peptoid "threaded loop"

A threaded loop conformation has been previously described by Huang *et al.* by means of CD and NMR for a peptoid nonamer bearing *Nspe* side chains (α-$Nspe_9$),[29] which is stabilized by four intramolecular hydrogen bonds between carbonyl groups of the backbone and both C and N terminal hydrogen atoms (**Figure 7 A**). Here, we first built α-$Nspe_9$ conformers ranging from extended, helical, or globular shapes with Materials Studio 6.0 without periodic boundary conditions and optimized their geometries using the Conjugate Gradient algorithm and a cutoff value of 200 Å. In a next step, we submitted the optimized geometries to multiple successive quenched molecular dynamics (36 MD in total, NVT, Nosé-Hoover thermostat, 1 fs time step) with a duration of 10 ns at different temperatures (800, 600, and 400 K); 10,000 snapshots are

then extracted from the dynamical run and optimized at the Molecular Mechanics (MM) level. The most stable structures of each successive quenched MD (selected among the 10,000 optimized snapshots) were then resubmitted to a quenched MD with the same parameters as in the previous MD runs, but at lower temperature (200 K) for 10 ns. This method has already proven efficient to scan the PES of complex systems.[41] The conformation of the most stable structure is displayed in **Figure 7 C** and compared to that inferred by Huang *et al.* (**Figure 7 B**).[29] The analysis of the backbone dihedrals (ω, φ, ψ) of the lowest energy optimized structure shows a very good agreement with those determined by NMR, as illustrated in **Figure 7**.[29] This structure was finally submitted to a 10 ns-long equilibration MD (NVT, 298 K, Nosé-Hoover thermostat, 1 fs timestep) followed by a second 10 ns-long analysis MD (NVT, 298 K, Nosé-Hoover thermostat, 1 fs timestep) to judge the quality of PEPDROID to describe the conformational dynamical aspects. Interestingly, the distribution of any couple of dihedrals (φ, ψ) calculated from 1000 structures extracted from the 10 ns-long MD are in good agreement with experimental results (see **Figures 7 D**, **E** & **S10**). The largest deviations are observed for the ψ distributions, which are shifted only by about 10°, with respect to the experimental values while the average value is within the experimental error.[29]

3.2.2. β-Peptoid helix

Over the years, researchers have developed strategies to induce and control the formation of helical structures in peptoidic structures.[8,42,43] Recently, a joint experimental and theoretical study has shown that this control can be achieved by an appropriate choice of bulky aromatic side chains, such as *N1snpe* (**Scheme 1 B**), despite the increased conformational flexibility due to the additional methylene in the backbone.[13] These side chains induce a large energetical preference for the *cis*-amide bond conformation, leading to well-organized helical structures. This has been illustrated recently by Laursen *et al.* for a β-*N1snpe*$_6$ hexamer through CD and XRD experiments.[13]

We have used PEPDROID to model the β-*N1snpe*$_6$ hexamer capped at the C terminus extremity by a tert-butyl ester (-O-tBu) (**Figure 8 A**). The complete procedure for this study is detailed in the Supporting Information. Briefly, we generated a helical structure and a globular one that we introduced into a large unit cell (30 Å x 30 Å x 30 Å) using periodic boundary conditions (**Figure 8 B** & **C**). These structures were submitted to several MD runs, using Ewald summation method to account for the non-bonded interactions, first to equilibrate the system, and then to analyze the stability of the conformations scanned by the dynamics. After equilibration of the systems, the average potential energy of these conformations along a MD run of 10 ns (NPT, 298 K) is in favor of the helical structure (**Figure 8 D**). The distribution of the radius of gyration (R_{Gyr}) along the 10 ns MD run is centered around 7.1 Å, in good agreement with previous results obtained by molecular dynamics simulations by Laursen *et al.* (R_{Gyr} around 7.5 Å, **Figure 8 E**).[13] Note also that the helical structure is conserved during the MD at 298 K and only fluctuates around the equilibrium geometry, as attested by the evolution of the radius of gyration. We also performed similar calculations for cells containing four molecules (four helices or four globules) to account for the possible influence of intermolecular interactions, with adapted dimensions of the unit cell (60 Å x 60 Å x 60 Å). The same picture still holds true, with helical conformations favored over globular shapes, **Figure 8 D**.

4. Conclusion

Robust theoretical tools dedicated to peptoids are nowadays required to improve the understanding of the relationship between their primary and secondary structures, and to allow for the prediction of structures for specific applications in diverse areas. In this context, we developed PEPDROID, a generic peptoid force field based on the DREIDING force field which was reparametrized for a series of different side chains,[28] based on high-level QM calculations. The key advantage is the decoupling of the backbone and side chain dihedral angles, which permits to easily integrate any new desired side chain. Moreover, this force field is suitable for α- and β-peptoids, for which a growing interest is encountered in the current literature.[12,13,44]

The validation of PEPDROID was performed in two steps. First, we generated Ramachandran-like plots, for which QM data were available in the literature, and obtained a good agreement between the two sets of data following the reparameterization of the dihedral terms.[20] The second step was to assess the ability of PEPDROID to accurately describe the static and dynamic structural properties of well-known structures, either for α- or β-peptoids. PEPDROID successfully reproduces the dihedral preferences of the "threaded loop" structure for the α-peptoid (α-*Nspe*$_9$),[29] and the conformational preference of a β-peptoid hexamer to form helices (β-*N1snpe*$_6$).[13] We hope that this new peptoid force field will strive further efforts to gain a better understanding on the secondary structure of the peptoid foldamers.

Supporting Information

Supporting Information is available from the Wiley Online Library or from the author.
PEPDROID parameters are available as Supporting Information in the form of a .csv file as well as a topology file.

Acknowledgements

The work in the Laboratory for Chemistry of Novel Materials was supported by the European Commission / Région Wallonne (FEDER – BIORGEL project), the Consortium des Équipements de Calcul Intensif (CÉCI) funded by the Fonds National de la Recherche Scientifique (F.R.S.-FNRS) under Grant No. 2.5020.11, and FRS-FNRS. The UMONS MS laboratory acknowledges FRS-FNRS for the continuous support. JC and QD are FNRS Research fellows. SH and EH thank the "Fonds pour la Recherche Industrielle et Agricole" for their PhD grants. FS thanks the University of Mons for his PhD grant. The S^{2}MOs lab is grateful to the Fonds National de la Recherche Scientifique (F.R.S.-FNRS) for continuing support.

References

[1] R. J. Simon, R. S. Kania, R. N. Zuckermann, V. D. Huebner, D. a Jewell, S. Banville, S. Ng, L. Wang, S. Rosenberg, C. K. Marlowe, Proc. Natl. Acad. Sci. U. S. A. 1992, 89, 9367.

[2] R. N. Zuckermann, J. M. Kerr, S. B. H. Kent, W. H. Moos, J. Am. Chem. Soc. 1992, 114, 10646.

[3] C. W. Wu, T. J. Sanborn, R. N. Zuckermann, A. E. Barron, J. Am. Chem. Soc. 2001, 123, 2958.

[4] S. a Fowler, H. E. Blackwell, Org. Biomol. Chem. 2009, 7, 1508.

[5] P. Armand, K. Kirshenbaum, A. Falicov, R. L. Dunbrack, K. a Dill, R. N. Zuckermann, F. E. Cohen, Fold. Des. 1997, 2, 369.

[6] C. W. Wu, T. J. Sanborn, K. Huang, R. N. Zuckermann, A. E. Barron, J. Am. Chem. Soc. 2001, 123, 6778.

[7] P. Armand, K. Kirshenbaum, R. A. Goldsmith, S. Farr-Jones, A. E. Barron, K. T. V Truong, K. A. Dill, D. F. Mierke, F. E. Cohen, R. N. Zuckermann, E. K. Bradley, Proc. Natl. Acad. Sci. U. S. A. 1998, 95, 4309.

[8] N. H. Shah, G. L. Butterfoss, K. Nguyen, B. Yoo, R. Bonneau, D. L. Rabenstein, K. Kirshenbaum, J. Am. Chem. Soc. 2008, 130, 16622.

[9] K. H. A. Lau, C. Ren, T. S. Sileika, S. H. Park, I. Szleifer, P. B. Messersmith, Langmuir 2012, 28, 16099.

[10] S. Lingfeng, C. Co, S. Heqi, C. Co, A. C. Co, C. Co, S. Hanhong, F. Silysia, P. Csp, B. Avance, E. Vario, E. L. Iii, W. Acquity, Analyst 2011, 136, 4409.

[11] A. S. Norgren, S. Zhang, P. I. Arvidsson, Org. Lett. 2006, 8, 4533.

[12] J. S. Laursen, J. Engel-Andreasen, C. A. Olsen, Acc. Chem. Res. 2015, 48, 2696.

[13] J. S. Laursen, P. Harris, P. Fristrup, C. a Olsen, Nat. Commun. 2015, 6, 7013.

[14] E. De Santis, T. Hjelmgaard, C. Caumes, S. Faure, B. D. Alexander, S. J. Holder, G. Siligardi, C. Taillefumier, A. A. Edwards, Org. Biomol. Chem. 2012, 10, 1108.

[15] K. Moehle, H.-J. Hofmann, Biopolymers 1996, 38, 781.

[16] G. L. Butterfoss, P. D. Renfrew, B. Kuhlman, K. Kirshenbaum, R. Bonneau, J. Am. Chem. Soc. 2009, 131, 16798.

[17] G. L. Butterfoss, B. Yoo, J. N. Jaworski, I. Chorny, K. A. Dill, R. N. Zuckermann, R. Bonneau, K. Kirshenbaum, V. A. Voelz, Proc. Natl. Acad. Sci. U. S. A. 2012, 109, 14320.

[18] D. T. Mirijanian, R. V. Mannige, R. N. Zuckermann, S. Whitelam, J. Comput. Chem. 2014, 35, 360.

[19] B. C. Gorske, J. R. Stringer, B. L. Bastian, S. A. Fowler, H. E. Blackwell, J. Am. Chem. Soc. 2011, 1, 93.

[20] P. D. Renfrew, T. W. Craven, G. L. Butterfoss, K. Kirshenbaum, R. Bonneau, J. Am. Chem. Soc. 2014, 136, 8772.

[21] S. Mukherjee, G. Zhou, C. Michel, V. A. Voelz, J. Phys. Chem. B 2015, 119, 15407.

[22] V. a Voelz, K. a Dill, I. Chorny, Biopolymers 2011, 96, 639.

[23] T. K. Haxton, R. V. Mannige, R. N. Zuckermann, S. Whitelam, J. Chem. Theory Comput. 2015, 11, 303.

[24] A. D. MacKerell, D. Bashford, M. Bellott, R. L. Dunbrack, J. D. Evanseck, M. J. Field, S. Fischer, J. Gao, H. Guo, S. Ha, D. Joseph-McCarthy, L. Kuchnir, K. Kuczera, F. T. K. Lau, C. Mattos, S. Michnick, T. Ngo, D. T. Nguyen, B. Prodhom, W. E. Reiher, B. Roux, M. Schlenkrich, J. C. Smith, R. Stote, J. Straub, M. Watanabe, J. Wiórkiewicz-Kuczera, D. Yin, M. Karplus, J. Phys. Chem. B 1998, 102, 3586.

[25] D. A. Case, T. E. Cheatham, T. Darden, H. Gohlke, R. Luo, K. M. Merz, A. Onufriev, C. Simmerling, B. Wang, R. J. Woods, J. Comput. Chem. 2005, 26, 1668.

[26] J. M. Wang, R. M. Wolf, J. W. Caldwell, P. a Kollman, D. a Case, J. Comput. Chem. 2004, 25, 1157.

[27] L. J. Weiser, E. E. Santiso, AIMS Mater. Sci. 2017, 4, 1029.

[28] S. L. Mayo, B. D. Olafson, W. A. Goddard, J. Phys. Chem. 1990, 94, 8897.

[29] K. Huang, C. W. Wu, T. J. Sanborn, J. A. Patch, K. Kirshenbaum, R. N. Zuckermann, A. E. Barron, I. Radhakrishnan, J. Am. Chem. Soc. 2006, 128, 1733.

[30] C. Decroo, E. Colson, M. Demeyer, V. Lemaur, G. Caulier, I. Eeckhaut, J. Cornil, P. Flammang, P. Gerbaux, Anal. Bioanal. Chem. 2017, 409, 3115.

[31] V. Lemaur, L. Muccioli, C. Zannoni, D. Beljonne, R. Lazzaroni, J. Cornil, Y. Olivier, Macromolecules 2013, 46, 8171.

[32] B. Guillerm, V. Lemaur, B. Ernould, J. Cornil, R. Lazzaroni, J.-F. Gohy, P. Dubois, O. Coulembier, RSC Adv. 2014, 4, 10028.

[33] K. Broch, D. Venkateshvaran, V. Lemaur, Y. Olivier, D. Beljonne, M. Zelazny, I. Nasrallah, D. J. Harkin, M. Statz, R. Di Pietro, A. J. Kronemeijer, H. Sirringhaus, Adv. Electron. Mater. 2017, 3, 1700225.

[34] W. Mästle, U. Link, W. Witschel, U. Thewalt, T. Weber, M. Rothe, Biopolymers 1991, 31, 735.

[35] K. B. Borisenko, H. J. Reavy, Q. Zhao, E. W. Abel, J. Biomed. Mater. Res. - Part A 2008, 86, 1113.

[36] J. Gasteiger, M. Marsili, Tetrahedron Lett. 1978, 19, 3181.

[37] S. Saiev, L. Bonnaud, P. Dubois, D. Beljonne, R. Lazzaroni, Polym. Chem. 2017, 8, 5988.

[38] L. Sun, L. Yang, Y.-D. Zhang, Q. Shi, R.-F. Lu, W.-Q. Deng, J. Comput. Chem. 2017, 38, 1991.

[39] A. R. Kulkarni, D. S. Sholl, Langmuir 2015, 31, 8453.

[40] G. N. Ramachandran, V. Sasisekharan, Adv. Protein Chem. 1968, 23, 283.

[41] J. De Winter, V. Lemaur, R. Ballivian, F. Chirot, O. Coulembier, R. Antoine, J. Lemoine, J. Cornil, P. Dubois, P. Dugourd, P. Gerbaux, Chem. - A Eur. J. 2011, 17, 9738.

[42] J. R. Stringer, J. A. Crapster, I. A. Guzei, H. E. Blackwell, J. Am. Chem. Soc. 2011, 133, 15559.

[43] O. Roy, C. Caumes, Y. Esvan, C. Didierjean, S. Faure, C. Taillefumier, Org. Lett. 2013, 15, 2246.

[44] J. S. Laursen, J. Engel-Andreasen, P. Fristrup, P. Harris, C. A. Olsen, J. Am. Chem. Soc. 2013, 135, 2835.

[45] P. D. Renfrew, T. W. Craven, G. L. Butterfoss, K. Kirshenbaum, R. Bonneau, J. Am. Chem. Soc. 2014, 136, 8772.

[1] R. J. Simon, R. S. Kania, R. N. Zuckermann, V. D. Huebner, D. a Jewell, S. Banville, S. Ng, L. Wang, S. Rosenberg, C. K. Marlowe, *Proc. Natl. Acad. Sci. U. S. A.* **1992**, *89*, 9367.

[2] R. N. Zuckermann, J. M. Kerr, S. B. H. Kent, W. H. Moos, *J. Am. Chem. Soc.* **1992**, *114*, 10646.

[3] C. W. Wu, T. J. Sanborn, R. N. Zuckermann, A. E. Barron, *J. Am. Chem. Soc.* **2001**, *123*, 2958.

[4] S. a Fowler, H. E. Blackwell, *Org. Biomol. Chem.* **2009**, *7*, 1508.

[5] P. Armand, K. Kirshenbaum, A. Falicov, R. L. Dunbrack, K. a Dill, R. N. Zuckermann, F. E. Cohen, *Fold. Des.* **1997**, *2*, 369.

[6] C. W. Wu, T. J. Sanborn, K. Huang, R. N. Zuckermann, A. E. Barron, *J. Am. Chem. Soc.* **2001**, *123*, 6778.

[7] P. Armand, K. Kirshenbaum, R. A. Goldsmith, S. Farr-Jones, A. E. Barron, K. T. V Truong, K. A. Dill, D. F. Mierke, F. E. Cohen, R. N. Zuckermann, E. K. Bradley, *Proc. Natl. Acad. Sci. U. S. A.* **1998**, *95*, 4309.

[8] N. H. Shah, G. L. Butterfoss, K. Nguyen, B. Yoo, R. Bonneau, D. L. Rabenstein, K. Kirshenbaum, *J. Am. Chem. Soc.* **2008**, *130*, 16622.

[9] K. H. A. Lau, C. Ren, T. S. Sileika, S. H. Park, I. Szleifer, P. B. Messersmith, *Langmuir* **2012**, *28*, 16099.

[10] S. Lingfeng, C. Co, S. Heqi, C. Co, A. C. Co, C. Co, S. Hanhong, F. Silysia, P. Csp, B. Avance, E. Vario, E. L. Iii, W. Acquity, *Analyst* **2011**, *136*, 4409.

[11] A. S. Norgren, S. Zhang, P. I. Arvidsson, *Org. Lett.* **2006**, *8*, 4533.

[12] J. S. Laursen, J. Engel-Andreasen, C. A. Olsen, *Acc. Chem. Res.* **2015**, *48*, 2696.

[13] J. S. Laursen, P. Harris, P. Fristrup, C. a Olsen, *Nat. Commun.* **2015**, *6*, 7013.

[14] E. De Santis, T. Hjelmgaard, C. Caumes, S. Faure, B. D. Alexander, S. J. Holder, G. Siligardi, C. Taillefumier, A. A. Edwards, *Org. Biomol. Chem.* **2012**, *10*, 1108.

[15] K. Moehle, H.-J. Hofmann, *Biopolymers* **1996**, *38*, 781.

[16] G. L. Butterfoss, P. D. Renfrew, B. Kuhlman, K. Kirshenbaum, R. Bonneau, *J. Am. Chem. Soc.* **2009**, *131*, 16798.

[17] G. L. Butterfoss, B. Yoo, J. N. Jaworski, I. Chorny, K. A. Dill, R. N. Zuckermann, R. Bonneau, K. Kirshenbaum, V. A. Voelz, *Proc. Natl. Acad. Sci. U. S. A.* **2012**, *109*, 14320.

[18] D. T. Mirijanian, R. V. Mannige, R. N. Zuckermann, S. Whitelam, *J. Comput. Chem.* **2014**, *35*, 360.

[19] B. C. Gorske, J. R. Stringer, B. L. Bastian, S. A. Fowler, H. E. Blackwell, *J. Am. Chem. Soc.* **2011**, *1*, 93.

[20] P. D. Renfrew, T. W. Craven, G. L. Butterfoss, K. Kirshenbaum, R. Bonneau, *J. Am. Chem. Soc.* **2014**, *136*, 8772.

[21] S. Mukherjee, G. Zhou, C. Michel, V. A. Voelz, *J. Phys. Chem. B* **2015**, *119*, 15407.

[22] V. a Voelz, K. a Dill, I. Chorny, *Biopolymers* **2011**, *96*, 639.

[23] T. K. Haxton, R. V. Mannige, R. N. Zuckermann, S. Whitelam, *J. Chem. Theory Comput.* **2015**, *11*, 303.

[24] A. D. MacKerell, D. Bashford, M. Bellott, R. L. Dunbrack, J. D. Evanseck, M. J. Field, S. Fischer, J. Gao, H. Guo, S. Ha, D. Joseph-McCarthy, L. Kuchnir, K. Kuczera, F. T. K. Lau, C. Mattos, S. Michnick, T. Ngo, D. T. Nguyen, B. Prodhom, W. E. Reiher, B.

Roux, M. Schlenkrich, J. C. Smith, R. Stote, J. Straub, M. Watanabe, J. Wiórkiewicz-Kuczera, D. Yin, M. Karplus, *J. Phys. Chem. B* **1998**, *102*, 3586.

[25] D. A. Case, T. E. Cheatham, T. Darden, H. Gohlke, R. Luo, K. M. Merz, A. Onufriev, C. Simmerling, B. Wang, R. J. Woods, *J. Comput. Chem.* **2005**, *26*, 1668.

[26] J. M. Wang, R. M. Wolf, J. W. Caldwell, P. a Kollman, D. a Case, *J. Comput. Chem.* **2004**, *25*, 1157.

[27] L. J. Weiser, E. E. Santiso, *AIMS Mater. Sci.* **2017**, *4*, 1029.

[28] S. L. Mayo, B. D. Olafson, W. A. Goddard, *J. Phys. Chem.* **1990**, *94*, 8897.

[29] K. Huang, C. W. Wu, T. J. Sanborn, J. A. Patch, K. Kirshenbaum, R. N. Zuckermann, A. E. Barron, I. Radhakrishnan, *J. Am. Chem. Soc.* **2006**, *128*, 1733.

[30] C. Decroo, E. Colson, M. Demeyer, V. Lemaur, G. Caulier, I. Eeckhaut, J. Cornil, P. Flammang, P. Gerbaux, *Anal. Bioanal. Chem.* **2017**, *409*, 3115.

[31] V. Lemaur, L. Muccioli, C. Zannoni, D. Beljonne, R. Lazzaroni, J. Cornil, Y. Olivier, *Macromolecules* **2013**, *46*, 8171.

[32] B. Guillerm, V. Lemaur, B. Ernould, J. Cornil, R. Lazzaroni, J.-F. Gohy, P. Dubois, O. Coulembier, *RSC Adv.* **2014**, *4*, 10028.

[33] K. Broch, D. Venkateshvaran, V. Lemaur, Y. Olivier, D. Beljonne, M. Zelazny, I. Nasrallah, D. J. Harkin, M. Statz, R. Di Pietro, A. J. Kronemeijer, H. Sirringhaus, *Adv. Electron. Mater.* **2017**, *3*, 1700225.

[34] W. Mästle, U. Link, W. Witschel, U. Thewalt, T. Weber, M. Rothe, *Biopolymers* **1991**, *31*, 735.

[35] K. B. Borisenko, H. J. Reavy, Q. Zhao, E. W. Abel, *J. Biomed. Mater. Res. - Part A* **2008**, *86*, 1113.

[36] J. Gasteiger, M. Marsili, *Tetrahedron Lett.* **1978**, *19*, 3181.

[37] S. Saiev, L. Bonnaud, P. Dubois, D. Beljonne, R. Lazzaroni, *Polym. Chem.* **2017**, *8*, 5988.

[38] L. Sun, L. Yang, Y.-D. Zhang, Q. Shi, R.-F. Lu, W.-Q. Deng, *J. Comput. Chem.* **2017**, *38*, 1991.

[39] A. R. Kulkarni, D. S. Sholl, *Langmuir* **2015**, *31*, 8453.

[40] G. N. Ramachandran, V. Sasisekharan, *Adv. Protein Chem.* **1968**, *23*, 283.

[41] J. De Winter, V. Lemaur, R. Ballivian, F. Chirot, O. Coulembier, R. Antoine, J. Lemoine, J. Cornil, P. Dubois, P. Dugourd, P. Gerbaux, *Chem. - A Eur. J.* **2011**, *17*, 9738.

[42] J. R. Stringer, J. A. Crapster, I. A. Guzei, H. E. Blackwell, *J. Am. Chem. Soc.* **2011**, *133*, 15559.

[43] O. Roy, C. Caumes, Y. Esvan, C. Didierjean, S. Faure, C. Taillefumier, *Org. Lett.* **2013**, *15*, 2246.

[44] J. S. Laursen, J. Engel-Andreasen, P. Fristrup, P. Harris, C. A. Olsen, *J. Am. Chem. Soc.* **2013**, *135*, 2835.

[45] P. D. Renfrew, T. W. Craven, G. L. Butterfoss, K. Kirshenbaum, R. Bonneau, *J. Am. Chem. Soc.* **2014**, *136*, 8772.

[46] D. P. Smith, T. W. Knapman, I. Campuzano, R. W. Malham, J. T. Berryman, S. E. Radford, A. E. Ashcroft, *Eur. J. Mass Spectrom.* **2009**, *15*, 113.

[47] E. W. McDaniel, D. W. Martin, W. S. Barnes, *Rev. Sci. Instrum.* **1962**, *33*, 2.

[48] Q. Duez, F. Chirot, R. Liénard, T. Josse, C. Choi, O. Coulembier, P. Dugourd, J. Cornil, P. Gerbaux, J. De Winter, *J. Am. Soc. Mass Spectrom.* **2017**, *28*, 2483.

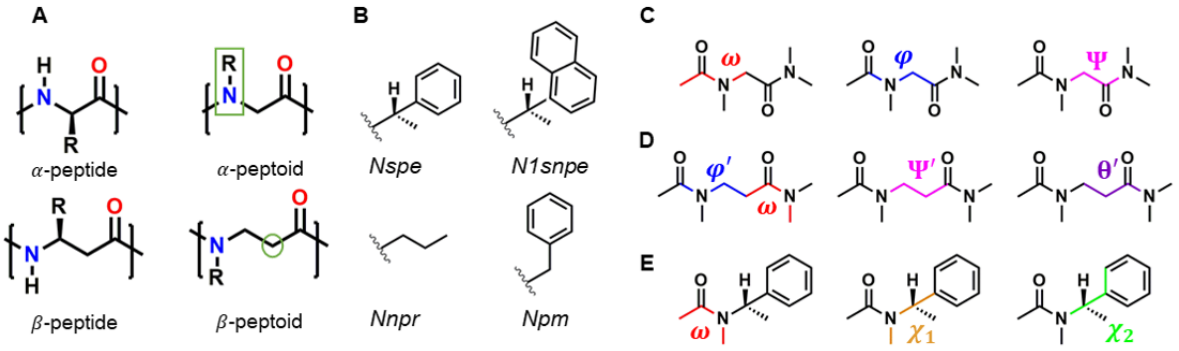

Scheme 1. (**A**) Comparison of the structures of α- and β-peptides with respect to α- and β-peptoids. α-peptoids are peptide regioisomers in which the side chain is appended to the nitrogen. β-peptoids incorporate an additional methylene unit into the backbone in analogy to β-peptides; **(B)** Peptoid side chains under study; **(C)** α-peptoid backbone dihedrals; **(D)** β-peptoid backbone dihedrals. Note that β-peptoids have the same amide bond (ω) as in α-peptoids; (**E**) *Nspe* side chain dihedrals. The same dihedrals are found in other side chains than *Nspe* but have been omitted here for sake of clarity.

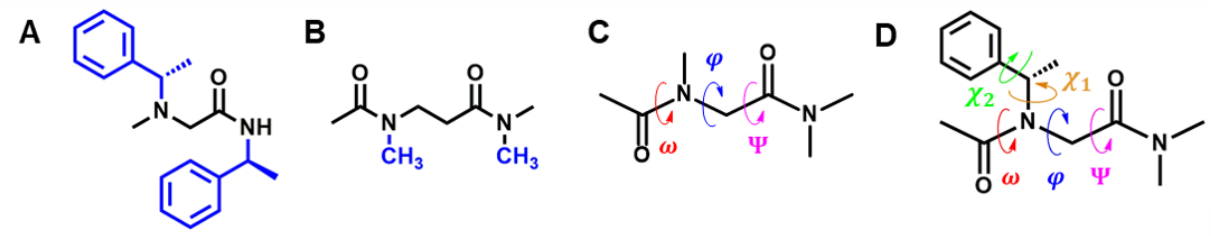

Scheme 2. Structure of: (**A**) the α-peptoid monomer bearing two (*S*)-1-phenylethyl (*Nspe*) side chains; (**B**) the β-peptoid monomer bearing two methyl side chains; (**C**) the model peptoid bearing methyl side chains used to generate the Ramachandran-like plots (φ, ψ). The backbone

dihedrals ω, φ, and ψ are highlighted; (**D**) the model peptoid bearing a (*S*)-1-phenylethyl (*Nspe*), used to generate the Ramachandran-like plots in **Figure 5**. Backbone and side chain dihedrals are highlighted.

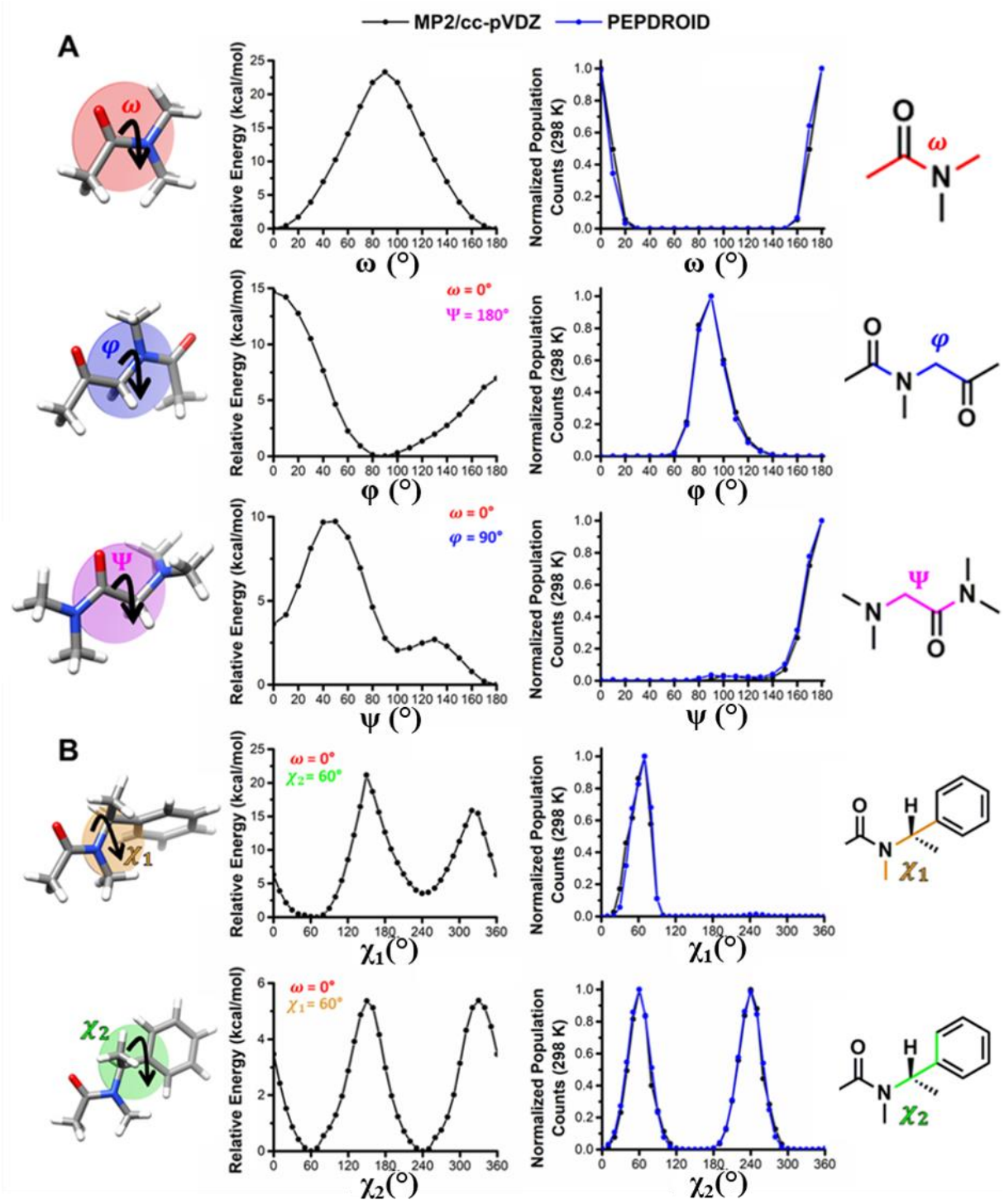

Figure 1. (**A**) Torsion energy (center) and relative population (right) profiles for α-peptoid backbone dihedrals (ω,φ,ψ), as calculated at the QM level (MP2/cc-pVDZ) and with the fitting procedure of the dihedral parameters at the MM level (PEPDROID); (**B**) Torsion energy and relative population profiles for the *Nspe* side chain dihedrals (χ_1, χ_2) as calculated at the QM level (MP2/cc-pVDZ) and with the fitting procedure of the dihedral parameters at the MM level

(PEPDROID). The constrains over the other dihedral angles are displayed in the relative energy panel.

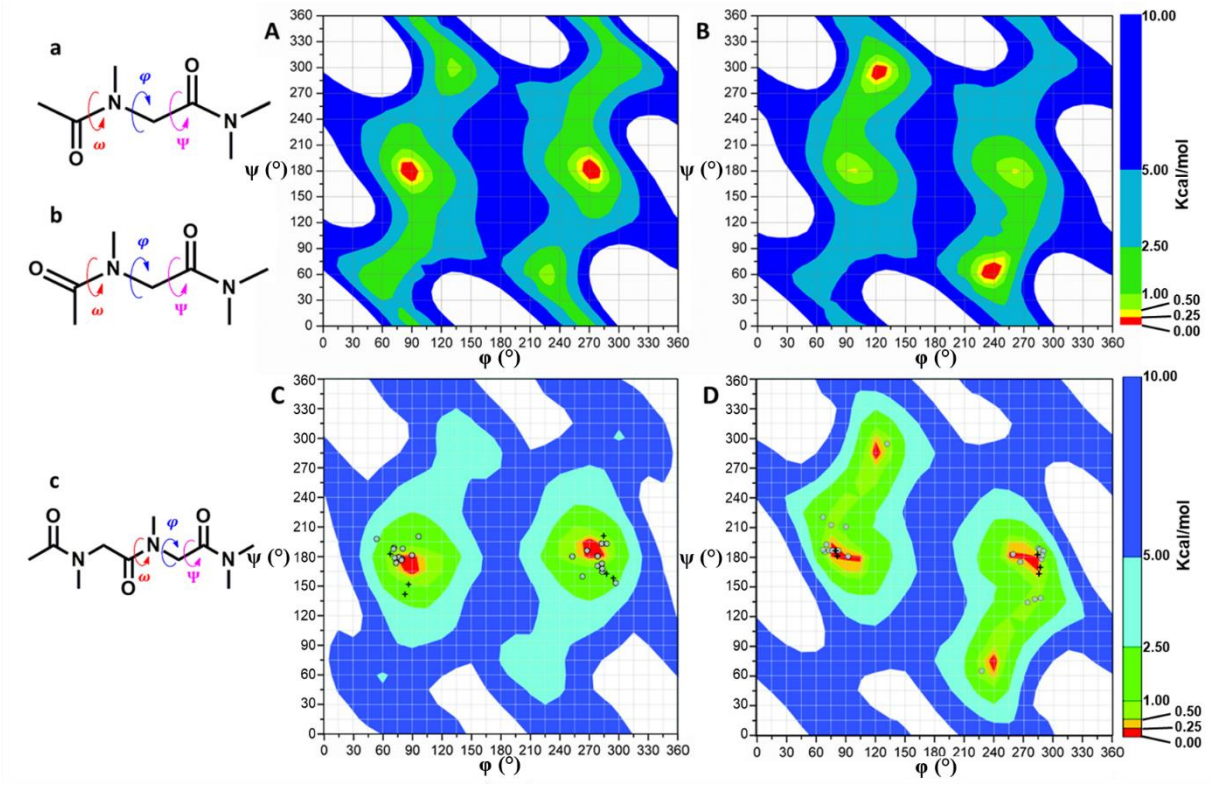

Figure 2. Ramachandran-like plots of α-peptoid backbone dihedrals (φ, Ψ) with methyl side chains for the (**A**) *cis* (ω = 0°, structure **a**) and (**B**) *trans* amide conformations (ω = 180°, structure **b**), as generated with PEPDROID. Ramachandran-like plots of structure **c** in (**C**) *cis* (ω = 0°) and (**D**) *trans* (ω = 180°) amide conformation (B3LYP/6-311+G(2d,p)//HF/6-31G*) adapted with permission from Butterfoss *et al.*[16] Copyright 2009 American Chemical Society. The energy range spans from 0 to 10 kcal/mol. The lowest energy structures (red) are set to 0 kcal/mol in each plot, while the highest energy structures (up to 10 kcal/mol) are displayed in blue. Structures with relative energies higher than 10 kcal/mol correspond to the white color.

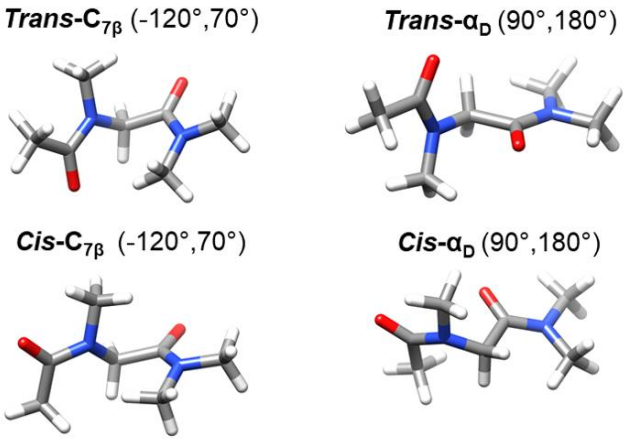

Conformation	MP2 Relative Energy (kcal/mol)
Trans-α_D	0.78
Trans-$C_{7\beta}$	0
Cis-α_D	0
Cis-$C_{7\beta}$	0.31

Figure 3. Structures and relative energies corresponding to the energy minima of an α-peptoid model bearing methyl side chains in *cis* or *trans* amide conformation, as obtained at the QM level (MP2/cc-pVDZ). Dihedral angle pairs (φ, ψ) are displayed on top of the structure.

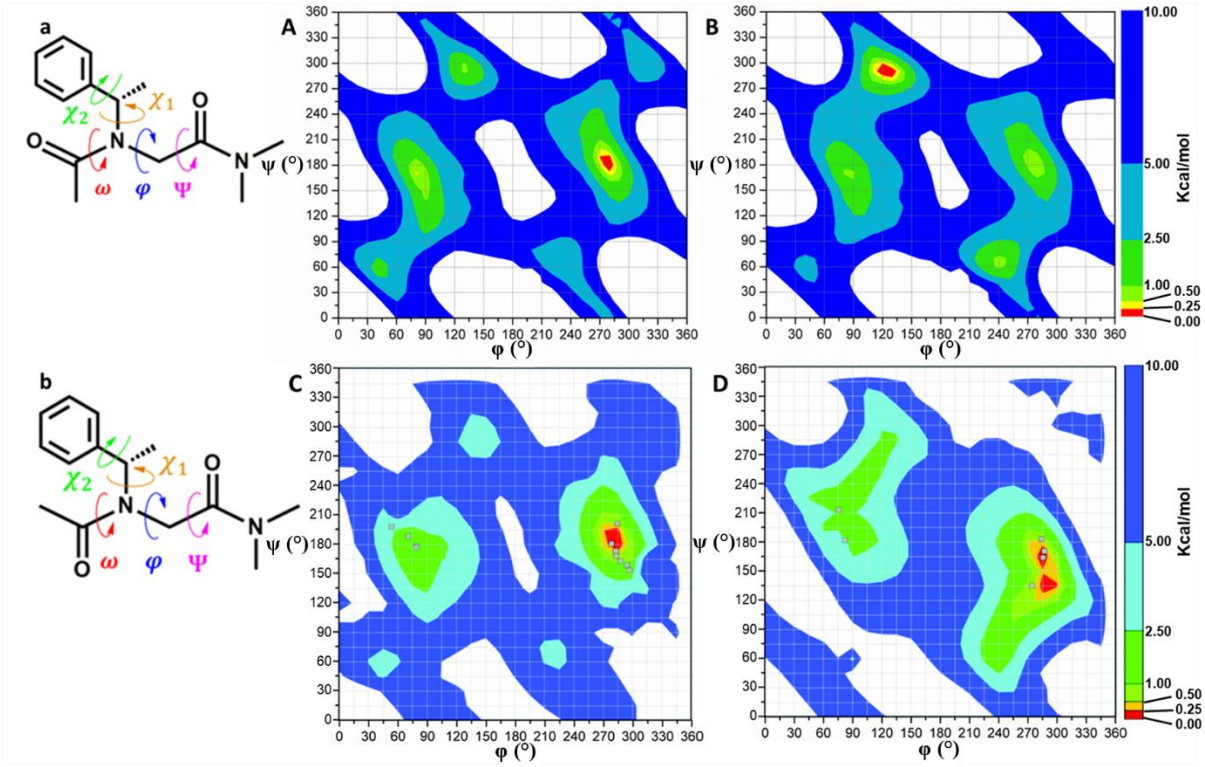

Figure 4. Ramachandran-like plots of α-peptoid backbone dihedrals (φ, ψ) with a *Nspe* side chain for the (**A**) *cis* (ω = 0°, structure **a**) and (**B**) *trans* amide (ω = 180°, structure **b**) conformations. Ramachandran-like plots of (**C**) *cis* (ω = 0°) and (**D**) *trans* (ω = 180°) amide conformation (structure **a** and **b,** respectively) (B3LYP/6-311+G(2d,p)//HF/6-31G*) are adapted with permission from Butterfoss *et al.*[16] Copyright 2009 American Chemical Society. The energy range spans from 0 to 10 kcal/mol. The lowest energy structures (red) are set to 0 kcal/mol in each plot, while the highest energy structures (up to 10 kcal/mol) are displayed in blue. Structures with relative energies higher than 10 kcal/mol correspond to the white color.

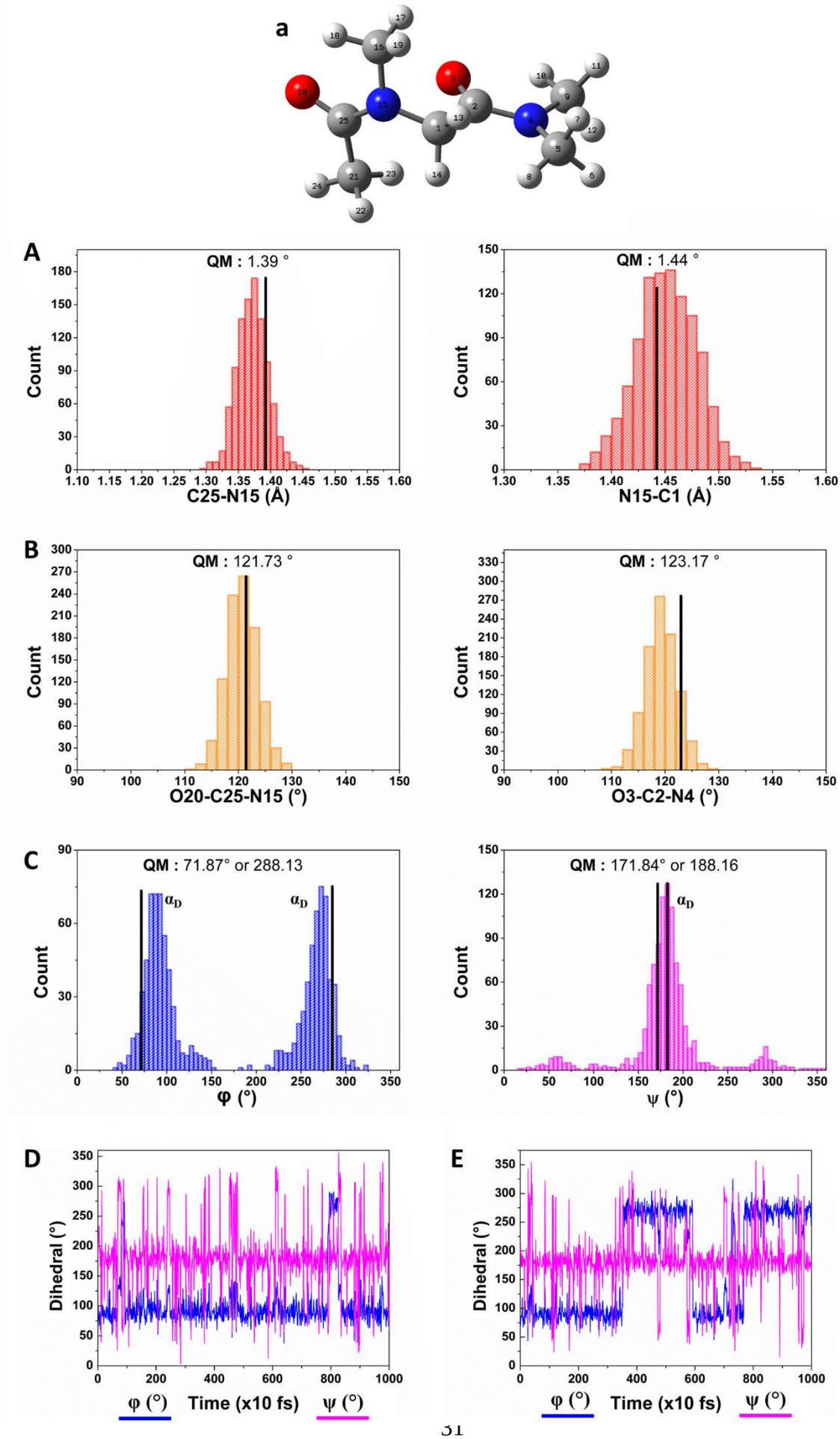
a
A
QM : 1.39 °
Count
C25-N15 (Å)
QM : 1.44 °
N15-C1 (Å)
B
QM : 121.73 °
O20-C25-N15 (°)
QM : 123.17 °
O3-C2-N4 (°)
C
QM : 71.87° or 288.13
αD
φ (°)
QM : 171.84° or 188.16
ψ (°)
D
Dihedral (°)
φ (°) Time (x10 fs) ψ (°)
E
Dihedral (°)
φ (°) Time (x10 fs) ψ (°)

Figure 5. Histograms representing the evolution of the structural parameters over a 10 ns-long analysis MD run for the model peptoid sketched in **Scheme 2 C** in the *cis*-α_D conformation as starting geometry. (**A**) Distributions of bond lengths around the QM reference value (MP2/cc-pVDZ); (**B**) Distributions of the bond angles around the QM reference value (MP2/cc-pVDZ); (C) Distributions of the dihedral angles (φ, ψ) around the QM reference value (MP2/cc-pVDZ) and their time evolution along (**D**) the equilibration MD run and (**E**) analysis MD run. Switching occurs along the first and second MD runs between the two isoenergetic forms of the *cis*-α_D conformations.

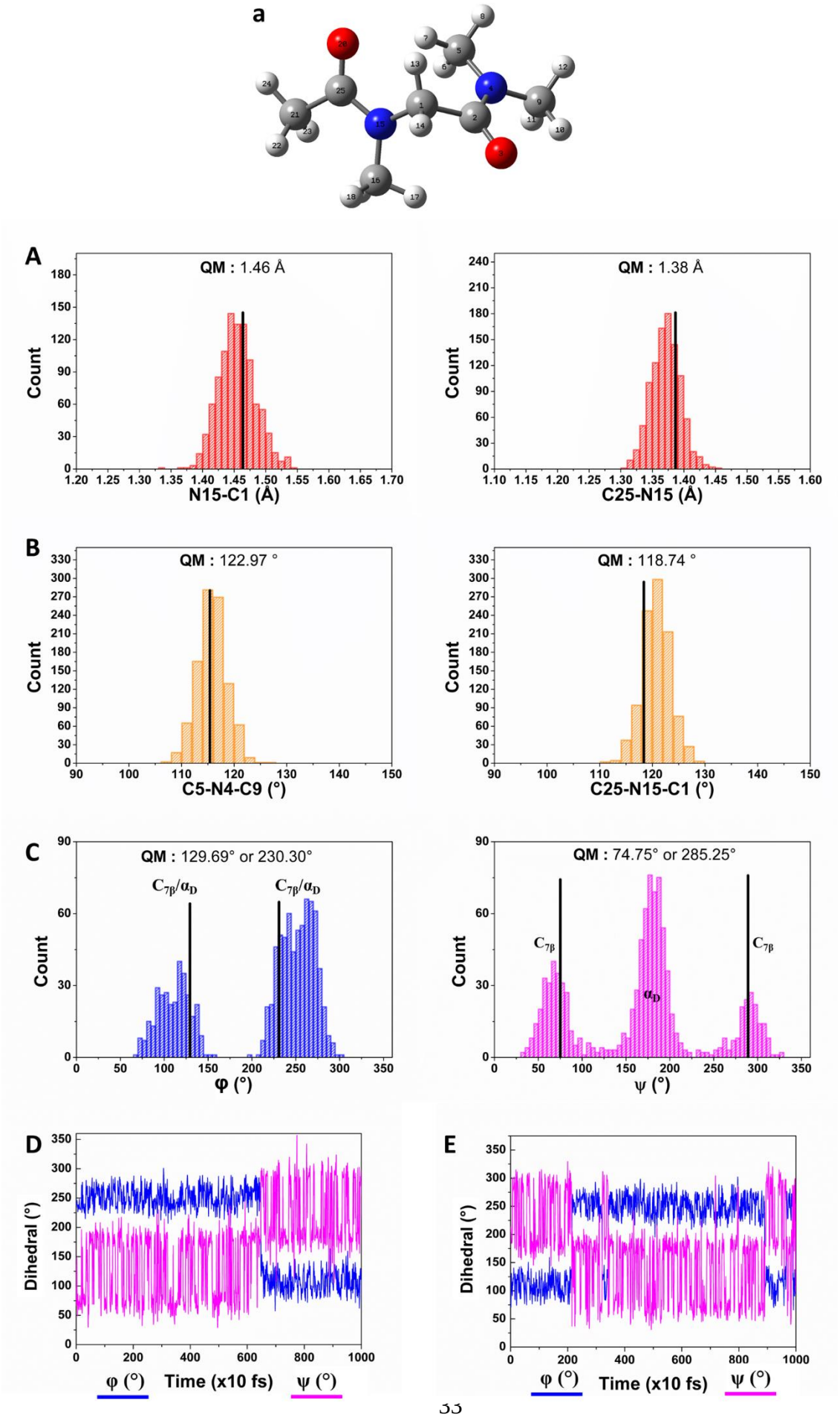
a
A
QM : 1.46 Å
Count
N15-C1 (Å)
QM : 1.38 Å
C25-N15 (Å)
B
QM : 122.97 °
C5-N4-C9 (°)
QM : 118.74 °
C25-N15-C1 (°)
C
QM : 129.69° or 230.30°
C7β/αD
φ (°)
QM : 74.75° or 285.25°
C7β
αD
ψ (°)
D
Dihedral (°)
φ (°) Time (x10 fs) ψ (°)
E
Dihedral (°)
φ (°) Time (x10 fs) ψ (°)

Figure 6. Histograms representing the evolution of the structural parameters over a 10 ns-long analysis MD for the model peptoid of **Scheme 2 C** in the *trans*-$C_{7\beta}$ conformation as starting geometry. (**A**) Distributions of the bond lengths around the QM reference value (MP2/cc-pVDZ); (**B**) Distributions of the bond angles around the QM reference value (MP2/cc-pVDZ); (**C**) Distributions of the dihedral angles (φ, ψ) around the QM reference value (MP2/cc-pVDZ) and their time evolution along (**D**) the equilibration MD and (**E**) analysis MD run. The starting geometry for the second MD is different from the first one due to switching between the *trans*-$C_{7\beta}$ and *trans*-α_D conformations.

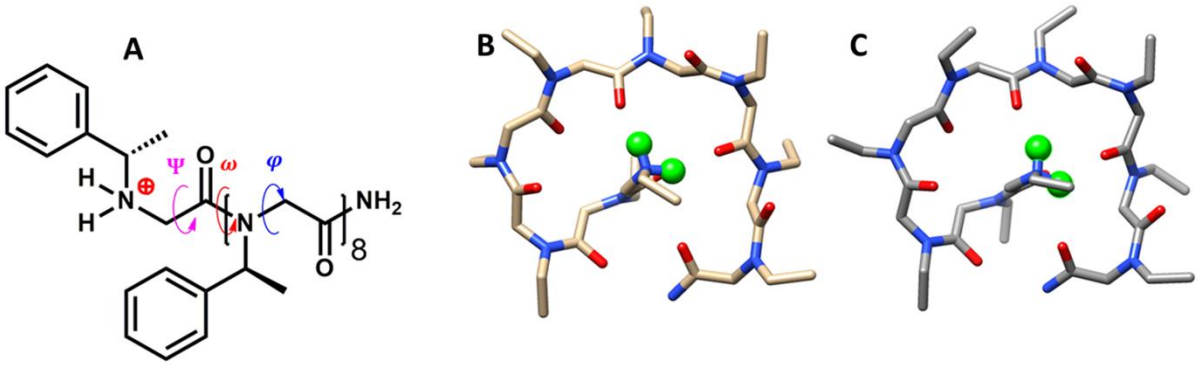

Residue	NMR Exp. [29]	φ PEPDROID (MM)	PEPDROID (average MD)	NMR Exp. [29]	Ψ PEPDROID (MM)	PEPDROID (average MD)	ω NMR Exp. [29]	PEPDROID
1				-175.34 ± 4.35	176	177.22 ± 10.66	*cis*	*cis*
2	-68.40 ± 3.73	-69	-68.49 ± 8.62	154.92 ± 4.37	150	156.04 ± 8.08	*cis*	*cis*
3	-69.92 ± 3.15	-76	-72.32 ± 7.90	159.83 ± 4.31	156	160.34 ± 6.69	*trans*	*trans*
4	76.08 ± 4.78	80	79.13 ± 7.44	-177.68 ± 6.29	170	174.08 ± 7.00	*trans*	*trans*
5	-72.85 ± 4.72	-84	-82.90 ± 7.37	172.54 ± 6.04	-164	-166.92 ± 8.88	*trans*	*trans*
6	-76.68 ± 6.30	-83	-79.89 ± 8.60	-177.96 ± 4.38	-171	-169.48 ± 8.37	*cis*	*cis*
7	-78.04 ± 3.57	-71	-71.71 ± 8.14	-158.13 ± 6.59	177	-178.04 ± 7.57	*trans*	*trans*
8	-70.73 ± 4.35	-71	-74.74 ± 8.62	170.14 ± 5.08	176	-176.74 ± 7.87	*cis*	*cis*
9	-77.46 ± 4.63	-73	-75.91 ± 9.24					

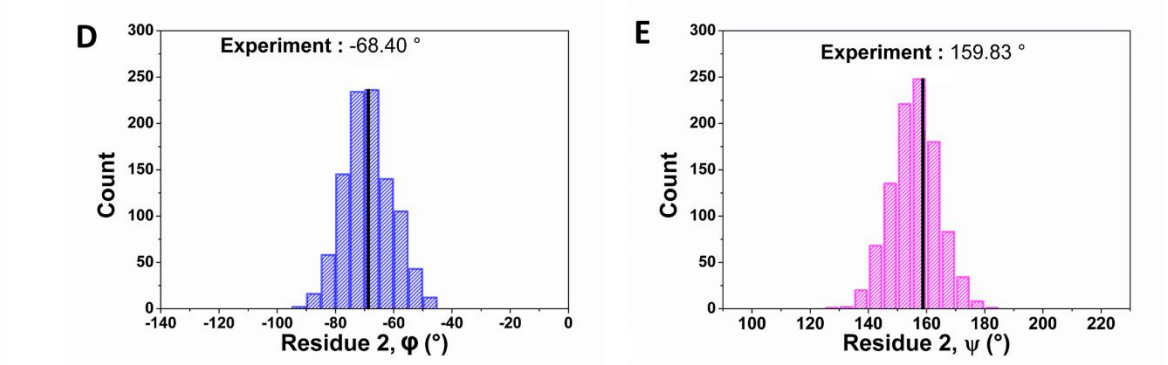

Figure 7. (**A**) Primary structure of the α-*Nspe*$_9$ threaded loop whose terminal amine is protonated and comparison with the backbone dihedrals obtained with PEPDROID and those obtained in the literature, as adapted with permission from Huang *et al.*[24] Copyright 2006 American Chemical Society; (**B**) Threaded loop backbone structure reported in Ref. 29 and (**C**) obtained with PEPDROID. Protons on the terminal amine have been highlighted in green while other hydrogens and the phenyl rings have been omitted for clarity. (**D**) and (**E**) are histograms representing the distribution, binned at every 5°, of the dihedral angle couple (φ,ψ) for the residue 6 along a 10 ns MD run at 298 K. The experimental NMR value is represented as a black line with arbitrary units.[29]

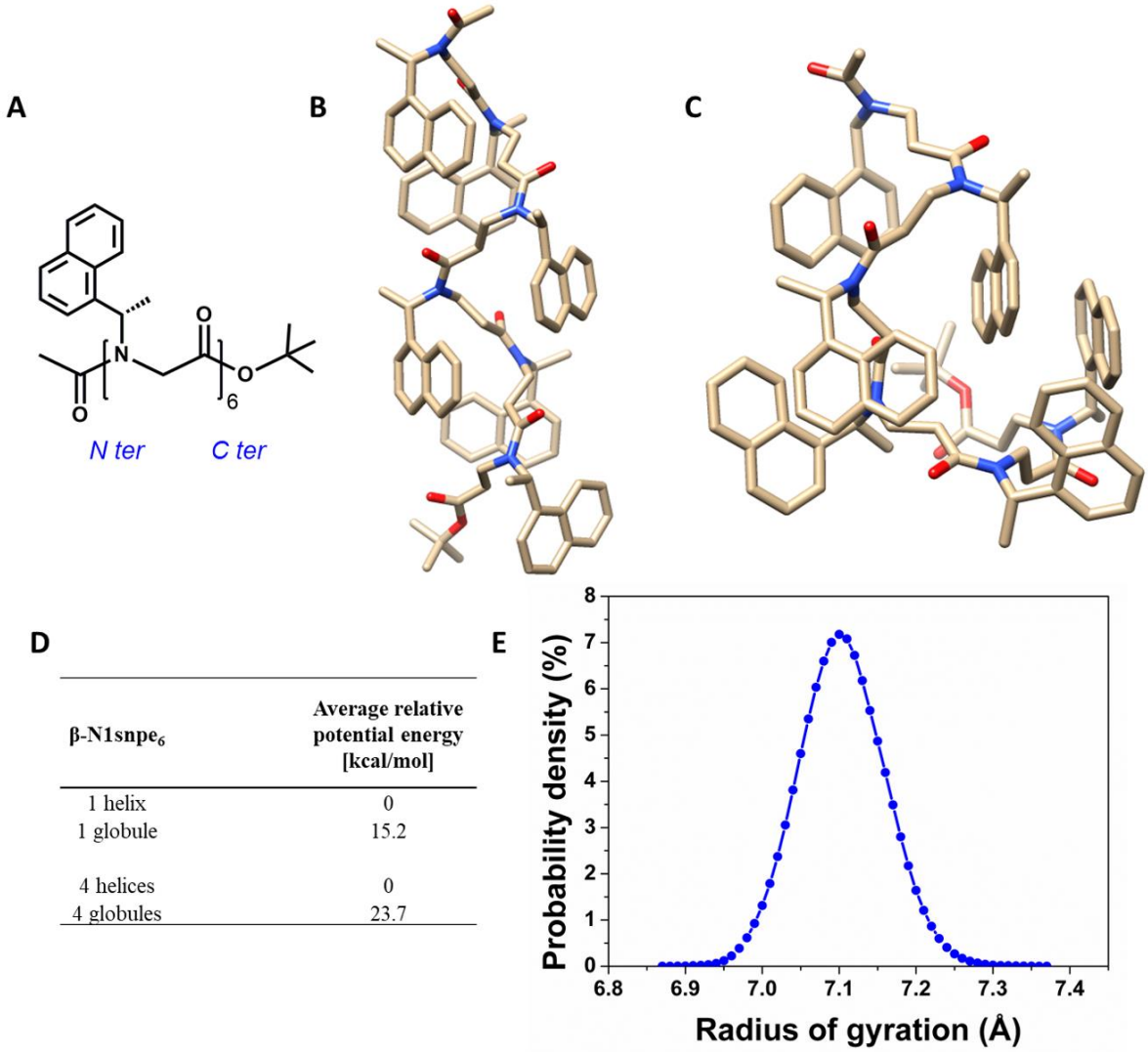

β-N1snpe$_6$	Average relative potential energy [kcal/mol]
1 helix	0
1 globule	15.2
4 helices	0
4 globules	23.7

Figure 8. (**A**) Primary structure of β-*N1snpe*$_6$ with the corresponding helical (**B**) and globular (**C**) conformations. *N ter* and *C ter* refer to N terminal and C terminal extremity, respectively. (**D**) Average relative energies along a 10 ns-long MD run for a single molecule (helix or globule) or four molecules (four helices or four globules) in the unit cell. (**E**) Probability density (%) of the radius of gyration along the 10 ns-long MD run for the single helical β-peptoid.

The table of contents entry should be 50–60 words long, and the first phrase should be bold. The entry should be written in the present tense and impersonal style. The text should be different from the abstract text.

Keyword

C. Author 2, D. E. F. Author 3, A. B. Corresponding Author* ((same order as byline))

PEPDROID: Development of a Generic DREIDING-based Force Field for the Assessment of Peptoid Secondary Structures

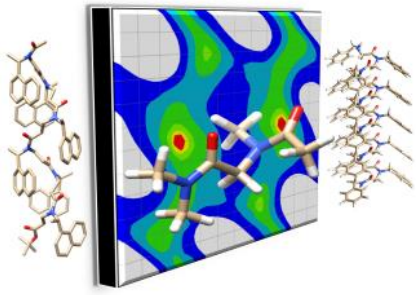

Supporting Information

PEPDROID: Development of a Generic DREIDING- based Force Field for the Assessment of Peptoid Secondary Structures

*Sébastien Hoyas, Vincent Lemaur, Quentin Duez, Fabrice Saintmont, Emilie Halin, Julien De Winter, Pascal Gerbaux, Jérôme Cornil**

Table S1. Comparison of the bond lengths and bond angles for an α-peptoid monomer (bearing two (*S*)-1-phenylethyl side chains) calculated at the MP2/cc-pVDZ and MM levels and the associated RMSD.

Bond	MP2 (Å)	DREIDING (Å)
C25-N4	1.474	1.431
N4-H42	1.013	0.973
N4-C2	1.338	1.347
C2-O3	1.235	1.249
C2-C1	1.539	1.476
C1-N7	1.491	1.485
C25-H26	1.097	1.093
C25-C27	1.532	1.540
C27-H30	1.091	1.091
C25-C31	1.523	1.486
C31-C32	1.398	1.413
C32-H35	1.087	1.021
C1-H6	1.093	1.091
RMSD	**2.593%**	

Angle	MP2 (°)	DREIDING (°)
H42-N4-C25	118.362	117.229
H42-N4-C2	114.680	116.473
N4-C2-O3	124.755	116.759
O3-C2-C1	117.609	118.435
C2-C1-N7	104.266	112.611
C2-C1-H6	110.212	107.035
C25-N4-C2	126.546	126.290
N4-C25-H26	108.030	109.052
N4-C25-C27	108.083	108.597
C25-C27-C29	111.043	109.656
N4-C25-C31	112.355	111.742
H26-C25-C31	108.703	109.770
C27-C25-C31	111.512	110.437
C25-C31-C32	119.495	119.579
C31-C32-H35	119.734	120.330
C31-C32-C34	120.500	120.683
H6-C1-N7	109.621	108.278
RMSD	**2.700%**	

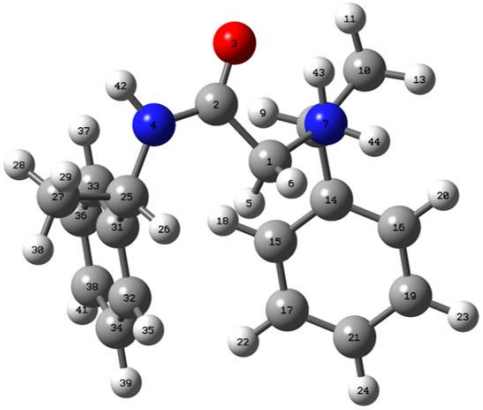

Table S2. Comparison of the bond lengths and bond angles for a β-peptoid monomer (bearing two methyl side chains) calculated at the MP2/cc-pVDZ and MM levels and their associated RMSD.

Bond	MP2 (Å)	DREIDING (Å)
C21-H24	1.098	1.091
C21-C25	1.520	1.473
C25-O20	1.231	1.254
C25-N15	1.386	1.370
N15-C16	1.455	1.441
N15-C1	1.453	1.446
C1-H14	1.096	1.090
C1-C26	1.535	1.551
C26-C2	1.528	1.484
RMSD	**1.681%**	

Angle	MP2 (°)	DREIDING (°)
H24-C21-H22	109.131	108.941
H24-C21-C25	107.067	110.709
C21-C25-O20	121.684	114.789
C25-N15-C16	117.816	119.941
C25-N15-C1	125.250	123.041
N15-C1-H13	109.775	107.914
N15-C1-C26	111.882	114.232
C9-N4-C5	114.478	114.968
RMSD	**2.862%**	

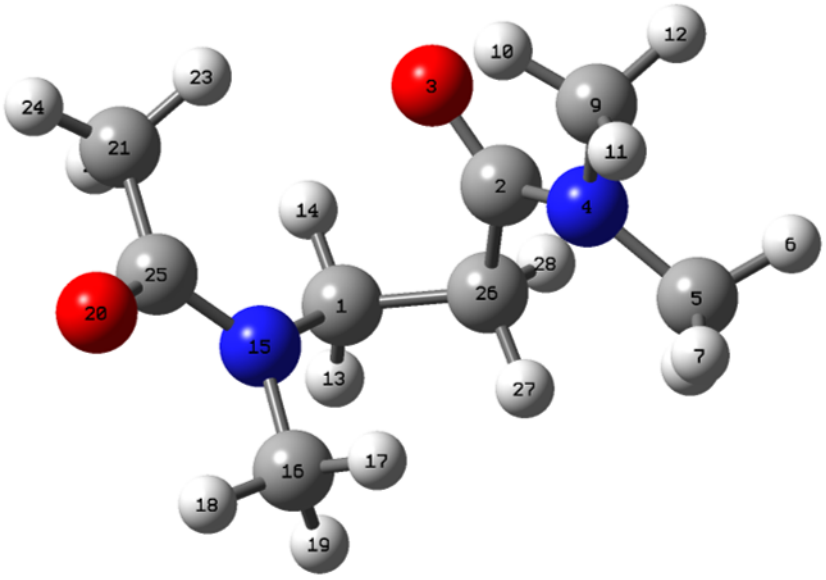

Table S3. Structures and relative energies corresponding to the energy minima of an α-peptoid model bearing (*S*)-1-phenylethyl (*Nspe*) side chain in *trans* amide conformation, as obtained at the QM (MP2/cc-pVDZ) and MM (PEPDROID) levels.

	MP2 Relative Energy (kcal/mol)	PEPDROID Relative Energy (kcal/mol)
Nspe trans-$C_{7\beta}$	0	0
Nspe trans-α_D	0.41	0.61

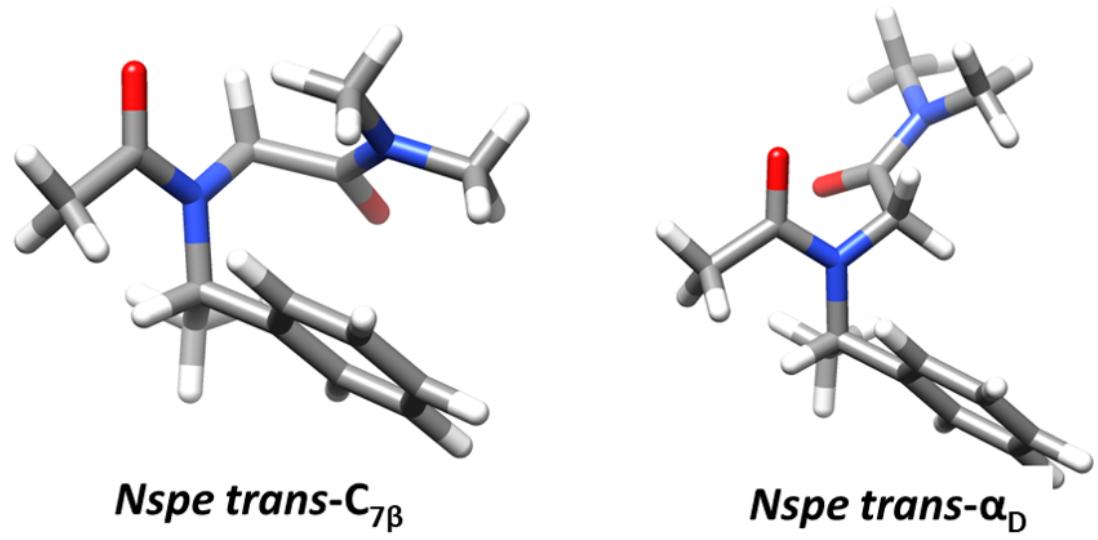

Table S4. RMSD values obtained between QM and MM torsional scans for the optimized dihedral parameters (B_n barrier height, d_n phase factor and n periodicity).

Dihedral angle	RMSD (%)
α-peptoid backbone ω	1.82
α-peptoid backbone φ	0.97
α-peptoid backbone ψ	1.14
Side chain *Nspe* χ1	1.38
Side chain *Nspe* χ2	1.86
Side chain *Npm* χ1	1.06
Side chain *Npm* χ2	1.95
Side chain *Nnpr* χ1	0.93
Side chain *Nnpr* χ2	2.45
β-peptoid backbone φ'	3.95
β-peptoid backbone ψ'	0.45
β-peptoid backbone θ	0.20

Table S5. Relative energies obtained at the MP2/cc-pVDZ level for the different local minima of the peptoid model bearing methyl side chains in *cis* or *trans* conformation (**Scheme 2**). The geometries were fully relaxed during the optimization.

	Dihedrals (φ,ψ)	Relative MP2 energy (kcal/mol)
cis-α_D	(71.87°, 171.84°)	0.00
cis-α_D	(-71.87°, -171.88°)	0.00
cis-$C_{7\beta}$	(156.30°, -59.54°)	1.66
cis-$C_{7\beta}$	(-156.31°, 59.52°)	1.66
cis-α	(61.33°, 49.55°)	1.75
trans-$C_{7\beta}$	(129.69°, -74.73°)	0.00
trans-$C_{7\beta}$	(-129.70°, 74.75°)	0.00
trans-α_D	(74.44°, -176.92°)	0.50
trans-α_D	(-74.40°, 176.88°)	0.50

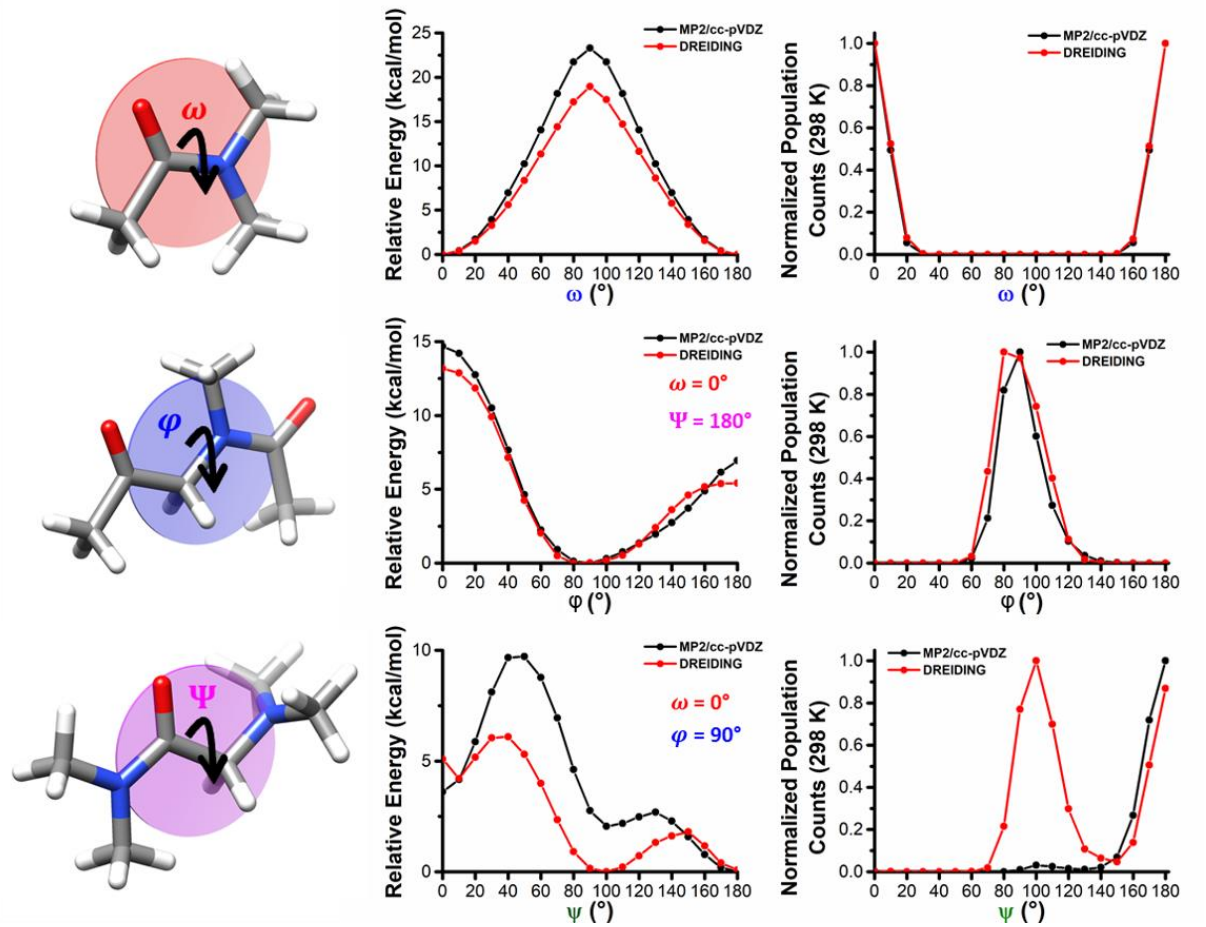

Figure S1. Torsion energy (left) and relative population (right) profiles for α-peptoid backbone dihedrals at the QM level (MP2/cc-pVDZ) and MM level (DREIDING default parameters). The restrains over the other dihedrals are displayed in the central panel.

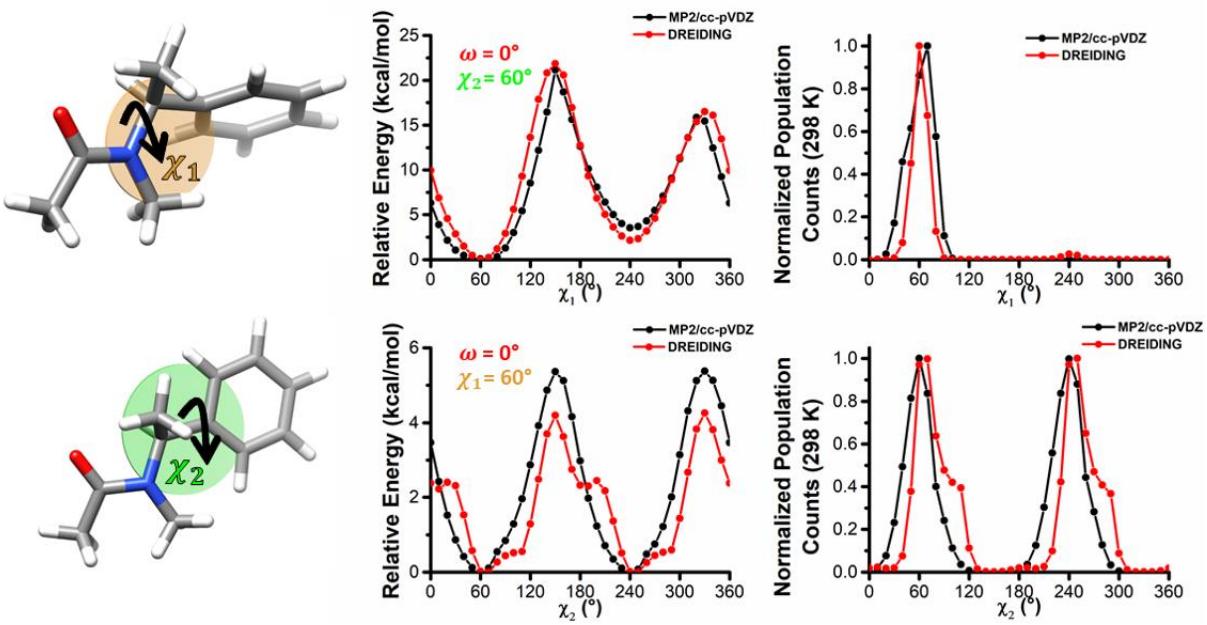

Figure S2. Torsion energy (left) and relative population (right) profiles for the backbone dihedrals of *Nspe* side chain at the QM level (MP2/cc-pVDZ) and MM level (DREIDING default parameters). Restrains over other dihedrals are displayed in the central panel.

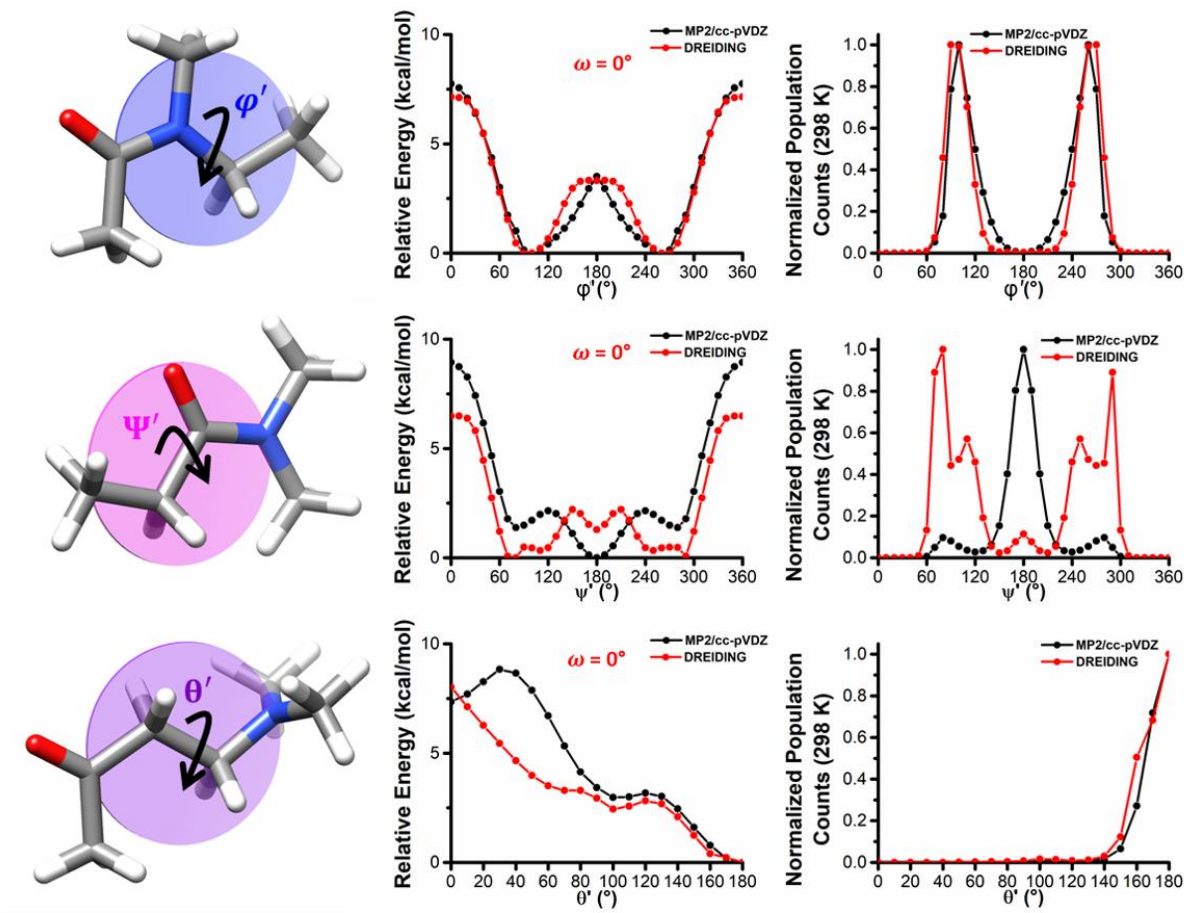

Figure S3 a. Torsion energy (left) and relative population (right) profiles for the backbone dihedrals of the β-peptoid backbone at the QM level (MP2/cc-pVDZ) and MM level (DREIDING default parameters). Restrains over the other dihedrals are displayed in the central panel. Note that the torsional profile associated to the amide bond dihedral angle (ω) is not displayed since it was previously reparametrized for the α-peptoid backbone and is kept for β-peptoids.

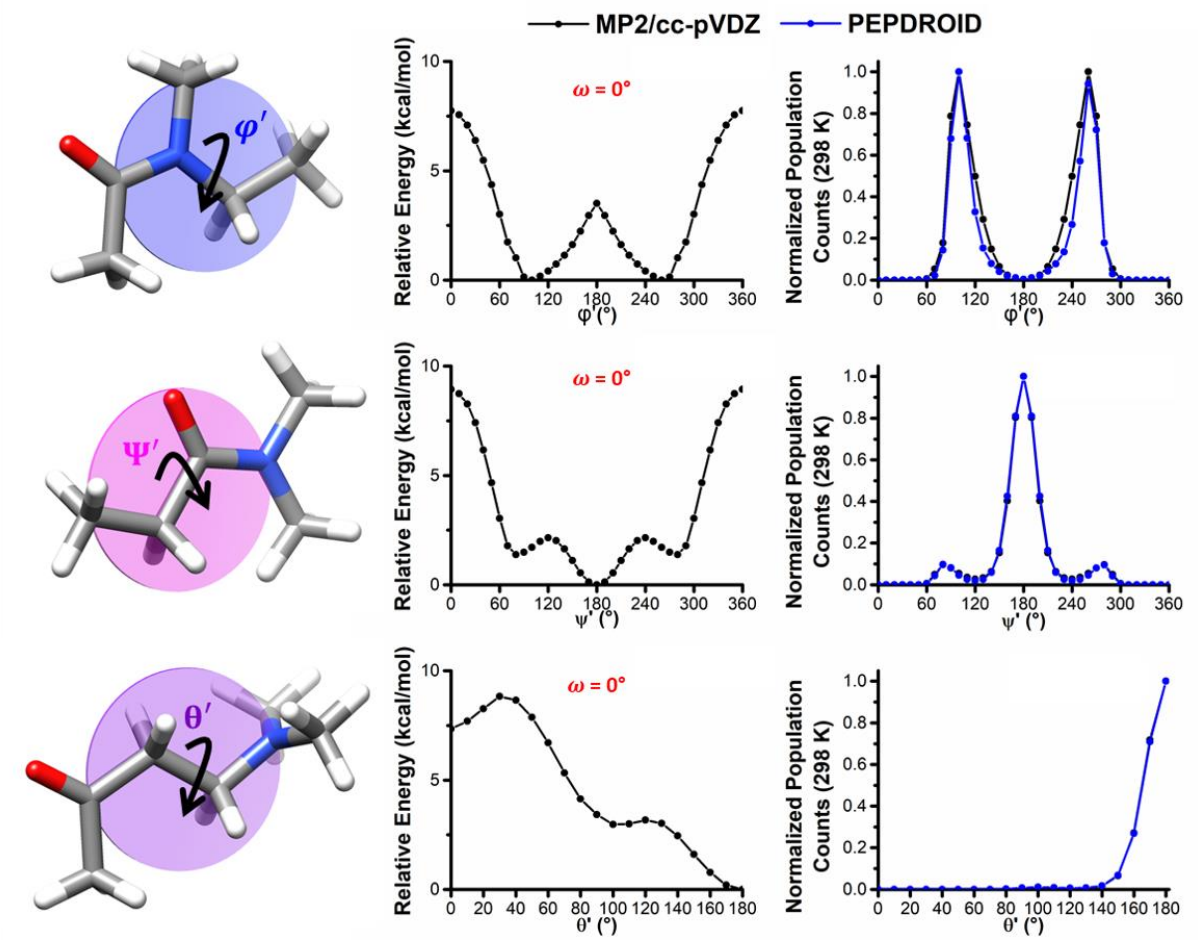

Figure S3 b. Torsion energy (center) and relative population (right) profiles for β-peptoid backbone dihedrals as calculated at the QM level (MP2/cc-pVDZ) (center) and with the fitting procedure of the dihedral parameters at the MM level (PEPDROID). Note that the torsional potential associated to the amide bond dihedral angle (ω) is not displayed since it was previously reparametrized for the α-peptoid backbone and is kept for β-peptoids.

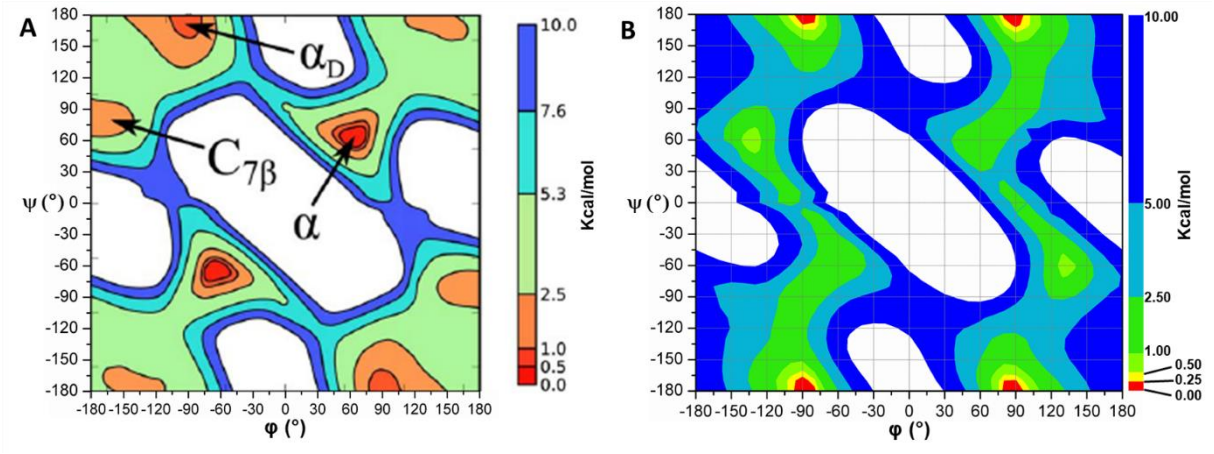

Figure S4. Comparison of the Ramachandran-like plots associated to the dihedrals (φ, Ψ) of the α-peptoid backbone bearing methyl side chains in vacuum and with the amide bond in the *cis* conformation (ω = 0°), as generated with (**A**) the MF-TOID force field and (**B**) with PEPDROID.[18] For plot (**A**), the α conformation is the global minimum, while it is the $C_{7\beta}$ for plot (**B**). The energy range spans from 0 to 10 kcal/mol. The lowest energy structures (red) are set to 0 kcal/mol in each plot, while the highest energy structures (up to 10 kcal/mol) are displayed in blue. Structures with relative energies higher than 10 kcal/mol correspond to the white color. Plot (**A**) was adapted by permission of John Wiley and Sons via the Rightslink service of CCC. Development and use of an atomistic CHARMM-based forcefield for peptoid simulation 35 by Dina T. Mirijanian.[18]

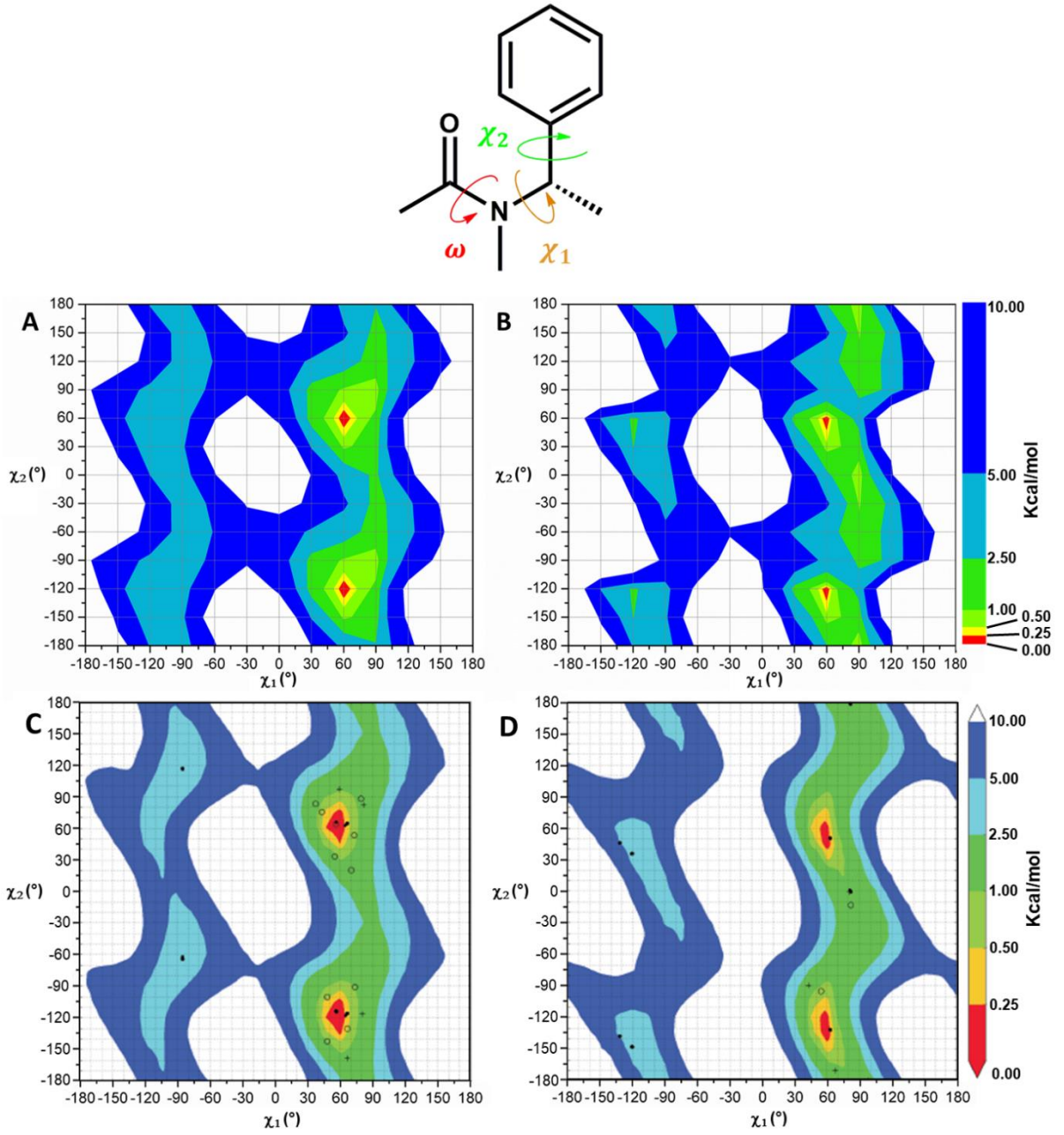

Figure S5. Ramachandran-like plots of side chain dihedrals (χ_1, χ_2) for *Nspe* in the (**A**) *cis* and (**B**) *trans* amide conformation obtained with PEPDROID. Ramachandran-like plots in *cis* (**C**) (ω = 0°) and (**D**) *trans* (ω = 180°) amide conformation (B3LYP/6-311+G(d,p)) adapted with permission from Renfrew *et al.*[45] Copyright 2014 American Chemical Society. Note that the scale of the plots is different (0° to 360° versus -180° to 180°). The energy range spans from 0 to 10 kcal/mol. The lowest energy structures (red) are set to 0 kcal/mol for each plot, while the

highest energy structures (up to 10 kcal/mol) are displayed in blue. Structures with relative energies higher than 10 kcal/mol correspond to the white color.

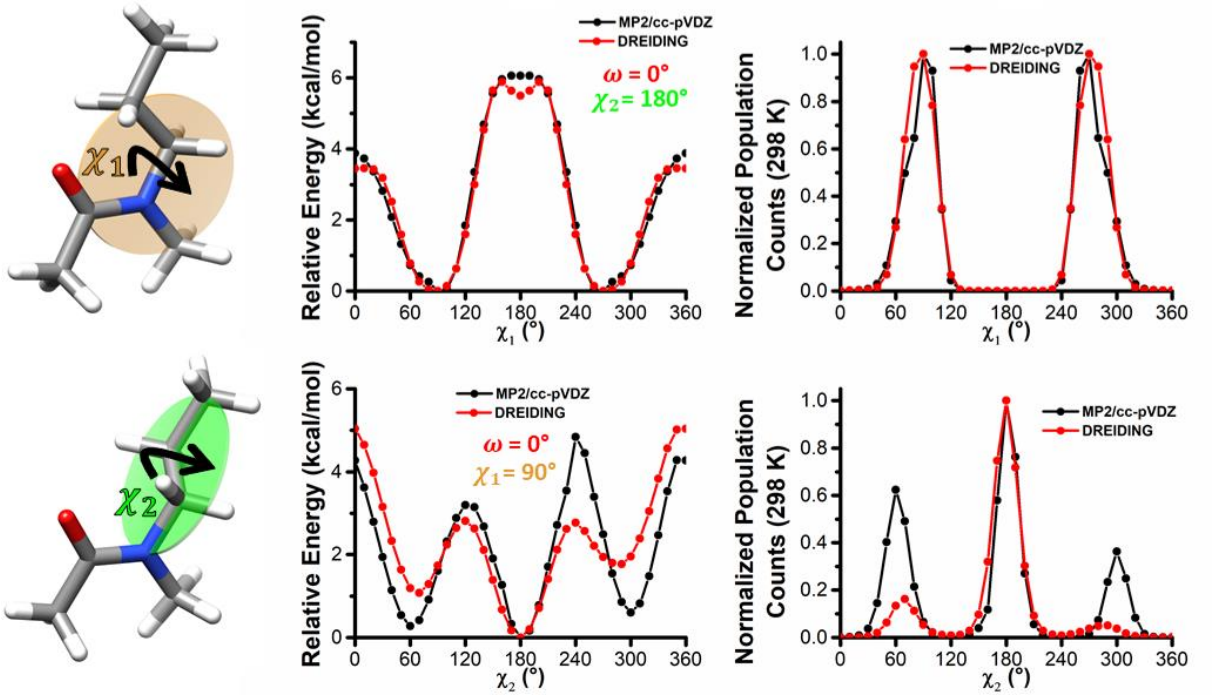

Figure S6 a. Torsion energy (left) and relative population (right) profiles for *Nnpr* side chain dihedrals (χ_1 & χ_2) of at the QM level (MP2/cc-pVDZ) and MM level (DREIDING default parameters). Restrains over the other dihedrals are displayed in the central panel.

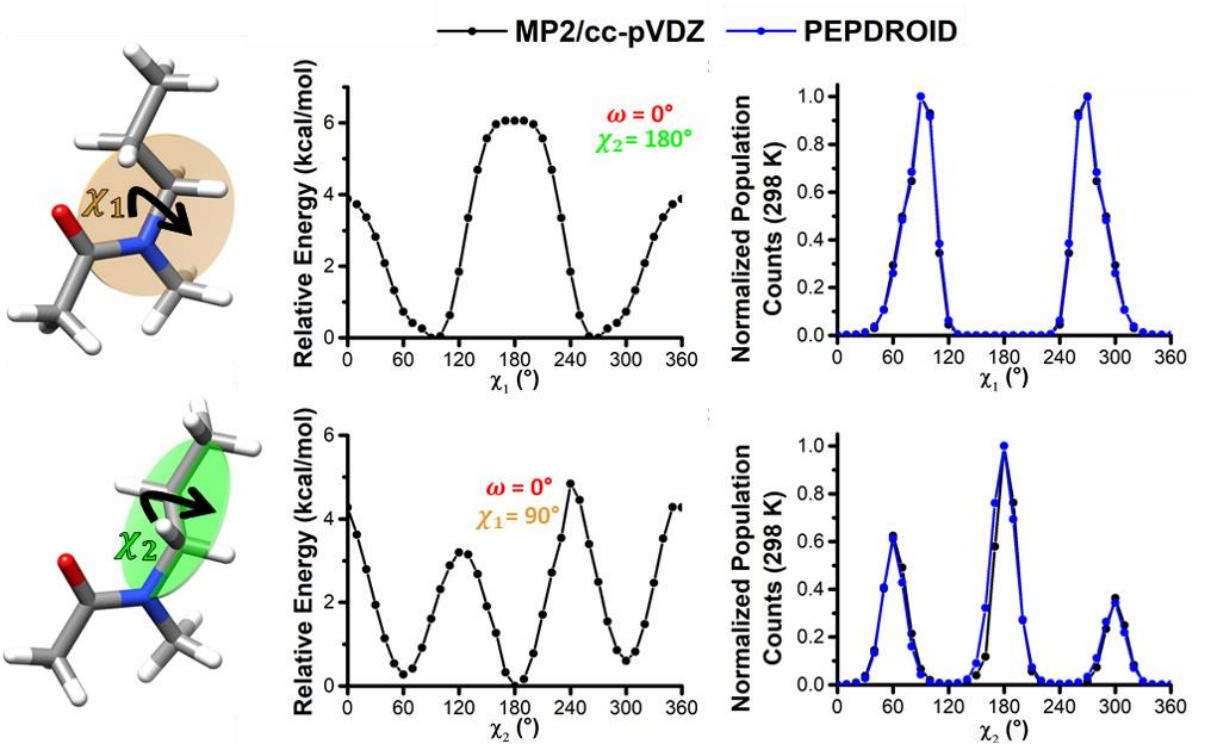

Figure S6 b. Torsion energy (center) and relative population (right) profiles for *Nnpr* side chain dihedrals (χ_1 & χ_2) as calculated at the QM level (MP2/cc-pVDZ) (center) and after the fitting procedure of the dihedral parameters at the MM level (PEPDROID). Restrains over the other dihedrals are displayed in the central panel.

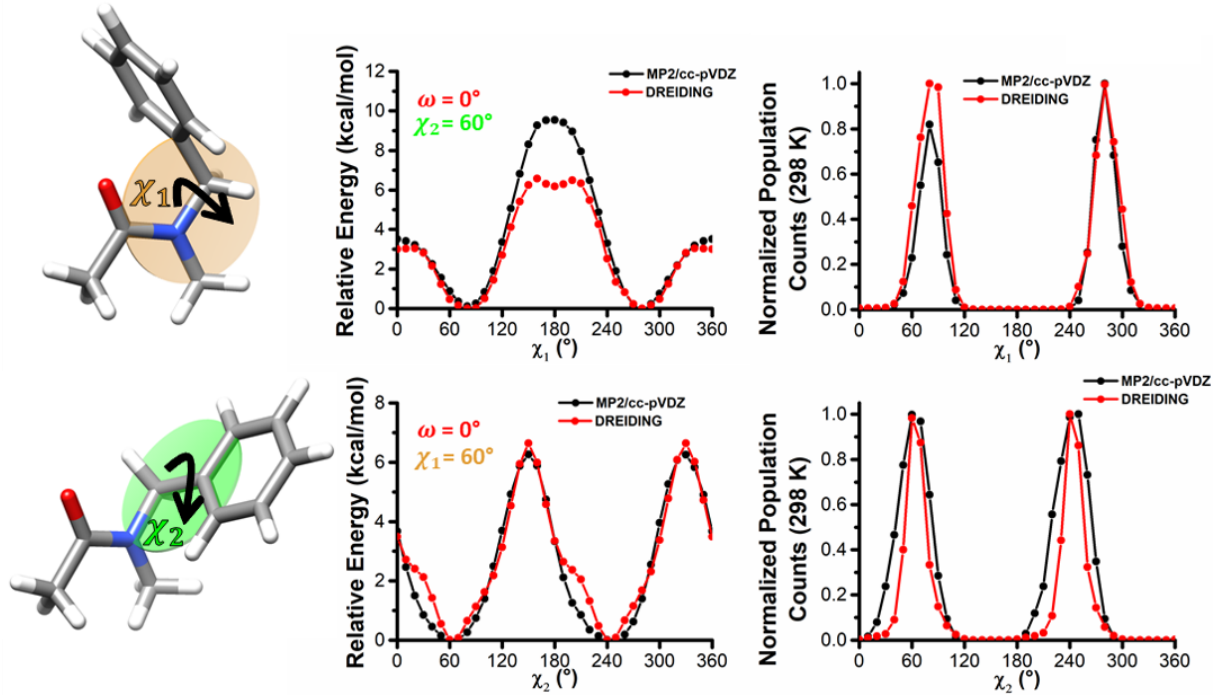

Figure S6 c. Torsion energy (left) and relative population (right) profiles for *Npm* side chain dihedrals (χ_1 & χ_2) of at the QM level (MP2/cc-pVDZ) and MM level (DREIDING default parameters). Restrains over other the dihedrals are displayed in the central panel.

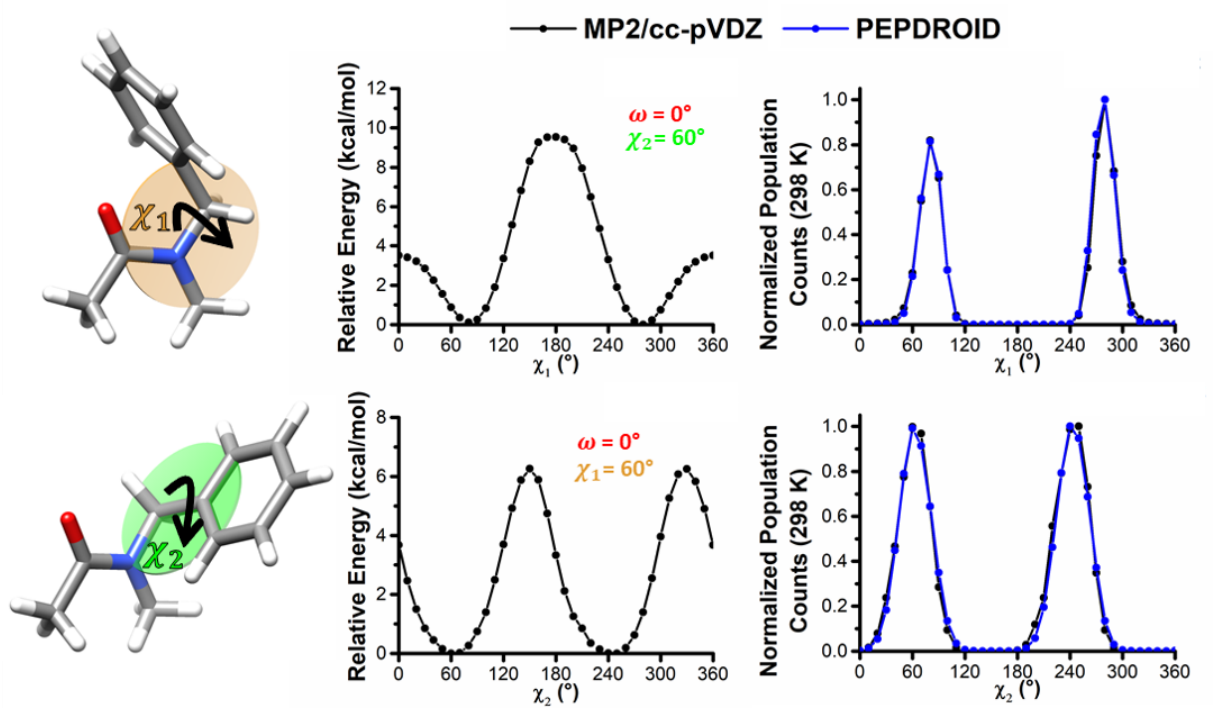

Figure S6 d. Torsion energy (center) and relative population (right) profiles for *Npm* side chain dihedrals (χ_1 & χ_2) as calculated at the QM level (MP2/cc-pVDZ) (center) and after the fitting procedure of the dihedral parameters at the MM level (PEPDROID). Restrains over other the dihedrals are displayed in the central panel.

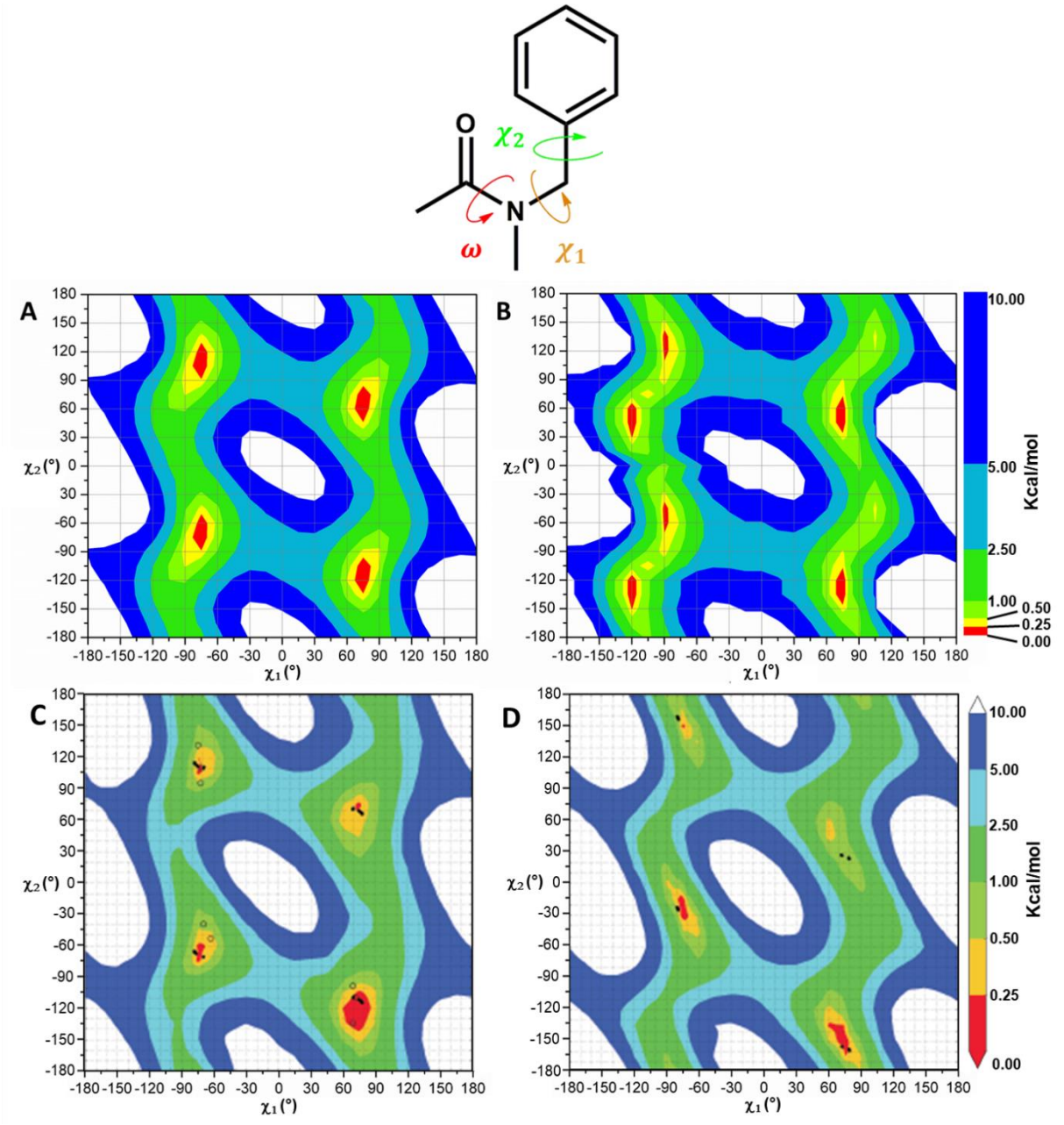

Figure S7. Ramachandran-like plots of side chain dihedrals (χ_1, χ_2) for *Npm* with the (**A**) *cis* (ω = 0°) and (**B**) *trans* (ω = 180°) amide conformation obtained with PEPDROID. The structure on the top corresponds to the *cis* amide bond. Ramachandran-like plots of (**C**) *cis* (ω = 0°) and (**D**) *trans* (ω = 180°) amide conformation (B3LYP/6-311+G(d,p)) adapted with permission from Renfrew *et al.*[45] Copyright 2014 American Chemical Society. The energy range spans

from 0 to 10 kcal/mol. The lowest energy structures (red) are set to 0 kcal/mol for each plot, while the highest energy structures (up to 10 kcal/mol) are displayed in blue. Structures with relative energies higher than 10 kcal/mol correspond to the white color.

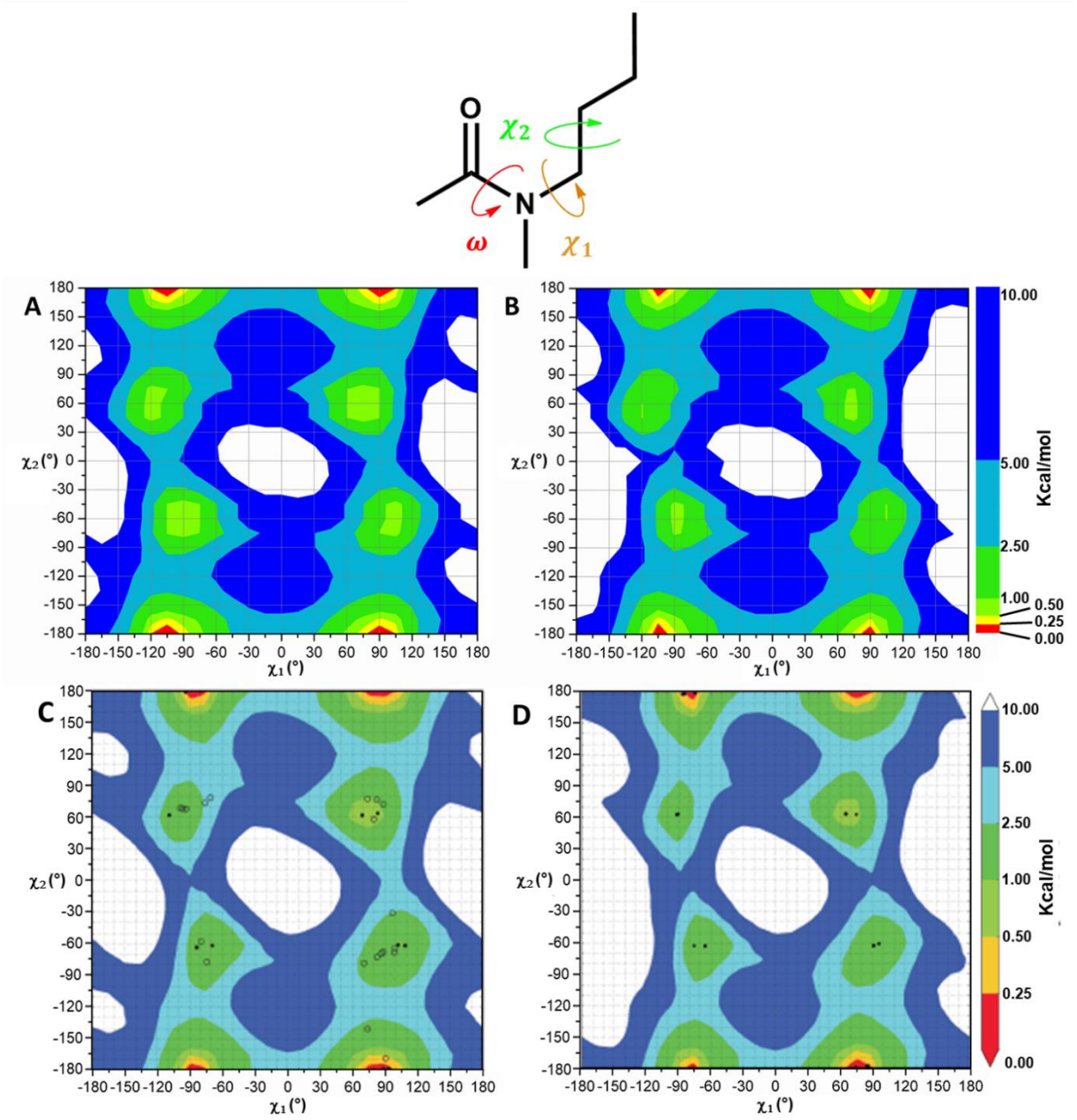

Figure S8. Ramachandran-like plots of side chain dihedrals (χ_1, χ_2) for *Nnpr* with the (**A**) *cis* (ω = 0°) and (**B**) *trans* (ω = 180°) amide conformation obtained with PEPDROID. The structure on the top corresponds to the *cis* amide bond. Ramachandran-like plots of (**C**) *cis* (ω = 0°) and (**D**) *trans* (ω = 180°) amide conformation (B3LYP/6-311+G(d,p)) adapted with permission

from Renfrew *et al.*[45] Copyright 2014 American Chemical Society. The energy range spans from 0 to 10 kcal/mol. The lowest energy structures (red) are set to 0 kcal/mol for each plot, while the highest energy structures (up to 10 kcal/mol) are displayed in blue. Structures with relative energies higher than 10 kcal/mol correspond to the white color.

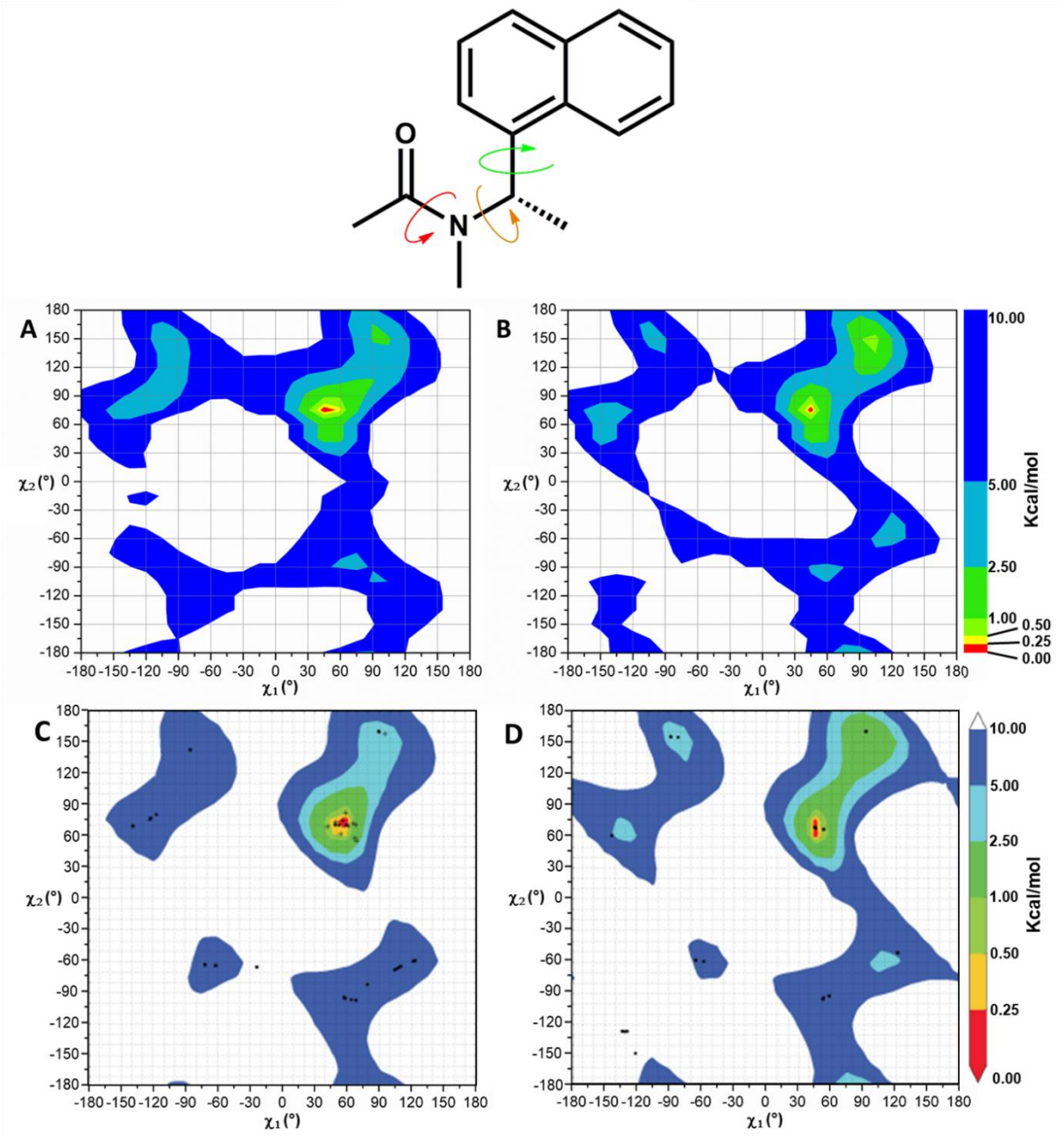

Figure S9. Ramachandran-like plots of side chain dihedrals (χ_1, χ_2) for *N1snpe* in the (**A**) *cis* (ω = 0°) and (**B**) *trans* (ω = 180°) amide conformation obtained with PEPDROID. The structure on the top corresponds to the *cis* amide bond. Ramachandran-like plots of (**C**) *cis* (ω = 0°) and (**D**) *trans* (ω = 180°) amide conformation (B3LYP/6-311+G(d,p)) adapted with permission from Renfrew *et al.*[45] Copyright 2014 American Chemical Society. The energy range spans from 0 to 10 kcal/mol. The lowest energy structures (red) are set to 0 kcal/mol for each plot, while the highest energy structures (up to 10 kcal/mol) are displayed in blue.

Structures with relative energies higher than 10 kcal/mol correspond to the white color.

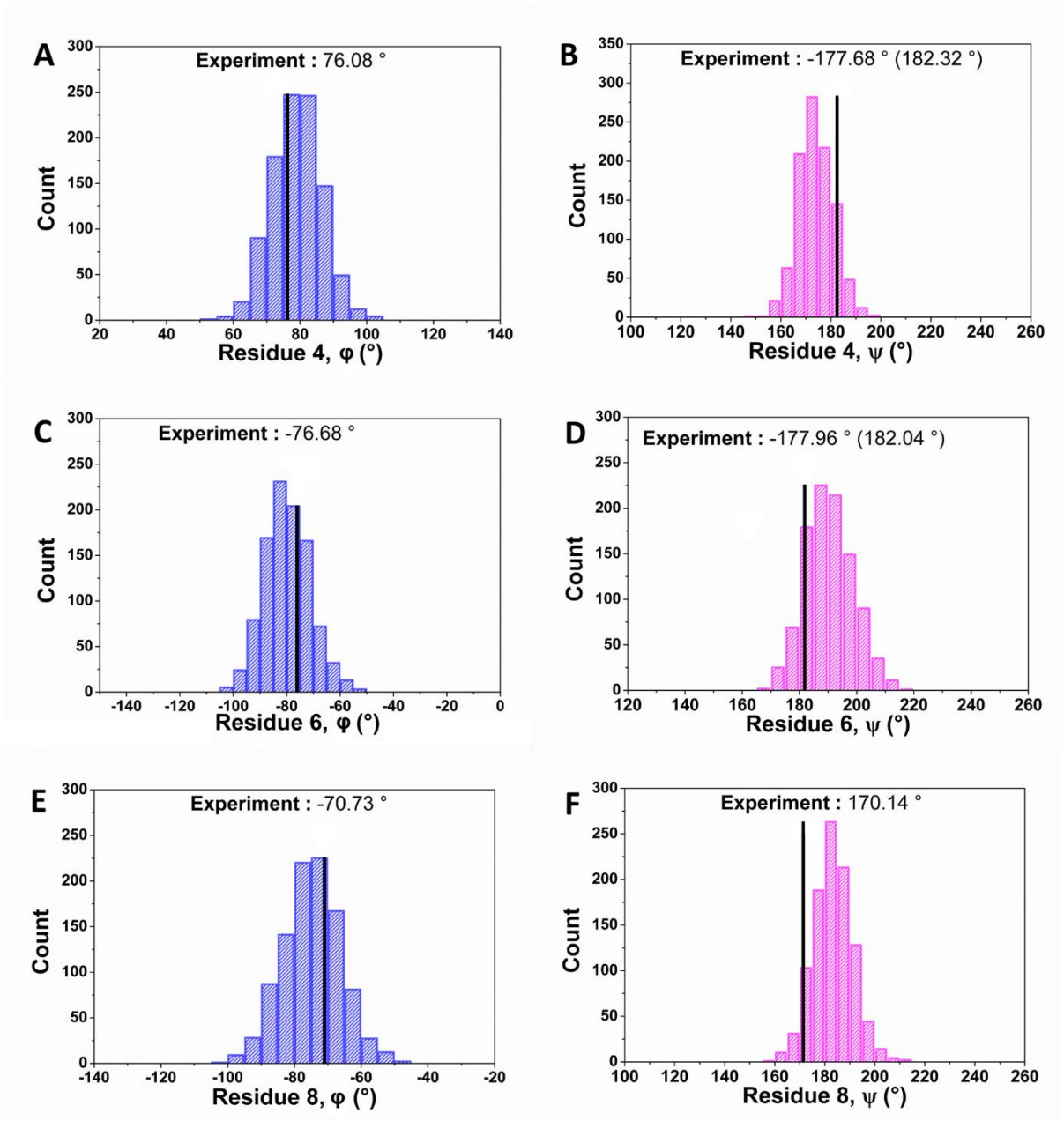

Figure S10. Histograms of dihedral couples for residues 4, 6 and 8 of α-*Nspe*$_9$. The experimental values from NMR are displayed with arbitrary intensity as black lines.[29]

van der Waals reparameterization

1. **Equilibrium distance**

We should recall that vdW parameters (R_0, D_0) are defined for homonuclear pairs in DREIDING. For hydrogen, equilibrium distance and well depth are defined for the H – H bonds, while parameters for interactions with other atoms is defined by an arithmetic/geometric mean of the homonuclear parameters. The methodology to optimize the equilibrium distance

(R_0) for hydrogen has been achieved in an independent and not yet published study where we compared experimental collision cross sections (CCS) obtained by Ion Mobility Mass Spectrometry in gas phase (IMMS) and corresponding theoretical estimates in gas phase. IMMS is an analytical method allowing for the separation of ions in gas phase through their interactions with a buffer gas, typically helium or nitrogen, and hence allowing to get information on their 3D structures.[46,47]

In this work, we considered polymer solutions (poly(ethylene glycol) - PEG, α-methyl, ω-hydroxy poly(lactide) - PLA, poly-ε-caprolactone - PCL) prepared at a concentration of 15 µM in acetonitrile and cationized by 10 µL of sodium iodide solution (13mM). The structures bear one or two positive charge(s) and have a degree of polymerization ranging from 3 to 70. Polymers were analyzed with a Waters Synapt G2-S*i* mass spectrometer. All solutions were directly infused in the Electrospray ionization source (ESI) with a flow rate of 5 µL/min, a capillary voltage of 3.1 kV, a source temperature of 100 °C and a desolvation gas temperature of 200 °C. IM spectrometry was carried out with nitrogen as the drift gas at a pressure of 2.89 mbar, an IM wave velocity of 800 $m.s^{-1}$ and wave height of 40 V. Data were analyzed in the Waters MassLynx program, and an arrival time distribution (ATD) was extracted for each polymer ion composition.[48] ATD were then converted into collision cross sections (CCS) through the **Equation (1)**, where Ω corresponds to the CCS, t_D to the time associated to the peak maximum for a given ion, µ to the reduced mass between the ion and the drift gas (N_2), and A' as well as B are parameters determined from the calibration (full description in Ref. 47).

$$\Omega = \frac{z}{\sqrt{\mu}} A' t_D^B \quad (1)$$

To obtain the theoretical CCS (CCS_{th}), we used the DREIDING force field adapted with reparametrized torsional terms for PEG, PLA and PCL. We modeled ions of increasing chain length in different charge states in Materials Studio 6.0. To best parameterize the van der Waals parameters, we first used a fixed value of well depth (default value: 0.0152 kcal/mol) while

varying the equilibrium distance between 2.75 and 3.195 Å, which is the default DREIDING value. Each polymer ion (see **Table S6**) was submitted to two consecutive quenched molecular dynamics (MD) at 600 K and 200 K for 10 ns each. Next, two consecutive MD at 298 K for 10 ns each were performed on the most stable structures provided by the last quenched MD run at 200K. CCS_{th} were computed on the second MD by injecting 100 extracted frames into the MOBCAL program and using the Trajectory Method to provide average CCS values from each individual structure.

Table S6. List of all polymer ions selected from IMMS experiments (with the associated CCS_{exp}) and submitted to calculations (MD and CCS_{th}).

Polymer	**CCS_{exp} (Å²)**	**CCS_{th} (Å²)**
PEG_{20}^{1+}	228	229
PEG_{40}^{1+}	362	366
PEG_{15}^{2+}	221	213
PEG_{60}^{2+}	483	480
PEG_{70}^{2+}	531	535
PLA_{3}^{1+}	140	148
PLA_{5}^{1+}	185	191
PLA_{20}^{2+}	499	493
PLA_{26}^{2+}	584	598
PLA_{30}^{2+}	637	643
PCL_{26}^{2+}	531	535
PCL_{30}^{2+}	586	581

The lowest RSMD between the experimental and theoretical data was obtained for an equilibrium distance of 2.83 Å (**Figure S11**).

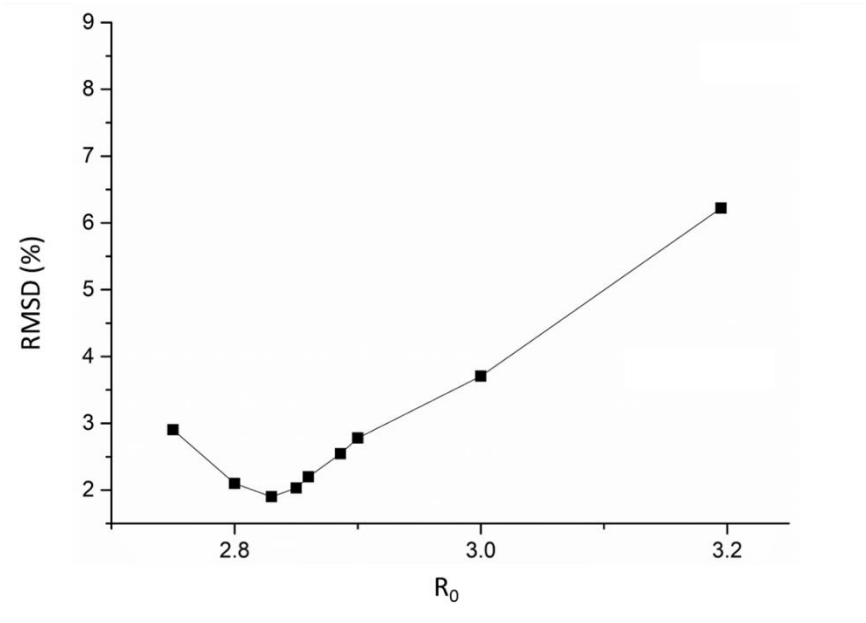

Figure S11. Plot of the RMSD between CCS_{exp} and CCS_{th} for all polymer ions as a function of the equilibrium distance. The optimum distance is 2.83 Å.

2. Well depth

To assess the reliability of the well depth parameter introduced in DREIDING for hydrogen, we compared experimental and theoretical data of vaporization enthalpies. To do so, we built different solvent boxes (propane, butane, pentane, hexane, cyclohexane and methyl acetate) with the Materials Studio 6.0 package and computed their vaporization enthalpies as shown in **Equation (2)**, where E_{total} is the total energy of the box and E_{intra} is the total energy of the isolated solvent molecules. These data were compared to experimental values in the NIST database around RT.

$$\Delta H_{vap} = \langle E_{intra} \rangle - \langle E_{total} \rangle + RT \quad (2)$$

Solvent boxes were generated explicitly in Materials Studio 6.0 with around 1000 atoms and the cell parameters were adjusted to reproduce the experimental densities. The atomic charges were assigned with the COMPASS force field while all remaining calculations were carried out using the DREIDING force field with the equilibrium distance for H – H set to 2.83 Å and the

well depths varied between 0.01 and 0.044 kcal/mol. The Ewald summation method was used to describe the electrostatic and van der Waals interactions.

The solvent boxes were first subjected to a high-temperature MD (NVT, 750K,50 ps). The systems were then submitted to another MD at 298 K for 100 ps. Before fully relaxing the systems, a MD in the NPT ensemble was performed at high pressure (3 GPa, 298 K) for 10 ns, followed by another MD at ambient pressure until energy is converged. When the systems are converged, a last MD run (NPT, Nosé-Hoover thermostat at 298 K, Berendsen barostat at ambient pressure, 300 ps) is performed and the calculation of vaporization enthalpies performed through the Forcite module implemented in Materials Studio.

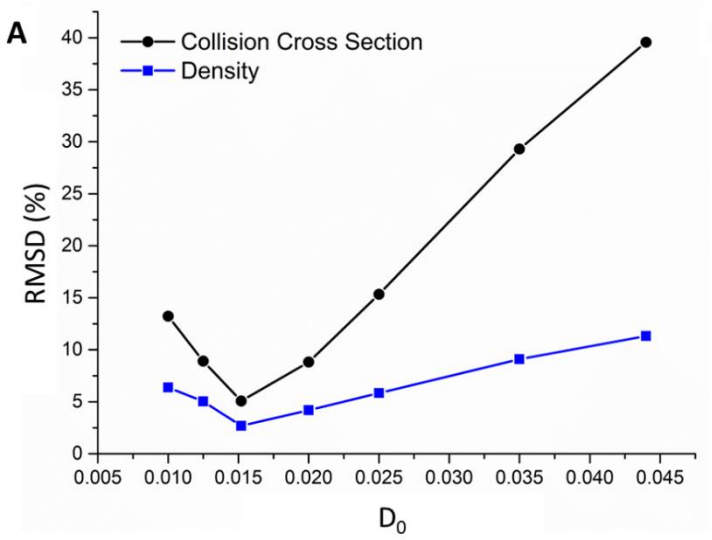

B

Solvent	Experimental density	Theoretical density (after fitting procedure)
Propane	0.51	0.48
Butane	0.58	0.55
Pentane	0.626	0.631
Hexane	0.655	0.669
Cyclohexane	0.779	0.796
Acetate	0.897	0.859

Figure S12. Plot of the RMSD between CCS_{exp} and CCS_{th} (black curve) for all polymer ions and between experimental and theoretical densities (blue curve) for all solvents used as a function of the well depth. The optimum well depth is 0.0152 kcal/mol.

β-peptoids

Isolated β-peptoids in the helical or globular conformation were first built and optimized (conjugated gradient algorithm, cutoff of 200Å) with the Materials Studio 6.0 package. Then, unit cells containing one of these singly-optimized helical or globular β-peptoids were built and optimized using the conjugate gradient algorithm and the Ewald summation method for non-bonded interactions among periodic cells. Four successive 100 ps-long molecular dynamics of increasing temperature (NPT – Berendsen barostat, Nose thermostat, 100 ps, 50-100-200-298 K) were performed to equilibrate the systems. Finally, 10 ns-long MD (NPT, 298 K) were performed to evaluate the relative stability between the two conformations (helical versus globular) as the average of the relative energies of 1000 snapshots of the systems extracted from the MD trajectory. The same procedure was adopted for unit cells containing four molecules. Note that no interconversion occurs during the MD.

XYZ coordinates

α-peptoid monomer bearing (S)-1-phenylethyl side chains *Nspe* (Table S1)

MP2

C	0.58401600	0.31915300	-1.74402100
C	-0.65584200	-0.22470800	-2.47668100
O	-0.51240800	-1.23534500	-3.17165000
N	-1.80380900	0.44782400	-2.33646300
H	0.40312300	0.56638000	-0.69790800
H	0.96860200	1.20333900	-2.25800900
N	1.57989400	-0.78649700	-1.83660400
C	1.59578200	-1.72480300	-0.61685000
H	0.53935100	-1.95114500	-0.45119400
C	2.34155400	-2.99470900	-1.00807100
H	1.85649400	-3.49509000	-1.85127900
H	2.33993900	-3.67976600	-0.15817500
H	3.38479800	-2.79533300	-1.26882400
C	2.15058000	-0.97002300	0.56480300
C	1.28761600	-0.53823700	1.57755800
C	3.51615900	-0.66155500	0.64405600
C	1.78364600	0.18801500	2.66027600
H	0.22838600	-0.77079100	1.52611600
C	4.00810900	0.06876700	1.72309200
H	4.20724200	-1.00159800	-0.12308200
C	3.14184800	0.49285300	2.73382800
H	1.10459300	0.51272400	3.44048100
H	5.06654900	0.29941000	1.78081600
H	3.52873200	1.05585600	3.57667000
C	-2.06365600	1.55465000	-1.39841500
H	-1.30536100	2.32861700	-1.56820500
C	-3.43386500	2.15183600	-1.73533000
H	-4.22235500	1.40855400	-1.58066600
H	-3.46587900	2.50155700	-2.77103600
H	-3.63922700	2.99577600	-1.07484100
C	-1.99060300	1.11027200	0.05620400
C	-1.49705400	1.99313000	1.02188200
C	-2.47314500	-0.14112400	0.45815500
C	-1.50337800	1.64143300	2.37228500
H	-1.11828300	2.96618600	0.71946500
C	-2.47601200	-0.49547800	1.80750600
H	-2.85892400	-0.83595100	-0.28171000
C	-1.99576200	0.39762100	2.76859700
H	-1.12689000	2.34041300	3.11201500
H	-2.86356300	-1.46308600	2.10967900
H	-2.00818600	0.12488800	3.81875700
H	-2.58342800	0.06808200	-2.86074100
H	1.23889200	-1.32941600	-2.66428700
H	2.52505200	-0.43476300	-1.99714800

PEPDROID
H -3.1991685 1.3353777 0.4068821
C -1.1962688 1.4012196 0.8574519
C -1.3505998 0.5119160 2.0270167
O -2.4892151 0.0686087 2.2870658
N -0.3534800 0.1236810 2.8465041
H -0.2408664 1.2169714 0.3636121
H -1.1871983 2.4244658 1.2358892
N -2.3163670 1.2724436 -0.1119705
C -2.3284289 0.0212902 -0.9165653
H -2.1026469 -0.8338932 -0.2716408
C -3.7561727 -0.2274262 -1.4491490
H -4.1013570 0.6184701 -2.0454445
H -4.4401501 -0.3725137 -0.6115205
H -3.7674049 -1.1271528 -2.0671317
C -1.3178343 0.0897904 -2.0041420
C -1.4890270 0.9184905 -3.1382711
C -0.1340106 -0.6747378 -1.8961418
C -0.5009463 0.9794208 -4.1365782
H -2.3322173 1.4831314 -3.2489830
C 0.8532718 -0.6138828 -2.8947848
H 0.0193165 -1.2834422 -1.0899381
C 0.6704613 0.2140258 -4.0143743
H -0.6338224 1.5783568 -4.9531013
H 1.7035480 -1.1727374 -2.8087486
H 1.3874592 0.2571985 -4.7403541
C 1.0228261 0.5031123 2.7493479
H 1.0834050 1.5606558 2.4802512
C 1.6743552 0.3500420 4.1365822
H 2.7196218 0.6594266 4.0908466
H 1.6233879 -0.6883003 4.4687062
H 1.1530111 0.9802269 4.8583008
C 1.7468372 -0.3147871 1.7420562
C 2.6114587 0.3176588 0.8209417
C 1.6020967 -1.7206072 1.6816449
C 3.3037039 -0.4332496 -0.1454278
H 2.7454765 1.3295264 0.8507219
C 2.2935451 -2.4721410 0.7153663
H 0.9930681 -2.2033103 2.3441561
C 3.1436576 -1.8280410 -0.1989849
H 3.9264476 0.0335616 -0.8061807
H 2.1819432 -3.4863832 0.6805772
H 3.6483321 -2.3737933 -0.8988765
H -0.5960479 -0.4872974 3.5637815
H -2.2740005 2.0646278 -0.7593934

β-peptoid bearing methyl side chains (from Table S2)

MP2

C	-0.89914900	0.83447500	1.32779800
C	1.20118000	-0.30566900	0.59459600
O	0.70216000	-1.40365000	0.85513600
N	2.23770600	-0.17620600	-0.30209900
C	3.13213800	0.96614500	-0.39125500
H	4.12719600	0.71077400	0.02034600
H	3.26609600	1.26592100	-1.44541200
H	2.74419300	1.82420400	0.16946600
C	2.74898600	-1.39318500	-0.92004500
H	1.94828200	-2.14231500	-0.94487800
H	3.08266900	-1.16140300	-1.94464700
H	3.60481200	-1.80593800	-0.35301000
H	-1.29629800	1.72492400	1.85493600
H	-1.14091100	-0.05291200	1.92362700
N	-1.51875600	0.72127400	0.01888600
C	-1.27962100	1.80812000	-0.91844700
H	-0.28856900	1.72968100	-1.40343600
H	-2.04731400	1.76307900	-1.70191600
H	-1.33941800	2.77466700	-0.38773200
O	-2.69906600	-0.40911000	-1.57239300
C	-2.55441200	-1.45952700	0.58741200
H	-3.07312400	-1.07026700	1.47887100
H	-1.61668500	-1.93901400	0.90713400
H	-3.19955700	-2.19427700	0.08786700
C	-2.27070400	-0.35743600	-0.41967800
C	0.62785500	0.96053000	1.22908700
H	0.88779300	1.87327400	0.67484800
H	1.04579400	1.06549100	2.24767100

PEPDROID

C	-0.88385500	0.78698400	1.23441100
C	1.32731500	-0.23203700	0.36380200
O	0.76178000	-1.34751200	0.46068100
N	2.56933700	-0.16066100	-0.21035500
C	3.38424900	1.02289000	-0.21116000
H	4.35097600	0.80270700	0.24589900
H	3.54635500	1.35147200	-1.23923300
H	2.93779200	1.84724500	0.34305900
C	3.18394200	-1.32126900	-0.79641100
H	2.43438100	-2.02549700	-1.16275100
H	3.81575200	-1.04213400	-1.64213700
H	3.79739400	-1.82311800	-0.04665500
H	-1.20549500	1.66339900	1.80023800
H	-1.01170400	-0.07539200	1.88916700
N	-1.70598200	0.69715600	0.04799300
C	-1.67738600	1.81983400	-0.85442600
H	-0.86780300	1.68484500	-1.57328700
H	-2.61676300	1.91613100	-1.40236400
H	-1.51638000	2.75150900	-0.30898100
O	-3.13742800	-0.44731700	-1.31018800
C	-2.60544600	-1.58327400	0.61809100
H	-2.93742800	-1.27565500	1.60930900
H	-1.64152400	-2.08208500	0.70225900
H	-3.33061000	-2.28521400	0.20377200
C	-2.47555700	-0.39742600	-0.24644900
C	0.63215200	0.94232300	0.94792100
H	0.76959400	1.79679800	0.28647600
H	1.12468300	1.17000300	1.89313700

Energy minima from Ramachandran plots at Figure 2

cis-α_D (φ = 90°)
C 0.7168289 0.1291606 -0.2773112
C -0.4294183 0.2626622 0.6630340
O -0.7699631 -0.7580040 1.3090289
N -1.1103980 1.4372940 0.8532373
C -0.7967562 2.6629570 0.1714441
H -1.6455252 2.9607545 -0.4468385
H -0.6050784 3.4500800 0.9033500
H 0.0787945 2.5829952 -0.4713456
C -2.1892167 1.5267477 1.8006890
H -2.6847456 0.5633504 1.9349012
H -1.7958475 1.8530187 2.7646132
H -2.9441710 2.2417247 1.4670655
H 1.4715196 0.8556376 0.0280538
H 0.3723666 0.4507521 -1.2601085
N 1.3296394 -1.1797432 -0.3714894
C 2.3550973 -1.4843736 0.5909733
H 1.8892379 -1.8352632 1.5132594
H 3.0300570 -2.2603142 0.2250419
H 2.9563047 -0.6010793 0.8129370
O 1.4525680 -3.2517006 -1.3182039
C -0.1901584 -1.9115984 -2.2259010
H 0.0903665 -1.1343382 -2.9361719
H -1.0875875 -1.6068781 -1.6875041
H -0.4037356 -2.8306830 -2.7736030
C 0.9098210 -2.1231588 -1.2691515

cis-α_D (φ = -90°)
C 0.3873598 -0.0167578 -0.6826299
C -0.8028760 0.1056988 0.2029342
O -1.1261680 -0.9003650 0.8800065
N -1.5287188 1.2620212 0.3282678
C -1.2237856 2.4780246 -0.3744270
H -2.0612381 2.7412790 -1.0231379
H -1.0708473 3.2864250 0.3431981
H -0.3295226 2.4030376 -0.9915146
C -2.6497685 1.3427001 1.2261352
H -3.1191745 0.3673405 1.3679159
H -2.3093803 1.7094749 2.1956305
H -3.4122942 2.0219695 0.8393483
H 1.0978111 0.7524969 -0.3803444
H 0.0699474 0.2485151 -1.6923388
N 1.0440424 -1.3072921 -0.7113605
C 0.5188397 -2.2781177 -1.6344481
H 0.1865626 -1.7990994 -2.5569942
H 1.2694912 -3.0243865 -1.9012085
H -0.3301211 -2.7873708 -1.1754284
O 2.6037780 -2.7617576 0.0986756
C 2.5835994 -0.7245296 1.1792894
H 1.7654293 -0.3837765 1.8137827
H 3.0566563 0.1334116 0.7023692
H 3.3211150 -1.2349553 1.8004493
C 2.0592627 -1.6339866 0.1458296

cis-$C_{7\beta}$ (φ = 120°)
C 1.0684072 0.8256646 0.0909963
C -0.0871675 1.1363581 0.9781513
O 0.2243203 1.6931068 2.0583406
N -1.4008766 0.8610901 0.7087141
C -1.8021389 0.2196467 -0.5069658
H -2.8890128 0.1723342 -0.6012253
H -1.4195073 0.7779608 -1.3615414
H -1.4138629 -0.7996916 -0.5304603
C -2.4327515 1.1248959 1.6751664
H -2.1525460 1.9353784 2.3504444
H -3.3618608 1.4149880 1.1810559
H -2.6114532 0.2252687 2.2659531
H 1.9557971 1.3317755 0.4777629
H 0.8464628 1.2695398 -0.8776847
N 1.3843744 -0.5839831 -0.0348567
C 1.7302405 -1.2681028 1.1861855
H 0.8218323 -1.6508650 1.6540596
H 2.4062151 -2.1048929 1.0001490
H 2.2269385 -0.5912794 1.8844676
O 1.6358365 -2.4891315 -1.2613015
C 1.0363056 -0.6703084 -2.5293293
H 1.6364653 0.2249886 -2.6894318
H -0.0196086 -0.4132862 -2.5614004
H 1.2473653 -1.3765353 -3.3339143
C 1.3702252 -1.2649199 -1.2233350

cis-$C_{7\beta}$ (φ = -120°)
C 0.0002844 0.5894265 -1.2176723
C -1.1758969 0.8675197 -0.3469644
O -2.2412220 1.0899232 -0.9710033
N -1.1723070 0.8877873 1.0218870
C 0.0177232 0.6315912 1.7759036
H -0.1372336 0.7905511 2.8450807
H 0.3315279 -0.4027698 1.6276099
H 0.8109331 1.3057783 1.4523133
C -2.3857267 1.0813483 1.7692291
H -3.1228657 1.6484908 1.1979368
H -2.8126936 0.1094122 2.0208937
H -2.1897010 1.6319803 2.6911412
H 0.7825508 1.2838247 -0.9168001
H -0.2603609 0.8336232 -2.2499677
N 0.4722861 -0.7814256 -1.1940284
C -0.4742385 -1.7855751 -1.6115053
H -1.1564457 -1.3879824 -2.3657682
H 0.0261480 -2.6541272 -2.0439361
H -1.0565656 -2.1122704 -0.7484978
O 2.0748927 -2.3520535 -0.7920119
C 2.7826169 -0.2088090 -0.3662626
H 2.5159105 0.2199456 0.5965942
H 2.8978837 0.5863949 -1.1022916
H 3.7376363 -0.7266892 -0.2643031
C 1.7348635 -1.1458952 -0.8075768

trans-α_D (φ = 90°)
C 0.3896617 -0.5097756 -0.2979075
C -0.7751382 -0.2521188 0.5948773
O -1.2273691 0.9183485 0.6393183
N -1.3875306 -1.2394626 1.3228414
C -0.9519054 -2.6081463 1.2818647
H -1.2632348 -3.1492953 2.1776501
H -1.3846552 -3.0995165 0.4091111
H 0.1349337 -2.6753007 1.2247083
C -2.5717782 -0.9713462 2.0941333
H -2.6149332 0.0722349 2.4113681
H -3.4533024 -1.1882831 1.4891585
H -2.5988569 -1.5887386 2.9938738
H 0.0916921 -1.2741640 -1.0169080
H 1.1735914 -0.9586307 0.3135728
N 0.9255769 0.6387308 -1.0004639
C 0.3050800 0.9779874 -2.2523867
H -0.5738884 1.5959769 -2.0613044
H 0.9838395 1.5270694 -2.9055168
H -0.0077287 0.0785936 -2.7859220
O 2.3965678 1.1022556 0.6761668
C 2.5119308 2.5789655 -1.0929074
H 1.7276785 3.2984401 -1.3279253
H 3.0131317 2.2734294 -2.0110462
H 3.2397976 3.0537853 -0.4333320
C 1.9168394 1.3989609 -0.4430244

trans-α_D (φ = -90°)
C 0.4821365 -0.4835214 -0.1721759
C -0.7045719 -0.2172256 0.6868853
O -1.0781390 0.9756816 0.8056908
N -1.3695255 -1.2005194 1.3734544
C -0.9979189 -2.5882903 1.3408733
H -0.8103000 -2.9407816 2.3568827
H -1.8156928 -3.1718723 0.9141681
H -0.1036248 -2.7777953 0.7488528
C -2.4899743 -0.8892405 2.2198939
H -3.0109266 0.0072917 1.8784331
H -3.2130719 -1.7074500 2.2275785
H -2.1366021 -0.7205305 3.2381501
H 0.1790047 -1.2180894 -0.9200938
H 1.2373872 -0.9708565 0.4464999
N 1.0685041 0.6667115 -0.8290580
C 2.0897996 1.3731443 -0.1051643
H 3.0625995 0.9350116 -0.3326877
H 2.1097823 2.4314893 -0.3674694
H 1.9157111 1.3058617 0.9708978
O -0.2497252 0.4152361 -2.6695005
C 1.1937820 2.2116891 -2.7993380
H 2.2776172 2.1201478 -2.8676102
H 0.9384778 3.1279726 -2.2674023
H 0.7793436 2.2607119 -3.8073444
C 0.6459275 1.0552235 -2.0704162

trans-$C_{7\beta}$ (φ = 120°)
C 0.0050764 -1.3069403 -0.6969169
C -1.1114196 -1.2129204 0.2808322
O -2.2216637 -1.6210661 -0.1376527
N -0.9952841 -0.7117935 1.5499765
C 0.2553774 -0.2304632 2.0645590
H 0.4445703 0.7723430 1.6787423
H 0.2480660 -0.1889469 3.1554267
H 1.0755121 -0.8856895 1.7691779
C -2.1466658 -0.5463172 2.3943227
H -2.9377873 -1.2525225 2.1359114
H -1.8869363 -0.7117989 3.4414872
H -2.5337107 0.4673672 2.2813017
H -0.3195329 -1.9233143 -1.5379505
H 0.8203863 -1.8425578 -0.2106390
N 0.4447105 -0.0307980 -1.2303110
C -0.5043813 0.7022586 -2.0290923
H -1.5210507 0.5650765 -1.6568166
H -0.2995006 1.7730759 -2.0224739
H -0.4598126 0.3434066 -3.0584540
O 2.5639545 -0.2812822 -0.4233919
C 2.2422234 1.6873143 -1.5746945
H 1.7079674 2.5081574 -1.0966620
H 2.0910609 1.7334736 -2.6530616
H 3.3078402 1.7890627 -1.3636472
C 1.7310002 0.4048748 -1.0599736

trans-$C_{7\beta}$ (φ = -120°)
C 0.9601777 -1.0046071 0.5702942
C -0.1853647 -0.7461647 1.4827674
O 0.1210467 -0.5904958 2.6894432
N -1.4928572 -0.6537384 1.0861024
C -1.8830312 -0.8101602 -0.2864200
H -1.6877739 0.1171243 -0.8270331
H -1.3276126 -1.6209135 -0.7590346
H -2.9448182 -1.0483194 -0.3739181
C -2.5288843 -0.2890026 2.0132114
H -2.2668869 -0.5662780 3.0358929
H -2.6845022 0.7900446 1.9735842
H -3.4656945 -0.7915182 1.7656925
H 0.7330684 -1.9118329 0.0103225
H 1.8457025 -1.2200102 1.1718583
N 1.2814737 0.1028022 -0.3102080
C 1.6554541 1.3426648 0.3199177
H 2.1432668 1.1565095 1.2791529
H 2.3494070 1.9168950 -0.2947038
H 0.7603479 1.9420500 0.4940133
O 0.9177095 -1.1211660 -2.1999729
C 1.5551894 1.0540526 -2.6154461
H 2.6104019 1.3125128 -2.5296672
H 0.9463404 1.9278957 -2.3838618
H 1.3495277 0.7432125 -3.6408533
C 1.2383122 -0.0315569 -1.6711341

Energy minima from Ramachandran plots at Figure 4

cis-α_D (φ = 80°)
C 0.0080035 1.1261873 0.4582219
C -0.7636792 0.9780084 -0.8074815
O -0.1560517 0.5374267 -1.8129554
N -2.0754550 1.3572228 -0.9265989
C -2.8136012 1.9304100 0.1648425
H -3.8891104 1.8041085 0.0248176
H -2.5525286 1.4552997 1.1108885
H -2.5932765 2.9970420 0.2299281
C -2.7570494 1.2928794 -2.1918248
H -2.3322058 0.5208069 -2.8361433
H -3.8142370 1.0589518 -2.0536961
H -2.6705841 2.2554334 -2.6979735
H -0.5375762 0.5786657 1.2268438
H -0.0379569 2.1750665 0.7517553
N 1.3947052 0.6836717 0.4503267
O 3.5807919 1.1140802 -0.0641252
C 2.1451709 2.8056328 -0.6715037
H 1.7346855 3.4743688 0.0843678
H 1.4434347 2.7183914 -1.5003638
H 3.0780063 3.2294823 -1.0464143
C 2.3810682 1.4760939 -0.0791768
C 1.7219323 -0.6029648 1.0500910
H 2.7417279 -0.8923930 0.7845286
C 1.7659717 -0.4496468 2.5886291
H 2.4956053 0.3156484 2.8560059
H 2.0648877 -1.3940987 3.0448893
H 0.7888883 -0.1572583 2.9736947
C 0.8761456 -1.7235658 0.5389528
C -0.1241314 -2.3655659 1.3084633
C 1.0766897 -2.1564232 -0.7914505
C -0.8961060 -3.4069184 0.7636555
H -0.3020617 -2.0780891 2.2703902
C 0.3057761 -3.1965020 -1.3391169
H 1.7865579 -1.7066739 -1.3722701
C -0.6812658 -3.8226403 -0.5606332
H -1.6136765 -3.8603432 1.3300256
H 0.4623453 -3.4942633 -2.3024945
H -1.2418407 -4.5775318 -0.9570956

cis-α_D (φ = -80°)
C -0.1809435 0.8073873 -0.0858075
C -0.2609689 1.8579716 0.9658136
O 0.8020124 2.1688824 1.5558719
N -1.4239789 2.5076320 1.2890336
C -2.6870412 2.2494628 0.6537128
H -3.3974996 1.8818268 1.3963492
H -3.0771200 3.1750317 0.2259125
H -2.6218962 1.5118063 -0.1449381
C -1.4447707 3.5433383 2.2870513
H -0.6581390 3.3982081 3.0299588
H -1.2948768 4.5108279 1.8056107
H -2.3995766 3.5565405 2.8167929
H -0.5462932 1.2454151 -1.0147727
H -0.9017715 0.0335244 0.1810493
N 1.1190115 0.1995029 -0.3258901
O 3.1769722 0.3105817 -1.3181620
C 1.8623766 2.1535200 -1.7236720
H 1.6300041 2.8955560 -0.9604647
H 1.0404745 2.0943469 -2.4364696
H 2.7641170 2.4662462 -2.2523171
C 2.0625743 0.8368725 -1.0909107
C 1.3962403 -1.1016310 0.2675286
H 2.4432223 -1.3717269 0.1111544
C 1.2831059 -1.0607940 1.8112333
H 1.9519325 -0.2934087 2.2025675
H 1.5748680 -2.0258192 2.2270974
H 0.2624796 -0.8323760 2.1186757
C 0.6110435 -2.1735720 -0.4144982
C -0.4134822 -2.9176868 0.2195611
C 0.8979021 -2.4548520 -1.7702582
C -1.1243887 -3.9094401 -0.4792047
H -0.6533501 -2.7428710 1.1951394
C 0.1886148 -3.4454223 -2.4716802
H 1.6313148 -1.9348320 -2.2550173
C -0.8234772 -4.1735303 -1.8253788
H -1.8595515 -4.4377051 -0.0080983
H 0.4097566 -3.6354088 -3.4496634
H -1.3388973 -4.8934054 -2.3329107

cis-$C_{7\beta}$ (φ = 120°)
C 1.6932440 -0.8212090 0.6271476
C 0.5908970 -0.5742746 1.5966544
O 0.0883106 -1.6156290 2.0838814
N 0.1238892 0.6519219 1.9870504
C 0.6782934 1.8684269 1.4752099
H 0.2054067 2.7478404 1.9172702
H 1.7429647 1.9101777 1.7057098
H 0.5340446 1.9159008 0.3954544
C -1.0086180 0.7743316 2.8645879
H -1.1179853 -0.1022763 3.5054339
H -0.9035482 1.6458235 3.5133236
H -1.9149831 0.8841906 2.2672808
H 1.9806367 -1.8723721 0.6821818
H 2.5441527 -0.2543124 0.9982929
N 1.4081802 -0.5029253 -0.7696646
O 1.8984874 0.6940025 -2.6592725
C 3.2813339 1.1947265 -0.9102746
H 4.0165708 0.5099191 -0.4884353
H 2.9302699 1.8744269 -0.1381335
H 3.7650882 1.7803919 -1.6938445
C 2.1488206 0.4269359 -1.4606144
C 0.3138131 -1.2019110 -1.4464600
H 0.4127266 -1.0793443 -2.5275187
C 0.4136622 -2.7407729 -1.2952724
H 1.4004572 -3.0736523 -1.6185971
H -0.3410049 -3.2203584 -1.9198193
H 0.2590841 -3.0400645 -0.2586778
C -1.0189073 -0.6095380 -1.1144886
C -2.0271263 -1.3026138 -0.4001961
C -1.2920731 0.7157756 -1.5259403
C -3.2572216 -0.6903436 -0.1027071
H -1.8717234 -2.2582768 -0.0805988
C -2.5200478 1.3322924 -1.2293320
H -0.5914373 1.2436823 -2.0471222
C -3.5036891 0.6285650 -0.5163283
H -3.9699244 -1.2041416 0.4162376
H -2.6963836 2.2904133 -1.5327790
H -4.3956603 1.0742715 -0.2996394

cis-$C_{7\beta}$ (φ = -120°)
C 0.5309120 -0.6818901 -0.9189332
C -0.9201539 -0.9931628 -1.0319909
O -1.3368522 -1.8473159 -0.2132470
N -1.7890285 -0.4433201 -1.9362462
C -1.3614690 0.5256350 -2.8996176
H -2.1801131 0.8409925 -3.5499157
H -0.9783013 1.4101000 -2.3890433
H -0.5808354 0.0965050 -3.5282303
C -3.1905568 -0.7659430 -1.9173330
H -3.3693066 -1.7552441 -1.4922399
H -3.7215945 -0.0270373 -1.3154415
H -3.6030857 -0.7628976 -2.9279876
H 0.9491010 -0.8530672 -1.9084027
H 0.9933925 -1.4207663 -0.2620402
N 0.8733035 0.6460849 -0.4150906
O 1.8798180 2.6772035 -0.7295439
C 2.1293519 1.2772638 -2.5201656
H 1.3066621 1.1813644 -3.2240252
H 2.7177903 0.3600646 -2.5178873
H 2.7708275 2.0978605 -2.8458889
C 1.6083256 1.5335054 -1.1645936
C 0.4416348 1.0332809 0.9284061
H 1.0650023 1.8568368 1.2854155
C -0.9754927 1.6534328 0.8810631
H -1.0010429 2.4493784 0.1360914
H -1.2209500 2.0779018 1.8551527
H -1.7218991 0.9034928 0.6241124
C 0.6548896 -0.0223641 1.9650681
C -0.3965692 -0.6606222 2.6659517
C 1.9833348 -0.4101918 2.2553767
C -0.1268830 -1.6525862 3.6251879
H -1.3684283 -0.4142669 2.4794049
C 2.2560213 -1.4015254 3.2141694
H 2.7622571 0.0319406 1.7645164
C 1.1997064 -2.0231403 3.8998506
H -0.8959216 -2.1048976 4.1205283
H 3.2206970 -1.6693128 3.4117123
H 1.3954564 -2.7432916 4.5958566

trans-α_D (φ = 80°)
C 0.0169359 1.2719301 0.4822948
C -0.8207604 1.2910975 -0.7503839
O -0.3283823 0.8130893 -1.8013840
N -2.0790461 1.8345212 -0.7835948
C -2.6865181 2.4311638 0.3734679
H -3.7714306 2.4919368 0.2666561
H -2.4804330 1.8451870 1.2697038
H -2.2927390 3.4397704 0.5088478
C -2.8171635 1.9300932 -2.0143705
H -2.5205662 1.1524029 -2.7205751
H -3.8882232 1.8198205 -1.8356533
H -2.6323020 2.9036659 -2.4706852
H -0.5556420 0.7564199 1.2530340
H 0.1193801 2.3040077 0.8216847
N 1.3381501 0.6684007 0.3732849
O 2.1686760 2.5817926 -0.5547487
C 3.7385314 0.9142646 -0.3423894
H 3.7370052 0.0599530 -1.0191601
H 4.1415722 0.6134518 0.6243821
H 4.3748351 1.6948947 -0.7621153
C 2.3598934 1.4036604 -0.1709389
C 1.5380821 -0.6792132 0.8857094
H 2.4967127 -1.0758511 0.5488257
C 1.6784735 -0.6179244 2.4250627
H 2.5072274 0.0399282 2.6891881
H 1.8828725 -1.6149795 2.8170834
H 0.7644045 -0.2338365 2.8785693
C 0.5367214 -1.6615362 0.3711573
C -0.4928774 -2.2212017 1.1660096
C 0.6138639 -2.0431975 -0.9876305
C -1.4116525 -3.1341574 0.6188015
H -0.5858364 -1.9659830 2.1487973
C -0.3038966 -2.9548609 -1.5376973
H 1.3398491 -1.6489201 -1.5881006
C -1.3171615 -3.5014266 -0.7335015
H -2.1486875 -3.5290538 1.2037565
H -0.2353330 -3.2165557 -2.5216389
H -1.9845350 -4.1627543 -1.1317492

trans-α_D (φ = -80°)
C -0.2502474 0.9716732 -0.3399262
C -0.5183461 2.1142469 0.5783893
O 0.3971865 2.4594786 1.3648305
N -1.7229319 2.7677250 0.6183930
C -2.8269374 2.3968186 -0.2232266
H -3.5244230 3.2272619 -0.3498147
H -2.4854292 2.1063803 -1.2172708
H -3.3600103 1.5586065 0.2280939
C -1.9783655 3.8016940 1.5851148
H -1.0565709 4.2998242 1.8912381
H -2.6419801 4.5643916 1.1736337
H -2.4468838 3.3630950 2.4672912
H -0.4174794 1.3277216 -1.3574876
H -1.0187087 0.2206948 -0.1540106
N 1.0711748 0.3627376 -0.2713152
O 1.9424166 2.0272158 -1.5675889
C 3.5003796 0.4620769 -0.9272696
H 3.5170749 -0.5355887 -1.3650871
H 3.8797525 0.4190188 0.0935456
H 4.1463956 1.1157899 -1.5152957
C 2.1186143 0.9721074 -0.9137732
C 1.2287004 -0.8687144 0.4897906
H 2.2691744 -1.1936718 0.4794742
C 0.9535856 -0.6217309 1.9927440
H 1.5926990 0.1859078 2.3514511
H 1.1770719 -1.5243433 2.5624980
H -0.0897111 -0.3469283 2.1509426
C 0.4791225 -2.0009343 -0.1367210
C -0.5266903 -2.7398821 0.5330928
C 0.7847976 -2.3543103 -1.4719077
C -1.2007667 -3.7931745 -0.1097695
H -0.7804847 -2.5174099 1.4953854
C 0.1126348 -3.4065713 -2.1177450
H 1.5030376 -1.8411374 -1.9846404
C -0.8811525 -4.1269122 -1.4357907
H -1.9230432 -4.3154072 0.3873847
H 0.3465229 -3.6465110 -3.0817316
H -1.3701796 -4.8912389 -1.9029212

trans-$C_{7\beta}$ (φ = 120°)
C 1.7223582 -0.7795467 0.9058488
C 0.5951460 -0.4273524 1.8072470
O -0.0208788 -1.4067751 2.2930678
N 0.2175296 0.8505461 2.1230008
C 0.8989943 1.9977981 1.5943954
H 0.6964916 2.8896361 2.1904103
H 1.9782589 1.8426700 1.5978026
H 0.5698355 2.1813040 0.5715664
C -0.9600847 1.1050738 2.9063343
H -1.1914100 0.2676460 3.5668811
H -0.8267612 1.9903515 3.5305465
H -1.8078823 1.2662096 2.2391034
H 1.9232069 -1.8470079 1.0034754
H 2.6013509 -0.2735852 1.3039709
N 1.5248583 -0.4828707 -0.5133319
O 3.3321728 0.9218629 -0.5309584
C 2.3021481 0.7649830 -2.5693253
H 1.3236333 1.1908700 -2.7833961
H 2.4583353 -0.1161358 -3.1913628
H 3.0655179 1.5053876 -2.8139722
C 2.3853777 0.3799536 -1.1479481
C 0.4478377 -1.1576379 -1.2376654
H 0.5446171 -0.9746120 -2.3077133
C 0.6054327 -2.6967300 -1.1600520
H 1.6148573 -2.9759168 -1.4641306
H -0.1084497 -3.1739225 -1.8325445
H 0.4281621 -3.0511127 -0.1442549
C -0.9104934 -0.6283881 -0.8988018
C -1.9441860 -1.4258581 -0.3478266
C -1.1879952 0.7382808 -1.1350002
C -3.2019859 -0.8769221 -0.0426266
H -1.7895068 -2.4149249 -0.1547989
C -2.4441695 1.2916356 -0.8322521
H -0.4700347 1.3459793 -1.5265325
C -3.4527214 0.4828558 -0.2852834
H -3.9321484 -1.4669175 0.3575108
H -2.6223051 2.2808575 -1.0080936
H -4.3651093 0.8823151 -0.0632904

trans-$C_{7\beta}$ (φ = -120°)
C 0.4921208 -0.8756889 -1.1015336
C -0.9679921 -1.1333916 -1.1959333
O -1.4220860 -1.9609901 -0.3695822
N -1.8060802 -0.5349859 -2.0990353
C -1.3296656 0.4199845 -3.0587630
H -2.0386854 0.5498192 -3.8786334
H -1.1822177 1.3839923 -2.5698385
H -0.3847567 0.0929314 -3.4939391
C -3.2259611 -0.7541755 -2.0570605
H -3.4690460 -1.7230697 -1.6171701
H -3.6935642 0.0280341 -1.4573809
H -3.6516045 -0.7328860 -3.0619151
H 0.9056830 -1.0653051 -2.0916178
H 0.9321504 -1.6268138 -0.4437299
N 0.8697322 0.4442068 -0.5970503
O 1.9846305 0.9325225 -2.5368600
C 2.0633204 2.6301177 -0.9996126
H 2.7630362 2.5551643 -0.1674393
H 1.2021840 3.2264736 -0.6993257
H 2.5606759 3.1286056 -1.8331876
C 1.6188749 1.2792868 -1.3894090
C 0.4677569 0.8451176 0.7498145
H 1.1098469 1.6554611 1.0971429
C -0.9403347 1.4876376 0.7257236
H -0.9742210 2.2713744 -0.0314150
H -1.1558983 1.9307986 1.6985909
H -1.7043901 0.7454925 0.4997268
C 0.6813377 -0.2124597 1.7844695
C -0.3666534 -0.8190034 2.5181823
C 2.0064665 -0.6356930 2.0392652
C -0.0968574 -1.8129167 3.4753355
H -1.3366584 -0.5482344 2.3577562
C 2.2792204 -1.6290851 2.9958590
H 2.7832403 -0.2197027 1.5230114
C 1.2264026 -2.2178621 3.7149435
H -0.8635540 -2.2420266 3.9944391
H 3.2413772 -1.9229904 3.1669704
H 1.4221702 -2.9397400 4.4092013

Threaded loop ($Nspe_9$) from Figure 7

C -1.3797398 -3.4727217 -3.8597735
C -1.8375218 -2.0577372 -3.7623219
O -2.4354604 -1.7302450 -2.7095049
N -1.5567406 -1.0920041 -4.6956772
H -0.3942537 -3.4914547 -4.3229470
H -2.0561119 -3.9804897 -4.5489305
N -1.2958970 -4.2039096 -2.6044573
C -2.3903934 -5.1159497 -2.2911676
H -3.0365705 -5.2080789 -3.1681119
C -1.9178038 -6.5773842 -2.0923388
H -1.3363215 -6.8898847 -2.9602750
H -2.7865930 -7.2302845 -1.9993355
H -1.3031493 -6.6845823 -1.2003352
C -3.2692033 -4.5918345 -1.2042887
C -3.0666272 -4.9077545 0.1598949
C -4.3486395 -3.7423026 -1.5378982
C -3.9052533 -4.3818536 1.1567974
H -2.3033008 -5.5236294 0.4389164
C -5.1938649 -3.2189269 -0.5437029
H -4.5251666 -3.4994292 -2.5139256
C -4.9703210 -3.5364408 0.8056520
H -3.7404717 -4.6205203 2.1344103
H -5.9706177 -2.6095026 -0.8030287
H -5.5837261 -3.1572447 1.5277992
C -1.0372183 -1.4060681 -6.0192122
H -0.9166334 -2.4830008 -6.1402451
C -2.0773929 -1.0656863 -7.1139476
H -3.0031532 -1.6063339 -6.9138896
H -1.6957122 -1.3726135 -8.0886122
H -2.2921267 0.0021433 -7.1388289
C 0.3218630 -0.8252816 -6.2305066
C 1.4390706 -1.4885217 -5.6730927
C 0.5442280 0.3817228 -6.9362153
C 2.7360540 -0.9675753 -5.8162585
H 1.3161121 -2.3580399 -5.1559891
C 1.8406218 0.9077593 -7.0760460
H -0.2367464 0.8933186 -7.3469071
C 2.9372086 0.2337937 -6.5145206
H 3.5314467 -1.4621632 -5.4116420
H 1.9850778 1.7800169 -7.5857313
H 3.8786342 0.6148390 -6.6154857
C -1.7376138 0.3123638 -4.3410786
C -0.6260869 0.9212824 -3.5517957
O 0.2599254 0.1471164 -3.1154582
N -0.5168601 2.2634248 -3.2837032
H -1.8654041 0.9099900 -5.2418483
H -2.6560633 0.4298991 -3.7650124
C -1.5689258 3.1960033 -3.6730709

H -2.5196466 2.6768792 -3.5357923
C -1.6966257 4.4678306 -2.7976000
H -0.8707980 5.1535280 -2.9912785
H -1.6890732 4.1925147 -1.7436730
H -2.6357102 4.9764587 -3.0196795
C -1.4835066 3.6033034 -5.1039844
C -2.6727396 3.9151515 -5.8017543
C -0.2529580 3.6973153 -5.7962925
C -2.6364151 4.2965538 -7.1544091
H -3.5750741 3.8640790 -5.3263158
C -0.2144969 4.0798346 -7.1484329
H 0.6245267 3.4849054 -5.3221941
C -1.4067702 4.3773342 -7.8284274
H -3.5030952 4.5163635 -7.6468668
H 0.6797055 4.1415238 -7.6366000
H -1.3795719 4.6543929 -8.8105156
C 0.8296558 -2.9718979 -1.9618918
C -0.2451242 -3.9811466 -1.7423648
O -0.1527914 -4.6329686 -0.6780493
H 0.4491661 -2.1540899 -2.5618864
H 1.5939225 -3.4661422 -2.5632894
N 1.4408710 -2.3857444 -0.7749637
C 2.8590906 -2.6269718 -0.5344640
H 3.1444489 -2.2227908 0.4388854
C 3.1327631 -4.1427185 -0.3704834
H 3.0263147 -4.6593332 -1.3245843
H 2.4276763 -4.5656593 0.3458878
H 4.1440693 -4.2959068 0.0078488
C 3.7256663 -1.8995509 -1.5172132
C 4.8948158 -2.4685045 -2.0792832
C 3.3912158 -0.5762146 -1.8966477
C 5.6888252 -1.7492450 -2.9900326
H 5.1839592 -3.4139450 -1.8297785
C 4.1746144 0.1408315 -2.8147519
H 2.5667112 -0.1204250 -1.5061111
C 5.3282278 -0.4437819 -3.3590956
H 6.5280990 -2.1764400 -3.3837562
H 3.9046268 1.0863895 -3.0846359
H 5.9019435 0.0782459 -4.0224454
C -0.7233362 -1.3171040 -0.0426371
C 0.7403864 -1.5240535 0.0314072
O 1.3374302 -0.8501992 0.9042439
H -1.2126002 -2.2872154 0.0479451
H -0.9520272 -0.8963106 -1.0193444
N -1.2343902 -0.3999817 0.9991618
C -2.7067784 -0.3756433 1.1449913
H -3.1282951 -1.3396897 0.8470181
C -3.0656291 -0.2037572 2.6361800
H -2.6971188 -1.0574430 3.2055350
H -4.1490251 -0.1477206 2.7523121
H -2.6166025 0.7051037 3.0367549

C -3.2886617 0.6970229 0.3008213
C -4.0459385 0.3584197 -0.8417997
C -3.1034003 2.0645632 0.6095306
C -4.6189043 1.3585951 -1.6464152
H -4.1906684 -0.6194762 -1.0941169
C -3.6834324 3.0652407 -0.1877639
H -2.5450988 2.3418905 1.4176347
C -4.4424050 2.7124132 -1.3159035
H -5.1670078 1.1014007 -2.4683584
H -3.5494496 4.0488567 0.0513893
H -4.8632296 3.4395825 -1.8957876
H -0.8140388 -0.6501834 1.8972919
H -0.9049099 0.5332002 0.7516090
C 0.6791836 2.7593149 -2.6164198
C 0.6797297 2.6679574 -1.1279593
O -0.1119420 1.8378668 -0.6114250
N 1.5560948 3.3468853 -0.3153596
H 1.5461223 2.1934484 -2.9624917
H 0.8556155 3.7848743 -2.9287335
C 2.3821372 4.4388049 -0.8192404
H 1.8163785 4.9617167 -1.5912128
C 2.6847177 5.5749155 0.1902840
H 3.1837824 6.3973679 -0.3242759
H 3.3288742 5.2246809 0.9968960
H 1.7502772 5.9451901 0.6131876
C 3.6504241 3.9385657 -1.4177754
C 4.6223023 3.2552771 -0.6495406
C 3.9140869 4.1669390 -2.7875836
C 5.8242087 2.8175135 -1.2328819
H 4.4653842 3.0771840 0.3412994
C 5.1157940 3.7306151 -3.3728219
H 3.2332895 4.6596104 -3.3674257
C 6.0724489 3.0580732 -2.5943964
H 6.5176681 2.3264974 -0.6673665
H 5.2947137 3.9043412 -4.3625912
H 6.9459643 2.7427389 -3.0179093
C 1.6333656 2.9790814 1.0892312
C 0.6122033 3.5833293 1.9906165
O -0.3331828 4.2027062 1.4481822
N 0.6608783 3.4633500 3.3587379
H 1.5475810 1.8956932 1.1772732
H 2.6157353 3.2292716 1.4837358
C -0.1767342 4.2496354 4.2547870
H 0.2789299 4.2412341 5.2484753
C -0.1817374 5.7688675 3.9446107
H -0.6916080 5.9893873 3.0085010
H 0.8460249 6.1272921 3.8791761
H -0.6876891 6.3015344 4.7508467
C -1.5300339 3.6491619 4.4205001
C -2.6484478 4.0543188 3.6541972
C -1.7130682 2.6376512 5.3903148

C -3.9133743 3.4763882 3.8618673
H -2.5494726 4.7733286 2.9374175
C -2.9782580 2.0664983 5.6068737
H -0.9238303 2.3161790 5.9530004
C -4.0796831 2.4845318 4.8421235
H -4.7111174 3.7802822 3.3024621
H -3.0951331 1.3509622 6.3233472
H -4.9987039 2.0695556 4.9991528
H 1.6226398 2.6560334 5.0444919
N 1.8921628 -0.0032264 4.2966779
C 3.2658038 0.1607142 4.7482241
H 3.5203518 1.2148854 4.8541790
C 3.4618000 -0.3751580 6.1884220
H 2.7537639 0.1167004 6.8565918
H 4.4751771 -0.1551953 6.5265587
H 3.2985532 -1.4518670 6.2321629
C 4.2013195 -0.3716793 3.7089859
C 4.2471825 0.2668849 2.4466230
C 5.0284792 -1.5032268 3.9097295
C 5.0815617 -0.2059343 1.4193863
H 3.6658282 1.0832807 2.2643796
C 5.8636453 -1.9805069 2.8835180
H 5.0276720 -1.9945759 4.8034401
C 5.8891449 -1.3330582 1.6374400
H 5.0989818 0.2666982 0.5148929
H 6.4527224 -2.7984850 3.0442591
H 6.4942287 -1.6800363 0.8920994
C 1.5314084 2.4737001 3.9724640
C 1.1399731 1.0436310 3.8240858
O 0.0458757 0.7999640 3.2568661
H 2.5349885 2.5994247 3.5696532
H 2.1337746 -2.0804400 4.4367017
N -0.3097583 -2.9159190 5.3702572
C -1.3626192 -3.2204426 6.3327034
H -1.4429224 -4.3058552 6.4337962
C -1.0178439 -2.8181307 7.7898660
H -1.7644548 -3.2354363 8.4667388
H -0.9980433 -1.7376398 7.9191680
H -0.0405246 -3.2228420 8.0545642
C -2.7008487 -2.7692330 5.8557770
C -3.4232786 -3.5922708 4.9620386
C -3.2913529 -1.5525656 6.2703664
C -4.7035095 -3.2228210 4.5131028
H -3.0225617 -4.4747108 4.6413641
C -4.5696252 -1.1788477 5.8190676
H -2.7943103 -0.9300964 6.9071986
C -5.2768750 -2.0145603 4.9401488
H -5.2200078 -3.8355378 3.8819322
H -4.9855503 -0.3016227 6.1332938
H -6.2067449 -1.7461403 4.6160790
C 1.3402308 -1.3507214 4.2768815

C 0.2470029 -1.6633005 5.2423433
O -0.1867497 -0.7087772 5.9289098
H 0.9609909 -1.5442029 3.2771389
C 0.1108069 -4.0051742 4.5050430
C -0.3530315 -3.9625385 3.1014456
O -0.9815301 -2.9947456 2.6158189
N -0.0029391 -4.9501307 2.2686300
H 1.2002734 -4.0501514 4.4889172
H -0.2066226 -4.9668111 4.9119121
H -0.1692339 -4.8646298 1.3236965
H 0.4167508 -5.7549836 2.6091523

β-*N1snpe*$_6$ (helix, last frame of analysis MD) from Figure 8

O -4.7496527 5.7286452 -2.1256386
C -4.0507651 3.9380169 -3.6310524
H -4.2494349 4.3956869 -4.6035059
H -3.0584198 4.1171308 -3.3192537
O -6.1926339 3.9541933 -2.6049813
C -5.0513166 4.5134281 -2.6982263
C -5.6227535 6.5342338 -1.2967691
C -4.8140302 2.1259480 -6.8034764
C -6.1961045 1.8369165 -6.8718574
H -6.4942487 0.9512246 -6.4122907
C -7.1334210 2.6920417 -7.5411838
H -8.1245754 2.4842097 -7.4737808
C -6.6705734 3.7606823 -8.3414570
H -7.2730567 4.4207819 -8.7382771
C -5.2681138 3.9131877 -8.3630593
C -4.3141483 3.1603309 -7.6004628
C -2.9343565 3.4271347 -7.8104596
C -2.5112839 4.4861030 -8.6069952
H -1.4764447 4.7310922 -8.7086139
C -3.4364836 5.2539420 -9.3073636
H -3.1195881 5.9603955 -10.0234534
C -4.7996918 4.9744297 -9.1898593
H -5.4221600 5.5071460 -9.7483080
H 1.1112078 4.1593172 -6.8543267
C -0.0949463 5.3542920 -5.6464226
H -0.5160968 5.7338919 -6.5164300
H -2.6471215 7.7690015 -2.7352904
C -1.5637735 6.7075247 -4.2868900
H -1.8951299 7.1588819 -5.1564416
N -1.1262640 -0.5368151 1.8592103
C 0.7891852 -2.0311328 1.2826366
H 0.7804382 -1.7017216 0.2194494
H 1.4738104 -1.3978337 1.8350175
C -2.4481082 -0.2658210 2.4333802
H -3.0129578 -1.2606314 2.5497507
O -1.1427258 -2.6861307 2.4752618
C -0.5162408 -1.7640372 1.9523357
C -0.4531596 0.6744656 1.3603740
H 0.6468041 0.5823106 1.4592834
H -0.6861738 1.5206407 2.0598970
C -3.4554995 0.3215407 1.5450042
C -4.0237638 1.5624597 1.8859848
H -3.7520649 2.0430638 2.7040594
C -4.9550735 2.2766606 1.0953728
H -5.2048746 3.2617654 1.3704084
C -5.4044682 1.6599526 -0.0539600
H -6.0500460 2.1737426 -0.6920001
C -4.9255622 0.4607229 -0.5180476

C -3.8925218 -0.2365750 0.2696416
C -3.3734300 -1.4500052 -0.2194698
H -2.6447940 -2.0135777 0.3346382
C -3.7771740 -1.9865635 -1.4290437
H -3.4406896 -2.8830189 -1.7247922
C -4.8753618 -1.3923762 -2.0991836
H -5.1180733 -1.7480901 -2.9887229
C -5.4171167 -0.1689150 -1.6519926
H -6.1934191 0.2189458 -2.1644490
C -2.2337500 0.2694490 3.8379707
H -1.5676955 -0.5011848 4.3776959
H -3.1207402 0.3883487 4.3001444
H -1.7316579 1.2364388 3.9029779
N -3.3823475 1.7332222 -4.7071286
C -1.4267511 1.6968767 -3.1426720
H -1.5268255 2.6583892 -2.8077376
H -2.0158213 1.2668857 -2.3896940
C -3.9576530 1.1900022 -5.9521593
H -3.1772109 0.8574601 -6.5729111
O -1.2321705 1.3755097 -5.4489902
C -2.0016072 1.5869876 -4.5020861
C -4.2406121 2.4126823 -3.7374386
H -3.9311250 2.0577703 -2.6763102
H -5.2797797 2.1457111 -3.8100713
C 1.7192694 -3.6181522 -1.5767310
C 0.3419126 -3.7334023 -1.7891639
H -0.2298157 -4.3490317 -1.2142525
C -0.3015546 -3.1490133 -2.9087998
H -1.2345525 -3.2115134 -3.0171827
C 0.3890751 -2.2084846 -3.6557788
H -0.0231186 -1.7275132 -4.4239644
C 1.8190701 -2.0220993 -3.4211615
C 2.4367153 -2.6972574 -2.3779855
C 3.8280229 -2.4384168 -2.1844770
H -2.1419976 2.9413664 -7.3309886
C 4.4814547 -1.4902583 -2.9104643
H 5.4557805 -1.3363674 -2.7661199
C 3.8242818 -0.7096708 -3.9494452
H 4.2954336 -0.0591091 -4.5258254
C 2.4900906 -1.0130195 -4.1535419
H 2.0876344 -0.5239237 -4.9038114
C -4.5884457 -0.1772588 -5.5555037
H -5.0098949 -0.7679186 -6.3743081
H -5.3220514 -0.0336017 -4.8003231
H -3.7911545 -0.8187822 -5.0703524
N 0.6955934 2.1673764 -1.8731985
C -0.7030578 1.0184790 -0.0583707
H -1.7093045 1.3801256 -0.1890753
H -0.7124640 0.1100124 -0.6115564
C 1.6404375 3.1584444 -2.3056375
H 1.7567410 3.8380943 -1.3919597

O 0.4014290 2.9801748 0.2707115
C 0.2299928 2.0677708 -0.5879011
C 0.0439065 1.3176311 -2.9095938
H 0.1815702 0.3139753 -2.5778637
H 0.6577954 1.2795354 -3.8128351
C 1.0630350 4.0040589 -3.4271431
C 1.4780841 3.7447106 -4.7738885
H 2.2934551 3.1369394 -4.9693117
C 0.9065024 4.4001251 -5.8485703
H 4.8149561 2.0338394 0.4898798
C 3.3032433 2.1074344 1.9408322
H 2.8513321 2.7890014 1.3388851
C -0.5432942 5.6983178 -4.3943799
C 0.0408696 5.0278267 -3.2486659
C -0.4506394 5.4147953 -1.9662702
H -0.1132814 4.9683964 -1.0992981
C -1.4593767 6.3488530 -1.8610073
H -1.8282290 6.5984684 -0.9029066
C -1.9948267 6.9977410 -3.0102196
H 0.0773580 1.9238895 5.2795412
C 1.6169044 2.1201120 3.7306855
H 1.1569838 2.9339961 3.2748460
C 3.0330921 2.5060725 -2.5232055
H 2.8582329 1.7936308 -3.4248939
H 3.4363596 2.0295646 -1.6114027
H 3.6701589 3.3260936 -2.8705922
N 4.7720251 -5.9458216 7.2904461
C 7.2573925 -6.6942893 7.3789450
H 7.5210287 -6.0368967 8.1974474
H 7.5169583 -6.2595386 6.4039609
C 3.3632740 -6.3803773 7.4898919
H 3.2516408 -7.4542740 7.2165815
O 5.5304313 -8.0721556 7.7695732
C 5.8125895 -6.8936160 7.4796134
C 5.1180231 -4.5998453 7.2252536
H 6.0826774 -4.5791761 7.6108626
H 4.5032856 -4.0813000 7.9303681
C 2.3315269 -5.7087664 6.6505955
C 1.5314981 -4.6213716 7.1065285
H 1.7816948 -4.2803089 8.0571284
C 0.4570509 -4.1139080 6.3657833
H 0.0034289 -3.2802799 6.6735941
C 0.1608402 -4.6873878 5.0903014
H -0.5842409 -4.2804099 4.5301031
C 0.9894766 -5.7360125 4.5868280
C 2.0776500 -6.1947461 5.3518904
C 2.9550073 -7.1825583 4.7515460
H 3.7694293 -7.6736709 5.1925208
C 2.6704423 -7.6954811 3.4833650
H 3.2522667 -8.3905744 3.1484768
C 1.4764486 -7.3228638 2.8004257

H 1.1942783 -7.7418780 1.9030882
C 0.6510540 -6.3221747 3.3294630
H -0.1597870 -6.0968904 2.8043201
C 3.0096179 -6.2993925 8.9748356
H 3.1059845 -5.2551987 9.3057198
H 3.7440985 -6.9939648 9.5546438
H 1.9818225 -6.5862579 9.1484822
N 2.4741473 -3.8277288 0.8309653
C 3.8205046 -3.0248948 2.7160517
H 3.2028060 -2.1181289 2.5231414
H 3.3072993 -3.5798562 3.4635819
C 2.4242423 -4.4187816 -0.4950919
H 3.4454637 -4.5280107 -0.8522729
O 4.7740325 -4.2865248 0.9848179
C 3.6916102 -3.7977430 1.4305035
C 1.2865082 -3.4729950 1.5015827
H 1.3962069 -3.7160569 2.5872351
H 0.4850066 -4.1651439 1.2112888
H 4.2336517 -2.8678214 -1.3608423
C 1.9894885 -5.8946609 -0.4141675
H 2.4229445 -6.3822038 0.4525528
H 2.3450169 -6.4182443 -1.2864145
H 0.9082467 -6.0001112 -0.2964220
N 5.4049165 -1.9609030 4.4518245
C 4.9208943 -3.9040456 5.8397715
H 3.8495065 -3.8931984 5.6604772
H 5.2809398 -4.6343611 5.0904826
C 5.7915912 -0.5821044 4.2847730
H 5.6809349 -0.1219914 5.2436610
O 5.9160246 -2.0258052 6.6567340
C 5.4116749 -2.5655471 5.6492140
C 5.2512286 -2.7221397 3.1887628
H 5.7203629 -3.6961069 3.2053839
H 5.6623755 -2.2334690 2.3916891
C 4.8629204 0.2561320 3.4545456
C 5.2654482 0.7207693 2.2021122
H 6.1298460 0.4276431 1.7004459
C 4.5148658 1.6483756 1.4236913
C 2.7893582 1.5281511 3.1545002
C 3.5626462 0.6371322 3.9238601
C 2.9928778 0.1841110 5.1675225
H 3.4734907 -0.5331847 5.6578549
C 1.7017382 0.5978538 5.6098743
H 1.3609481 0.1685561 6.5217705
C 0.9893327 1.5783275 4.8874045
C 7.2854231 -0.4696078 3.9464356
H 7.8268958 -1.0275802 4.7120022
H 7.5082734 0.5859823 3.9719750
H 7.4528690 -0.9680760 2.9980856
C -6.8399425 7.0485215 -2.0268215
H -7.5363839 7.4843670 -1.2677187

H -6.6299143 7.7581548 -2.8047183
H -7.3112635 6.1668005 -2.4817182
C -5.9838693 5.8354534 0.0810263
H -6.6432807 6.3443573 0.7327445
H -6.3405830 4.9092648 -0.2746934
H -5.1102815 5.6744442 0.6349991
C -4.8538771 7.6863410 -0.7756650
H -5.4605089 8.2692724 -0.1632665
H -3.9935651 7.4428817 -0.1581339
H -4.6746639 8.2539906 -1.7098176
H 7.8091345 -7.6579131 7.4488757

β-*N1snpe*$_6$ (loop, last frame of analysis MD) from Figure 8

C 2.7182079 1.4303210 4.6765243
O 3.6219033 2.1669593 5.0344228
C 1.3974351 3.6038868 4.7332267
H 1.9076374 4.0607814 5.4965036
H 1.9660793 3.8238984 3.8546652
C 1.3892192 2.0644480 4.9776889
H 1.1215777 1.7918290 6.0414648
H 0.6111108 1.5924220 4.2509802
N 0.1258429 4.2081642 4.5167590
C 0.6696333 -1.7532688 1.9459400
O -0.3326907 -1.9258673 2.5876105
C 1.8626564 -0.7076680 3.9715830
H 0.9432426 -0.4643817 4.5153045
H 2.0766533 -1.6979242 4.3585479
C 1.5411240 -0.6273787 2.4433133
H 1.1110558 0.3602467 2.2048076
H 2.4537167 -0.6967990 1.9023145
N 3.0270887 0.1936646 4.2297242
C 2.5826352 -0.0671287 -1.7031549
O 3.5663786 -0.8239270 -1.9795007
C 1.8628202 -1.9555587 -0.2100269
H 2.0649199 -2.7473142 -0.9131354
H 2.8039212 -1.8175717 0.2345041
C 1.4640753 -0.6192072 -0.8705394
H 0.5834033 -0.7490519 -1.4438105
H 1.3040849 0.1110362 -0.0816902
N 0.8725639 -2.3940897 0.7427333
C -0.8608143 1.6966436 -1.4709606
O -0.5858767 1.5799705 -0.2171221
C 1.6561360 2.2422768 -1.6421567
H 2.0543010 3.2156039 -1.7489966
H 1.5567091 2.2317541 -0.5321984
C 0.2895812 2.0874389 -2.3546545
H 0.0829175 3.1011674 -2.6123779
H 0.3437757 1.5252077 -3.3070645
N 2.6406874 1.2586113 -2.1175030
C -2.1795478 -0.3924117 -5.3161111
O -1.2798616 0.1236467 -6.0074797
C -2.3832766 1.2514943 -3.3425496
H -1.6523953 1.8879769 -3.7735118
H -3.3325741 1.5273740 -3.7414884
C -1.9547573 -0.2411821 -3.8095984
H -0.8945284 -0.3972933 -3.6061975
H -2.4369447 -1.0012301 -3.2072368
N -2.1875935 1.4129935 -1.9453083
C -3.8201714 -4.2136492 -3.9057470
O -5.0015700 -4.2125853 -3.3876861
C -4.0044523 -1.9680097 -5.0091986

H -4.9142019 -2.2150793 -5.4740884
H -4.1842041 -1.5846805 -4.0157677
C -3.2849619 -3.3210751 -4.9605274
H -3.0775242 -3.8423838 -5.8985969
H -2.2774344 -3.0310640 -4.6108856
N -3.2464875 -1.0752805 -5.8732358
H -0.3146938 2.8371780 1.8439307
H -0.0683068 4.4713985 1.2532325
C 0.2007346 3.7995474 2.0778025
C -0.4040550 4.4316888 3.2523899
O -1.4827435 5.0645576 2.9829994
H 1.2710497 3.6725344 2.0500089
O -2.9768465 -5.2440827 -3.5684609
C -3.3053360 -6.4882002 -2.9084914
C -3.9973823 -6.2905684 -1.5354767
C -1.9478138 -7.2308430 -2.7815902
C -4.2075274 -7.2986155 -3.8374076
H -4.0658991 -7.0883458 -0.8815026
H -4.9965304 -5.8030072 -1.6947007
H -3.2702624 -5.5869198 -1.0748224
H -1.4416794 -7.3342068 -3.7701985
H -2.0256282 -8.2324383 -2.3659792
H -1.2998886 -6.6915466 -2.0386664
H -5.1181237 -6.8071488 -4.2253115
H -4.6267302 -8.1261405 -3.2672575
H -3.7300310 -7.6941546 -4.7669060
C -0.6915131 4.6878437 5.6953279
C -1.3009714 3.5545113 6.5835774
H -1.8924818 2.9011175 5.9839298
H -1.9081665 3.9299561 7.3478841
H -0.5585550 2.9213954 6.9793699
C -0.1038145 5.7112496 6.5173572
C -0.3783303 7.1049018 6.2906822
C 0.7585826 5.4594876 7.5996248
C 0.2801875 8.1118305 7.0536684
C 1.3606607 6.3942844 8.3850273
H 0.8576217 4.5013478 7.7266143
C 1.1456713 7.7510165 8.0409455
H 2.0115557 6.2030801 9.0742285
H 1.7086786 8.4284164 8.5996962
H -1.6510717 5.0802088 5.3760112
C 0.1493546 9.4455357 6.6913819
C -0.5761742 9.7713654 5.6061256
C -1.3693509 8.8332366 4.8927769
C -1.2678495 7.4893331 5.2528674
H 0.6741879 10.1820525 7.2236777
H -0.5829030 10.7726127 5.3239448
H -1.8942916 9.1766623 4.0883031
H -1.8415515 6.8532350 4.7192102
C 4.3166900 -0.2247439 3.7795825
C 5.6313599 0.4996002 4.2457950

H 5.6093614 1.5993701 3.9959588
H 6.3792550 -0.0066899 3.6368125
H 5.7378211 0.4087686 5.2956134
C 4.5989946 -1.6885311 3.8028869
C 4.8194245 -2.4241137 5.0118164
C 4.7660924 -2.3744865 2.5990669
C 5.2804609 -3.7514692 4.9481855
C 5.1602013 -3.6992504 2.5623461
H 4.5551818 -1.7976083 1.7242058
C 5.3950125 -4.3949013 3.7062099
H 5.3282589 -4.1772413 1.7069048
H 5.6598213 -5.3573327 3.6707314
H 4.2294583 0.1210175 2.7703085
C 5.5014636 -4.5078311 6.0923596
C 5.2656613 -3.9808917 7.4018918
C 4.7951319 -2.6599827 7.4701022
C 4.6072173 -1.9059877 6.3433655
H 5.7556052 -5.5049378 6.1765764
H 5.2624198 -4.6354669 8.2091035
H 4.6769852 -2.2220724 8.3974542
H 4.3594856 -0.9859857 6.4378973
C 0.1806900 -3.6641456 0.5626706
C -0.8407651 -3.6249990 -0.5744557
H -1.4504289 -2.7242910 -0.5651117
H -1.4756529 -4.4759335 -0.7006994
H -0.2655563 -3.4484779 -1.4526818
C 1.1032571 -4.8811886 0.4943429
C 1.7473254 -5.3613698 1.7295628
C 1.2501996 -5.5706399 -0.7575804
C 2.5653554 -6.4931853 1.6015977
C 2.0245348 -6.7080033 -0.8186450
H 0.7245512 -5.2510286 -1.5851336
C 2.6544787 -7.1561232 0.3436279
H 2.0886865 -7.2037426 -1.7704333
H 3.2667547 -7.9772631 0.2498000
H -0.3851598 -4.0053345 1.4367813
C 3.2259247 -6.9837809 2.7339682
C 3.0476761 -6.4255807 4.0247848
C 2.2575328 -5.2596987 4.0970286
C 1.5789990 -4.7383516 2.9897774
H 3.8436661 -7.7652631 2.6882073
H 3.4283109 -6.9255705 4.8292750
H 2.0816246 -4.8285337 4.9953359
H 0.9215346 -3.9914867 3.2369404
C 3.6794739 1.6728498 -3.0176998
C 3.1116469 1.6083841 -4.4824089
H 3.8965330 1.4452954 -5.2060842
H 2.5299226 2.4885794 -4.7428954
H 2.3874036 0.7512945 -4.6360469
C 4.3921505 2.9330229 -2.6327987
C 5.0026720 3.2049618 -1.3589139

C 4.4549821 4.0232678 -3.5420193
C 5.4674890 4.4982141 -1.0595969
C 5.0412392 5.2476534 -3.3332023
H 3.9734287 3.8798551 -4.4759721
C 5.4987531 5.5071165 -2.0324362
H 5.1254378 5.8570565 -4.1083513
H 5.9098646 6.4268269 -1.7869562
H 4.4040243 0.9326594 -2.9810062
C 6.1290166 4.7253691 0.1366660
C 6.1611774 3.7561712 1.1568465
C 5.6253808 2.4793575 0.9422455
C 5.0981518 2.2397910 -0.3460210
H 6.5591996 5.5901919 0.3661540
H 6.5339365 4.0501656 2.0958863
H 5.7130970 1.7321588 1.7165289
H 4.7191876 1.2976457 -0.5166752
C -3.3336736 1.3066327 -1.0408208
C -3.9161945 2.6876361 -0.8135377
H -3.3104663 3.3240735 -0.1630934
H -4.9572437 2.5283436 -0.3758637
H -4.0030346 3.2858389 -1.7429569
C -4.3926163 0.1949959 -1.1801858
C -4.3961807 -1.0615043 -0.4640587
C -5.3114445 0.3836858 -2.2683275
C -5.4308192 -2.0234513 -0.7757512
C -6.2387011 -0.6052963 -2.5782471
H -5.4083045 1.1663932 -2.8653088
C -6.2905932 -1.7979721 -1.8665460
H -6.9472935 -0.4181570 -3.2739255
H -7.0747121 -2.4507586 -2.0755618
H -2.8436883 1.1957637 -0.0834038
C -5.6232948 -3.2438646 0.0050638
C -4.6413308 -3.5494349 0.9579281
C -3.5958385 -2.6636451 1.2439721
C -3.5322936 -1.4011049 0.6313799
H -6.3379892 -3.8928063 -0.1165849
H -4.7803901 -4.4544158 1.4680468
H -2.9925648 -2.9795833 1.9910327
H -2.8175366 -0.7605654 0.8650224
C -3.4846970 -0.9076583 -7.2989132
C -4.6974464 -1.7173815 -7.9207652
H -4.2579713 -2.7356111 -8.0153661
H -4.8997451 -1.3838748 -8.9391026
H -5.5972832 -1.7358857 -7.3459410
C -3.5280225 0.4530235 -7.8243449
C -4.3131386 1.5247554 -7.2351266
C -2.8945290 0.6975903 -9.0784148
C -4.3592689 2.7499321 -7.9869528
C -2.9906960 1.9351169 -9.7034957
H -2.2373777 -0.1241441 -9.4535676
C -3.7964907 2.9511616 -9.2642579

H -2.5634485 2.1463754 -10.6421002
H -4.0676518 3.7812219 -9.8483705
H -2.5614422 -1.3239120 -7.7432739
C -5.0914749 3.8999643 -7.3859293
C -5.7157798 3.7735424 -6.1416504
C -5.6603286 2.5421792 -5.5127541
C -4.9515172 1.4285989 -6.0175160
H -5.1045699 4.7731320 -7.8410028
H -6.1411559 4.6267156 -5.7387550
H -6.1693188 2.4309562 -4.5837699
H -4.9225211 0.5981469 -5.3106144

Structures of peptoid model bearing *Nspe* side chain (MP2) from Table S3

trans-α_D

C	-0.75080400	-0.31093400	-0.46203600
C	-2.07921800	-0.47341300	0.30021200
O	-2.38306800	0.28172100	1.22126900
N	-2.86536300	-1.53298300	-0.08967800
C	-2.60138200	-2.33598400	-1.27269700
H	-3.08667200	-3.31704200	-1.14297700
H	-3.00078700	-1.87228200	-2.19543600
H	-1.52551200	-2.51680100	-1.40246200
C	-4.20479500	-1.64483400	0.46956300
H	-4.27286300	-0.96976600	1.33170700
H	-4.96948000	-1.35780000	-0.27631100
H	-4.39661200	-2.68294700	0.79056400
H	-0.93227400	-0.38183400	-1.54542800
H	-0.04805000	-1.11222400	-0.17465800
N	-0.13465400	0.96948200	-0.17600800
O	-1.78865500	1.90834600	-1.41574500
C	-0.29212900	3.44376700	-0.31676700
H	0.74994200	3.59047500	-0.64535200
H	-0.33791600	3.61533700	0.77110200
H	-0.93480500	4.17636300	-0.82309500
C	-0.81324700	2.06297400	-0.68007700
C	0.95023000	1.02945300	0.80815200
H	1.34467100	2.05746200	0.76894900
C	0.46286700	0.77136200	2.23676500
H	-0.36490500	1.45476700	2.47388600
H	1.28538900	0.92659800	2.95536100
H	0.08002500	-0.25498600	2.35328600
C	2.08377000	0.11429800	0.34711100
C	2.67651300	-0.85459400	1.17923700
C	2.56301200	0.25442400	-0.97375000
C	3.72668900	-1.66258500	0.70377500
H	2.32493300	-0.98794000	2.20634900
C	3.61289100	-0.54489300	-1.44852100
H	2.09647100	0.99558500	-1.63278800
C	4.19865700	-1.51060800	-0.60915600
H	4.17412200	-2.41280600	1.36460800
H	3.97360800	-0.41783800	-2.47499400
H	5.01630300	-2.13895300	-0.97757200

trans-$C_{7\beta}$

C	1.41591000	1.11942100	0.98582100
C	-0.03923000	1.59423100	0.95694100
O	-0.70930000	1.57243100	1.99667100
N	-0.53734000	2.01307100	-0.24568900
C	0.20356000	2.07547100	-1.49271900
H	1.26731000	1.84688100	-1.35258900
H	-0.21809000	1.35783100	-2.22054900
H	0.11716100	3.08973100	-1.92353900
C	-1.94835000	2.35285100	-0.34256900
H	-2.39902000	2.23844100	0.65126100
H	-2.06872900	3.39491100	-0.68956900
H	-2.44775000	1.67562100	-1.05761900
H	1.68381000	1.05248100	2.05228100
H	2.10446000	1.82552100	0.50258100
N	1.61243000	-0.17507900	0.33038100
O	3.29043000	0.69915000	-0.95760900
C	2.98748000	-1.67477000	-1.10711900
H	2.13821000	-2.17025900	-1.60222900
H	3.33351000	-2.33087000	-0.29114900
H	3.80266000	-1.54801000	-1.83192900
C	2.64580000	-0.28506900	-0.58287900
C	0.78463000	-1.30381900	0.78780100
H	1.25124000	-2.21284900	0.38018100
C	0.80847000	-1.43049900	2.31432100
H	1.85346000	-1.47582900	2.66304100
H	0.30033000	-2.35957900	2.61919100
H	0.30570000	-0.57926900	2.79772100
C	-0.62156000	-1.23008900	0.18405100
C	-1.79169000	-1.22037900	0.96748100
C	-0.75318000	-1.20960900	-1.22133900
C	-3.06050000	-1.20282900	0.35979100
H	-1.72470000	-1.21179900	2.05795100
C	-2.01731000	-1.19672900	-1.83125900
H	0.14476000	-1.20204900	-1.84875900
C	-3.18013000	-1.19714900	-1.03914900
H	-3.95824000	-1.19205900	0.98719100
H	-2.09504000	-1.19293900	-2.92421900
H	-4.16913000	-1.19068900	-1.50959900

References

[45] P. D. Renfrew, T. W. Craven, G. L. Butterfoss, K. Kirshenbaum, R. Bonneau, J. Am. Chem. Soc. 2014, 136, 8772.

[46] D. P. Smith, T. W. Knapman, I. Campuzano, R. W. Malham, J. T. Berryman, S. E. Radford, A. E. Ashcroft, Eur. J. Mass Spectrom. 2009, 15, 113.

[47] E. W. McDaniel, D. W. Martin, W. S. Barnes, Rev. Sci. Instrum. 1962, 33, 2.

[48] Q. Duez, F. Chirot, R. Liénard, T. Josse, C. Choi, O. Coulembier, P. Dugourd, J. Cornil, P. Gerbaux, J. De Winter, J. Am. Soc. Mass Spectrom. 2017, 28, 2483.